Attachment 1
NRC3-13-0036

Action Item 3.7-12
(2 pages)

NRC Action Item 3.7-12

Provide digitalize data for FSAR Figures 3.7.1-230 and 3.7.1-231.

Response

See Attachment 14 for the CD containing the Requested Electronic Files.

Proposed COLA Markup

None

Attachment 2
NRC3-13-0036

Action Item 3.7-13
(8 pages)

NRC Action Item 3.7-13

Review and update FSAR Appendix 3C as required.

Response

See Proposed COLA Markup.

Proposed COLA Markup

See Proposed FSAR Markup to Appendix 3C.

Attachment 2
NRC3-13-0036
(following 5 pages)

Markup of Fermi 3 COLA

The following markup represents how DTE Electric intends to reflect this RAI response in the next submittal of the Fermi 3 COLA. However, the same COLA content may be impacted by responses to other COLA RAIs, other COLA changes, plant design changes, editorial or typographical corrections, etc. As a result, the final COLA content that appears in a future submittal may be different than presented here.

The COLA markups were made to Draft Revision 6 of the Fermi 3 FSAR. Draft Revision 6 of the FSAR incorporates the proposed FSAR changes submitted in DTE Electric correspondence since the submittal of Revision 5 in February 2013 until the NRC audit in November 2013. Thus, the markups represent proposed FSAR changes since the conclusion of the NRC audit.

Appendix 3A Seismic Soil-Structure Interaction Analysis

This section of the referenced DCD is incorporated by reference with the following departures and/or supplements.

3A.1 Introduction

Replace the last sentence in the second paragraph with the following.

EF3 CDI

Site-specific geotechnical data is described in Chapter 2. This data is compatible with the site enveloping parameters considered in the standard design.

3A.2 ESBWR Standard Plant Site Plan

Replace the first two sentences of the first paragraph with the following.

EF3 CDI

The site plan is shown in Figure 2.1-204. The plan orientation is denoted on the figure.

3A.5 SOIL-STRUCTURE INTERACTION ANALYSIS METHOD

3A.5.2 SASSI2000 Analysis Method

Replace the second sentence of the first paragraph with the following.

EF3 CDI

The program uses finite elements with complex moduli for modeling the structure and foundation properties and is based on the direct method and the frequency domain complex response method.

Appendix 3B Containment Hydrodynamic Load Definitions

This section of the referenced DCD is incorporated by reference with no departures or supplements.

Appendix 3C Computer Programs Used in the Design and Analysis of Seismic Category I Structures

Insert 3C →

~~This section of the referenced DCD is incorporated by reference with no departures or supplements.~~

Insert 3C

EF3 SUP 3C-1 Add the following at the end of this Appendix

3C.8 **SITE SPECIFIC SOIL- STRUCTURE INTERACTION**

3C.8.1 **Dynamic Soil-Structure Interaction Analysis Program – SASSI2010**

3C.8.1.1 **Description**

SASSI2010 is used to solve a wide range of dynamic SSI problems in two or three dimensions. SASSI was developed at the University of California, Berkeley in 1982 under the technical direction of John Lysmer. The program is based on the finite-element method formulated in the frequency domain using a substructuring technique.

3C.8.1.2 **Validation**

SASSI2010 was obtained from ISATIS, LLC, University of California, Berkley and validated by Sargent & Lundy, LLC. The program validation documentation is available at Sargent & Lundy.

3C.8.1.3 **Extent of Application**

This program is used to perform the site specific SSI analysis for Seismic Category I structures.

3C.8.2 **RSG**

3C.8.2.1 **Description**

RSG is used to generate artificial synthetic time histories for seismic analysis. It also generates response spectrum from an input acceleration time history. It can envelope spectra, combine spectra, and generate a spectrum consistent time history.

3C.8.2.2 **Validation**

RSG was developed and validated by Sargent & Lundy, LLC. The program validation documentation is available at Sargent & Lundy.

3C.8.2.3 **Extent of Application**

RSG is used to calculate maximum velocity of nodes in the structural model for evaluating the overturning stability of the structure.

3C.8.3 **Free-Field Site Response Analysis – SHAKE04**

3C.8.3.1 **Description**

SHAKE is a program, which can perform the free-field site response analysis. It was developed at the University of California, Berkeley

Insert 3C (continued)

by B. Schnabel, John Lysmer and H.B. Seed in 1972. The program is based on the theory of one-dimensional propagation of shear waves in the vertical direction in a horizontally-layered visco-elastic soils system overlying an elastic halfspace medium.

SHAKE also has a function to account for non-linearities in soil shear modulus and hysteresis damping as functions of shear strain in soil by the use of equivalent-linear soil properties using an iterative equivalent linearization procedure to obtain constant values of shear modulus and hysteresis damping ratio compatible with the effective shear strain in each soil layer.

SHAKE04 is a modified version of SHAKE in which the fast Fourier transform routines have been updated and the allowable limits on the number of soil layers, number of material types, and the length of time histories were increased.

3C.8.3.2 **Validation**

SHAKE04 was developed by AMEC E&I. The software validation documents are located in Black & Veatch's Nuclear Department Quality Assurance files.

3C.8.3.3 **Extent of Application**

SHAKE04 is used to generate the free-field site response motions required in the seismic SSI analysis.

SHAKE04 is also used to provide the site-specific earthquake-induced design ground motions and the associated strain-compatible soil properties for SSI analysis.

3C.8.4 **Time Domain Spectral Matching – RSPMATCH (RSPM06)**

3C.8.4.1 **Description**

RSPMATCH performs a time domain modification of an acceleration time history to make its response spectrum compatible with a user specified target spectrum. RSPMATCH is based on the procedure proposed in Reference 3C-1 and later modified in Reference 3C-2. This time-domain approach defines small-adjustment time histories that modify the original time history and preserves the nonstationary properties of the original time history. The time-domain approach can therefore develop a time history that matches a target spectrum yet still has a realistic displacement waveform.

RSPM06 is the AMEC E&I implementation of RSPMATCH.

Insert 3C (continued)

3C.8.4.2 **Validation**

RSPM06 was developed by AMEC E&I. The software validation documents are located in Black & Veatch's Nuclear Department Quality Assurance files.

3C.8.4.3 **Extent of Application**

RSPM06 was used to modify the seed acceleration time history in the time domain to make its response spectrum match the enhanced SCOR FIRS and SCOR FIRS of the RB/FB and CB for SSI analysis.

3C.8.5 **Two-Dimensional Free-Field Site Response Analysis – QUAD4MU**

3C.8.5.1 **Description**

QUAD4MU is a two-dimensional finite element program used to perform twodimensional dynamic response of soil structures using equivalent-linear material properties in the time domain. QUAD4 was originally developed in Reference 3C-3. QUAD4M was developed in Reference 3C-4 to incorporate a flexible elastic halfspace and base transmitting boundary dampers, and subsequently updated to QUAD4MU to correct the calculation of the seismic coefficients.

3C.8.5.2 **Validation**

QUAD4MU was developed by AMEC E&I. The software validation documents are located in Black & Veatch's Nuclear Department Quality Assurance files.

3C.8.5.3 **Extent of Application**

QUAD4MU was used to evaluate two-dimensional effects on the site response for the FWSC. Surface motions were computed using a two-dimensional model of the fill concrete beneath the FWSC and using a one-dimensional model of the fill concrete. The ratios of the response spectra for the two-dimensional and one-dimensional motions were used to develop the FWSC FIRS for comparison with 1.35 times the CSDRS in the Referenced DCD.

3C.8.6 **REFERENCES**

3C-1 Lilhanand, K., and W.S. Tseng, "Development and application of realistic earthquake time histories compatible with multiple-damping response spectra," Proceedings of the 9th World Conference on Earthquake Engineering, Tokyo-Kyoto, Japan, v. II, 1988.

Insert 3C (continued)

3C-2	Abrahamson, N., "Non-stationary spectral matching," Seismological Research Letters, Vol. 63, No. 1, 1992.
3C-3	Idriss, I.M., Lysmer J., Hwang R., and Seed H.B., QUAD-4: A Computer Program for Evaluating the Seismic Response of Soil Structures by Variable Damping Finite Element Procedures, EERC Report 73-16, 1973.
3C-4	Hudson M., Idriss I.M., and M. Beikae, User's Manual for QUAD4M. A Computer Program to Evaluate the Seismic Response of Soil Structures Using Finite Element Procedures and Incorporating a Compliant Base, Center for Geotechnical Modeling, Department of Civil & Environmental Engineering, University of California, Davis, 1994.

Attachment 3
NRC3-13-0036

Action Item 3.7-14
(6 pages)

NRC Action Item 3.7-14

Provide a description of MSM Benchmarking in the FSAR.

Response

See Proposed COLA Markup.

Proposed COLA Markup

See Proposed FSAR Markup to Section 3.7.2.4 and Section 3.7.2.4.1.3.

Attachment 3
NRC3-13-0036
(following 3 pages)

Markup of Fermi 3 COLA

The following markup represents how DTE Electric intends to reflect this RAI response in the next submittal of the Fermi 3 COLA. However, the same COLA content may be impacted by responses to other COLA RAIs, other COLA changes, plant design changes, editorial or typographical corrections, etc. As a result, the final COLA content that appears in a future submittal may be different than presented here.

The COLA markups were made to Draft Revision 6 of the Fermi 3 FSAR. Draft Revision 6 of the FSAR incorporates the proposed FSAR changes submitted in DTE Electric correspondence since the submittal of Revision 5 in February 2013 until the NRC audit in November 2013. Thus, the markups represent proposed FSAR changes since the conclusion of the NRC audit.

3.7.2 **Seismic System Analysis**

3.7.2.4 **Soil-Structure Interaction**

Add the following at the end of the first paragraph.

EF3 SUP 3.7-4

This subsection of the Referenced DCD, including associated Appendix 3A in its entirety, is incorporated by reference with the following supplement for the Fermi 3 site-specific soil-structure interaction (SSI) analyses for the RB/FB and CB. The site-specific SSI analyses for the RB/FB and CB were performed using ~~the direct method of the SASSI2010 computer program.~~ The SSI analysis approach and the structural models are the same as presented in Appendix 3A of the Referenced DCD.

either the direct method or the modified subtraction method of the SASSI2010 computer program. The subtraction method of the SASSI2010 program was not used.

The FWSC is essentially a surface founded structure in the Referenced DCD, Subsection 3.7.1.1 and there are no embedded walls for the FWSC. Therefore, the Referenced DCD backfill requirements surrounding Seismic Category I structures are not applicable to FWSC embedded basemat (embedded 2.35 m (7.7 feet)). The FWSC is founded on fill concrete which meets the Referenced DCD requirements for backfill underneath Seismic Category I structures. Therefore, there is no site-specific SSI analysis performed for the FWSC.

Add the following subsections following Subsection 3.7.2.4.

3.7.2.4.1 **Fermi 3 Site-Specific Soil-Structure Interaction Analysis**

This subsection presents the Fermi 3 site-specific SSI analyses performed in accordance with SRP 3.7.2 for the Seismic Category I RB/FB and CB. The Fermi 3 site-specific FIRS developed in Subsection 3.7.1 is in accordance with Regulatory Guide 1.208 and NRC Interim Staff Guidance (DC/COL-ISG-017) for ensuring hazard-consistent seismic input for site response and soil-structure interaction analyses. The Fermi 3 site-specific FIRS developed in and Subsection 3.7.1 are fully enveloped, in all cases, by the ESBWR CSDRS. Therefore, the Fermi 3 site-specific SSI analyses were not performed to address an exceedance of the CSDRS by the FIRS; rather, the Fermi 3 site-specific SSI analyses were performed to address the following Fermi 3 site-specific conditions:

- Partial embedment in the Bass Islands Group bedrock of the RB/FB and CB Seismic Catagory I structures, as shown on Figure 2.5.4-202

variability in the subsurface materials properties at the Fermi 3 site. The development of the Fermi 3 site-specific strain compatible dynamic subsurface material properties associated with the BE, LB, and UB profiles is discussed in Subsection 3.7.1.3. The strain compatible dynamic subsurface material properties of the BE, LB, and UB subsurface profiles used in the Fermi 3 site-specific SSI analyses are provided in Table 3.7.1-206 through Table 3.7.1-211. To demonstrate that the backfill surrounding the Seismic Category I RB/FB and CB above the top of the Bass Islands Group bedrock can be neglected, separate BE, LB, and UB subsurface profiles were used for the Fermi 3 SSI analyses that separately include and do not include backfill that will be placed during construction above the Bass Islands Group bedrock at Elevation 168.2 m (552.0 ft) NAVD 88 to finished ground level grade at Elevation 179.6 m (589.3 ft) NAVD 88.

3.7.2.4.1.2 FIRS Compatible Ground Motion Time HIstory

Subsection 3.7.1.1.5 describes development of the Fermi 3 site-specific ground motion time histories used in the SSI analyses. The Fermi 3 site-specific SSI analyses used three orthogonal components (two horizontal and one vertical) of a single ground motion time history that were developed to be in-column motions at the bottom of RB/FB and CB basemat levels. The site-specific ground motion time histories are compatible with the SSI FIRS developed in Subsection 3.7.1 and are used as input motions applied at the bottom of RB/FB and CB basemat levels in the Fermi 3 site-specific SSI analyses.

3.7.2.4.1.3 Soil-Structure Interaction Analysis Method

Insert 3.7.2.4.1.3 →

~~The Fermi 3 site-specific SSI analysis follows the methodology presented in DCD Section 3A.5.2 using the direct method of the SASSI2010 computer program.~~ The SASSI2010 program uses finite elements with complex moduli for modeling the structure and foundation properties and is based on the frequency domain complex response method. The lumped mass-beam model described in DCD Section 3A.5.1 is coupled with the soil model using site-specific strain compatible dynamic subsurface properties in SASSI2010. Structural responses in terms of accelerations, forces, and moments are computed directly. Floor response spectra are obtained from the calculated response acceleration time histories.

Insert 3.7.2.4.1.3

The Fermi 3 site-specific SSI analysis follows the methodology presented in DCD Section 3A.5.2 using either the direct method or the modified subtraction method of the SASSI2010 computer program. The method of analysis used for site-specific SSI and SSSI analyses are shown in Tables 3.7.2-201 and 3.7.2-202. The subtraction method of SASSI2010 program is not used for any of the site-specific SSI analyses.

As shown in Tables 3.7.2-201 and 3.7.2-202, modified subtraction method was used for SSI analysis of the RB/FB with engineered backfill and SSSI analysis of the CB and FWSC. When using modified subtraction method, the results from the modified subtraction method models were benchmarked against the results from the direct method models to ensure that the appropriate modified subtraction method models were being utilized. These benchmark analyses were performed using the site-specific soil properties and input motions using full, half, or quarter models as follows:

- For benchmark analyses of the RB/FB, quarter model of the RB/FB was used.
- For benchmark analyses of the CB, full model of the CB was used.
- For the benchmark analyses of the FWSC, half model of the CB was used.

Attachment 4
NRC3-13-0036

Action Item 3.7-20
(4 pages)

NRC Action Item 3.7-20

Provide Documentation in FSAR that explains the change in the number of rock damping layers between FSAR Tables 2.5.2-213 and 2.5.2-214 and Tables 3.7.1-201, 3.7.1-202, and 3.7.1-203.

Response

See Proposed COLA Markup.

Proposed COLA Markup

See Proposed FSAR Markup to Section 3.7.1.1.4.1.1.2.

Attachment 4
NRC3-13-0036
(following 1 page)

Markup of Fermi 3 COLA

The following markup represents how DTE Electric intends to reflect this RAI response in the next submittal of the Fermi 3 COLA. However, the same COLA content may be impacted by responses to other COLA RAIs, other COLA changes, plant design changes, editorial or typographical corrections, etc. As a result, the final COLA content that appears in a future submittal may be different than presented here.

The COLA markups were made to Draft Revision 6 of the Fermi 3 FSAR. Draft Revision 6 of the FSAR incorporates the proposed FSAR changes submitted in DTE Electric correspondence since the submittal of Revision 5 in February 2013 until the NRC audit in November 2013. Thus, the markups represent proposed FSAR changes since the conclusion of the NRC audit.

slightly higher response. The planned fill concrete with shear dowels is anticipated to remain essentially linear under the anticipated ground motion levels. Thus, the shear modulus reduction values for the fill concrete were set to 0.9999 for strain levels less than 3 percent and to 0.999 at higher strain levels.

Below the engineered granular backfill and fill concrete, the remaining portion of the full soil column and FWSC site response analysis profiles consists of dolomite and claystone bedrock, as discussed in Subsection 2.5.2.5.1.2. The bedrock is expected to remain essentially linear at low to moderate levels of shaking. Damping within the in-situ dolomite and claystone bedrock is characterized by a high-frequency attenuation parameter κ that ranges from 0.001 and 0.003 seconds (Subsection 2.5.2.5.1). The values of κ established in Subsection 2.5.2.5.1 were used to develop the site response analysis for the Fermi 3 site.

As part of the development of the SSI inputs, the representation of damping in the in-situ bedrock was simplified from the seven different damping layers indicated in FSAR Table 2.5.2-213 and Table 2.5.2-214 to the four different damping layers listed in FSAR Table 3.7.1-201, Table 3.7.1-202, and Table 3.7.1-203. Sensitivity studies indicated that this simplification in the number of layers produces less than 0.1 percent difference in the mean amplification functions.

3.7.1.1.4.1.1.3 **Randomization of Dynamic Properties**

Site response analyses for the full soil column and FWSC profiles were conducted using randomized dynamic soil properties following the methods described in Subsection 2.5.2.5.1.3. The randomized dynamic properties included shear wave velocity, modulus reduction, and damping. Additionally, the locations of velocity layer boundaries were randomized to vary uniformly within the range of layer thickness observed in the site borings.

Sixty randomized V_S profiles were generated for each of the LR, IR, and UR site response analysis profiles (a total of 180 randomized V_S profiles for development of the PBSRS and SCOR FIRS). Sixty randomized V_S profiles were also generated for the FWSC site response analysis profile. The statistics of the randomized profiles are summarized by comparing to the input target values for median velocity and standard deviation (sigma) of ln(V_S) for the LR, IR, UR, and FWSC profiles. As an example of this process, Figure 3.7.1-204 to Figure 3.7.1-206 show the 60 randomized velocity profiles and the statistics of the randomized shear wave velocity profiles for the IR site response analysis profile.

The modulus reduction and damping relationships associated with the LR, IR, and UR full column site response analysis profiles were also randomized as shown on Figure 3.7.1-207, Figure 3.7.1-208, and Figure 3.7.1-209, respectively. The standard deviation in the modulus reduction

Attachment 5
NRC3-13-0036

Action Item 3.7-21
(5 pages)

NRC Action Item 3.7-21

Provide additional FSAR Description to document development of deterministic soil profiles (LB, BE, and UB).

Response

See Proposed COLA Markup.

Proposed COLA Markup

See Proposed FSAR Markup to Section 3.7.1.1.4.3.3.

Attachment 5
NRC3-13-0036
(following 2 page)

Markup of Fermi 3 COLA

The following markup represents how DTE Electric intends to reflect this RAI response in the next submittal of the Fermi 3 COLA. However, the same COLA content may be impacted by responses to other COLA RAIs, other COLA changes, plant design changes, editorial or typographical corrections, etc. As a result, the final COLA content that appears in a future submittal may be different than presented here.

The COLA markups were made to Draft Revision 6 of the Fermi 3 FSAR. Draft Revision 6 of the FSAR incorporates the proposed FSAR changes submitted in DTE Electric correspondence since the submittal of Revision 5 in February 2013 until the NRC audit in November 2013. Thus, the markups represent proposed FSAR changes since the conclusion of the NRC audit.

model for V_{S30} values of 830 m/s (2,720 ft/s) and 421 m/s (1,380 ft/s). These V_{S30} values corresponded to the firm rock and soft rock categories of Campbell and Bozorgnia (Reference 3.7.1-213). The result suggests a trend similar to the Campbell and Bozorgnia (Reference 3.7.1-213) result.

Figure 3.7.1-220 shows V/H spectral ratios as a function of frequency used for generating the vertical PBSRS at the finished ground level grade, and the V/H spectral ratios recommended by NUREG/CR- 6728 (Reference 3.7.1-202) for CEUS bedrock sites with a PGA between 0.2 g and 0.5 g. The V/H spectral ratios used for generating the vertical PBSRS are based on the V/H spectral ratios recommended by NUREG/CR-6728 (Reference 3.7.1-202) for CEUS bedrock sites with a shift in the frequencies above 10 Hz to represent the shift in the peak V/H spectral ratios towards lower frequencies in the Campbell and Bozorgnia (Reference 3.7.1-213) and Gülerce and Abrahamson (Reference 3.7.1-215) comparisons. Additionally, at frequencies below 9 Hz, the V/H spectral ratio is reduced slightly to reflect the differences observed in the Campbell and Bozorgnia (Reference 3.7.1-213) and Gülerce and Abrahamson (Reference 3.7.1-215) comparisons. The resulting vertical PBSRS is listed in Table 3.7.1-205 along with the values of V/H. Figure 3.7.1-221 shows the horizontal and vertical PBSRS (5 percent damping) at the finished ground level grade.

The 60 randomized full soil column profiles were developed for each of the nine alternative sets of dynamic properties (three alternative sets of engineered granular backfill properties and three alternative sets of damping values in the in-situ bedrock). These 540 profiles were then used in site response analyses with the time histories matched to the 10^{-4} and 10^{-5} HF and LF DEL, DEM, and DEH response spectra. The results of these calculations produced a total of 1,620 profiles of strain-compatible dynamic properties for each of the 10^{-4} and 10^{-5} HF and LF exceedance levels of input motion. Each strain-compatible profile was assigned a weight equal to the product of the weights on the corresponding branches of the site response logic tree shown in Figure 3.7.1-210 times 1/60 for each randomization case. The resulting values of shear wave velocity and damping in each soil layer were then ranked in increasing order and the empirical 16th, 50th, and 84th percentile values were identified for the four loading levels.

3.7.1.1.4.3.3 **Deterministic Profiles for SSI Analyses**

Three deterministic profiles, the best estimate (BE), lower bound (LB), and upper bound (UB), were developed from the full soil column site response analysis following the requirements of Standard Review Plan (SRP) 3.7.2 and guidance from the Interim Staff Guidance DC/COL-ISG-017. These profiles were based on the statistics of the iterated soil properties for the randomized full soil column profile described in Subsection 3.7.1.1.4.1.1.3, and include the engineered granular backfill above the top of the Bass Islands Group bedrock.

The deterministic BE profile with engineered granular backfill above the top of the Bass Islands Group bedrock was set equal to values interpolated between the median iterated soil properties for the 10^{-4} and 10^{-5} exceedance level ground motions using linear interpolation based on the PGA values for the 10^{-4} and 10^{-5} UHRS and the PGA for the PBSRS. The resulting subsurface layers and the corresponding strain

The 50th percentile properties for the HF and LF input motions were averaged to produce the BE profile.

compatible dynamic engineering properties for the full soil column BE profile are listed in Table 3.7.1-206.

The deterministic LB profile with engineered granular backfill above the top of the Bass Islands Group bedrock was set equal to the 16th percentile of the distribution of randomized soil properties interpolated between the 10^{-4} and 10^{-5} exceedance level ground motions, and the deterministic UB profile with engineered granular backfill above the top of the Bass Islands Group bedrock was set equal to the 84th percentile of the distribution of randomized soil properties interpolated between the 10^{-4} and 10^{-5} exceedance level ground motions. The range in the UB and LB shear wave velocities was increased where necessary to maintain the minimum variation from the shear modulus for the deterministic BE profile (G_{BE}) required in SRP 3.7.2. The minimum variation is defined by a multiplicative factor of 1 plus the minimum coefficient of variation (COV) in shear modulus such that G_{UB} is greater than or equal to the G_{BE} x ($1+COV_{min}$) and G_{LB} is less than or equal to G_{BE} / ($1+COV_{min}$). SRP 3.7.2 specifies that the minimum COV for well studied sites is 0.5 and for sites less well investigated the minimum COV should be at least 1.0. The in-situ subsurface materials have been well investigated at the Fermi 3 site and a COV of 0.5 was used to establish the minimum variation in G between the LB, BE, and UB profiles in these materials. However, properties of the engineered granular backfill are estimates based on a range of possible characteristics. Therefore, a minimum COV of 1.0 was used in establishing the minimum variation in G between the LB, BE, and UB profiles in the engineered granular backfill. Table 3.7.1-207 and Table 3.7.1-208 list the resulting subsurface layers and the corresponding strain compatible dynamic engineering properties for the LB and UB deterministic profiles, respectively, with engineered granular backfill above the top of the Bass Islands Group bedrock.

To maximize the range of values, the minimum values from the LF and HF ground motions were used for the 16th percentile and the maximum of the LF and HF ground motions were used for the 84th percentile.

Figure 3.7.1-222 shows the full soil column LB, BE, and UB subsurface shear wave velocity profiles with engineered granular backfill above the top of the Bass Islands Group bedrock for the Fermi 3 site. The corresponding damping ratios were obtained from the statistics of the iterated profiles assuming negative correlation between shear wave velocity (V_S) and damping: that is, the 16th percentile damping for the full soil column UB profile and the 84th percentile damping for the full soil column LB profile. The compression wave velocities were based on the shear wave velocities in the LB, BE, and UB shear wave velocity profiles

Attachment 6
NRC3-13-0036

Action Item 3.7-22
(4 pages)

NRC Action Item 3.7-22

Show that comparisons between Fermi 3 SSI wall pressures and DCD wall dynamic pressures are acceptable. If not, show wall designs per governing load combination (including Fermi 3 SSI wall pressures) are acceptable.

Response

1. Sargent & Lundy Report SL-012018, "Evaluation of Reactor Building/Fuel Building and Control Building Dynamic Bearing Capacity, Foundation Stability, and Wall Seismic Soil Pressures Summary Report", Revision 1, December 10, 2013 (Attachment 18) has been revised to include material showing comparisons between Fermi 3 SSI wall pressures and DCD wall dynamic pressures are acceptable.

2. See Proposed FSAR Markup.

Proposed COLA Markup

See Proposed FSAR Markup to Section 3.8.4.5.6.

Attachment 6
NRC3-13-0036
(following 1 page)

Markup of Fermi 3 COLA

The following markup represents how DTE Electric intends to reflect this RAI response in the next submittal of the Fermi 3 COLA. However, the same COLA content may be impacted by responses to other COLA RAIs, other COLA changes, plant design changes, editorial or typographical corrections, etc. As a result, the final COLA content that appears in a future submittal may be different than presented here.

The COLA markups were made to Draft Revision 6 of the Fermi 3 FSAR. Draft Revision 6 of the FSAR incorporates the proposed FSAR changes submitted in DTE Electric correspondence since the submittal of Revision 5 in February 2013 until the NRC audit in November 2013. Thus, the markups represent proposed FSAR changes since the conclusion of the NRC audit.

3.7.4 Seismic Instrumentation

Add the following at the end of this section.

EF3 SUP 3.7-6

[START COM 3.7-001] The seismic monitoring program described in this subsection, including the necessary test and operating procedures, will be implemented prior to receipt of fuel on site. **[END COM 3.7-001]**

3.8 Seismic Category I Structures

This section of the Referenced DCD is incorporated by reference with the following departures and/or supplements.

3.8.4 Other Seismic Category I Structures

3.8.4.5 Structural Acceptance Criteria

Add the following subsections at the end of this section.

EF3 SUP 3.8-1

3.8.4.5.6 Exterior Wall Design

The Fermi 3 site-specific exterior wall designs for the RB/FB and CB are evaluated against lateral earth pressures based on the results from the Fermi 3 site-specific SSI and SSSI analyses for the RB/FB and CB presented in Subsection 3.7.2.4.1.

Figure 3.8.4-201a through Figure 3.8.4-201h show the lateral seismic soil pressures on the walls of the RB/FB from Fermi 3 SSI analyses, the Referenced DCD design soil pressures, and the Referenced DCD wall capacity passive pressures.

In some of the cases shown in Figures Figure 3.8.4-201a through Figure 3.8.4-201h, the lateral seismic soil pressures on the walls of the RB/FB from Fermi 3 SSI analyses exceed the Referenced DCD design soil pressures. For these cases, the induced out-of-plane bending moments and shear forces in the walls due to the seismic soil pressures from the Fermi 3 SSI analyses are bounded by either the corresponding induced out-of-plane bending moments and shear forces in the walls due to the Referenced DCD design soil pressures or the corresponding induced out-of-plane bending moments and shear forces in the walls due to the ~~Referenced DCD wall capacity passive pressures.~~

In the DCD design of the exterior walls, the DCD wall capacity passive pressures are combined with the at-rest soil pressures for wall design.

Figure 3.8.4-202a through Figure 3.8.4-202d and Figure 3.8.4-203a and Figure 3.8.4-203b show the lateral seismic soil pressures on the walls of

Attachment 7
NRC3-13-0036

Action Item 3.7-23
(16 pages)

NRC Action Item 3.7-23

Request that the PSD for the SSI Input time histories be recomputed using only the defined near constant power portion of the time histories.

Response

See Proposed COLA Markup,

Proposed COLA Markup

See Proposed FSAR Markup to Section 3.7.1.1.5 and Figures 3.7.1-251 to Figure 3.7.1-256.

Attachment 7
NRC3-13-0036
(following 13 pages)

Markup of Fermi 3 COLA

The following markup represents how DTE Electric intends to reflect this RAI response in the next submittal of the Fermi 3 COLA. However, the same COLA content may be impacted by responses to other COLA RAIs, other COLA changes, plant design changes, editorial or typographical corrections, etc. As a result, the final COLA content that appears in a future submittal may be different than presented here.

The COLA markups were made to Draft Revision 6 of the Fermi 3 FSAR. Draft Revision 6 of the FSAR incorporates the proposed FSAR changes submitted in DTE Electric correspondence since the submittal of Revision 5 in February 2013 until the NRC audit in November 2013. Thus, the markups represent proposed FSAR changes since the conclusion of the NRC audit.

presented in Table 3.7.1-219. Figure 3.7.1-245 to Figure 3.7.1-250 present the matched time histories (outcropping motions) compatible with the RB/FB and CB enhanced SCOR FIRS at the foundation levels. The duration and the value of PGV/PGA (Table 3.7.1-219) are generally consistent with the characteristic values reported in NUREG/CR-6728 (Reference 3.7.1-202); however, the values of $PGA*PGD/PGV^2$ are larger. The hard rock UHRS for the Fermi 3 site represents a combination of hazard from large, distant earthquakes and smaller, closer earthquakes. Thus, it is expected that the PGA is enriched to represent smaller magnitude, closer earthquakes. Spectral matching of the time histories to response spectra extended to a period of 10 seconds also enriches the PGD values, leading to an increase in the values of $PGA*PGD/PGV^2$.

Insert 3.7.1-1 →

~~As an additional demonstration of sufficient power in the spectrally matched time histories, the PSD were calculated for the frequency range of 0.3 to 50 Hz and compared to the target PSD based on the guidelines and procedures provided in Appendix B of SRP 3.7.1. The target PSD were developed by enveloping the magnitude distance bins for the CEUS rock sites given in of Appendix B of SRP 3.7.1 that correspond to the RE's in Table 2.5.2-212 for the 10^{-4} and 10^{-5} exceedance levels of ground motion. The target PSD for the RB/FB and CB were then determined by scaling the enveloping spectrum by the square of the PGA (spectral acceleration at 100 Hz) based on the enhanced SCOR FIRS in Table 3.7.1-214 and Table 3.7.1-215, respectively. The duration of near maximum and nearly stationary power used to calculate the PSD for the spectrally matched time histories was determined in accordance with SRP 3.7.1 and the additional guidance in NUREG/CR-5347 (Reference 3.7.1-221). Figure 3.7.1-251 presents the duration measurements for the horizontal components of the matched time histories compatible with the RB/FB enhanced SCOR FIRS. These measurements resulted in duration values of 30 and 31.5 seconds, which were slightly greater than the duration for the Arias Intensity to increase from 5 to 75 percent. Figure 3.7.1-252 and Figure 3.7.1-253 present the scaled target PSD based on Appendix B of SRP 3.7.1, 80 percent of the target PSD, and the PSD for the horizontal spectrally matched time histories for the RB/FB and CB, respectively. The PSD for the spectrally matched time histories envelop the corresponding target PSDs and, thus, satisfy the SRP 3.7.1 criterion of enveloping 80 percent of the target PSD to demonstrate there is no deficiency of power.~~

Insert 3.7.1-1

To demonstrate that there are no significant gaps in power for the spectrally-matched time histories, power spectral densities (PSD) were calculated for the frequency range of 0.3 to 50 Hz following the guidance in SRP 3.7.1, Appendix B. The equivalent stationary duration, T_D, used to calculate the PSD for the spectrally-matched time histories was established in general accordance with SRP 3.7.1 and the additional guidance in NUREG/CR-5347 (Reference 3.7.1-221). Figure 3.7.1-251 presents the normalized Arias intensities for the horizontal components, H1 and H2, of the spectrally matched time histories compatible with the RB/FB enhanced SCOR FIRS. The normalized Arias intensity plots for the spectrally matched time histories compatible with the CB enhanced SCOR FIRS are not presented since they are essentially identical to Figure 3.7.1-251.

The PSD was evaluated using the following two approaches for computing the Fourier amplitudes:

- Using the full duration of the spectrally matched time histories.
- Using only the portion of the spectrally matched time histories corresponding to the equivalent stationary duration.

Appendix B of NUREG/CR-5347 (Reference 3.7.1-221) indicates that T_D is estimated by identifying the portion of the time history where the slope (power) of a cumulative energy plot (represented by normalized Arias intensity) is nearly constant and near maximum. Figure 3.7.1-251 provides a range of estimates of constant power slopes for the two horizontal RB/FB components.

The Fermi 3 FIRS represent the combined effects of two distinct earthquakes, a nearby moderate magnitude earthquake and a distant large earthquake (New Madrid). The seed time history for spectral matching was selected to represent the long duration expected in a distant recording of a large magnitude earthquake. As illustrated by the spectrally matched acceleration and velocity time histories on Figures 3.7.1-245 and 3.7.1-246, the time histories exhibit non-stationarity that results in high frequency energy more prominent in the early portion of the records and low frequency energy more prominent in the latter portion of the records. Because of the long duration and non-stationarity of the recording, longer values of T_D are needed to better represent the energy content of the recordings. Therefore, the time for the Arias intensities to rise from 0 to 100 percent is used to establish T_D instead of the more commonly used time to rise from 5 to 75 percent Arias intensity. This time was established by extending the constant power slopes to 0 percent and 100 percent Arias intensity, as shown on Figure 3.7.1-251, and the time between the intersection with the 0 and 100 percent Arias intensity levels was used to establish a value of T_D.

Use of the full duration of the spectrally matched time history records to compute the Fourier amplitudes for the PSD captures the full frequency content of the records, which is consistent with the SSI analyses that also use the full duration time history records. Values of T_D of 30 seconds for the H1 component and 31.5 seconds for the H2 component were selected from the range of estimated values for the PSD calculation using the full duration of the spectrally

Insert 3.7.1-1 (Continued)

matched time histories. The resulting PSDs for the horizontal spectrally matched time histories are shown on Figure 3.7.1-252, Figure 3.7.1-253, Figure 3.7.1-254, and Figure 3.7.1-255 for the RB/FB H1 component, the RB/FB H2 component, the CB H1 component, and CB H2 component, respectively. As demonstrated in these figures, with the full duration considered, the spectrally matched time histories have no significant gaps in power over the frequency range of 0.3 to 50 Hz.

Appendix B of SRP 3.7.1 indicates the PSD is calculated using the portion of the spectrally matched time history corresponding to T_D. The effect of using only the T_D portion of the time histories to compute the PSD is illustrated on Figure 3.7.1-252 through Figure 3.7.1-255. On each figure, the different PSD are calculated using the portion of the spectrally matched time history windowed to the different T_D values shown on Figure 3.7.1-251. Outside of the T_D window, a two second duration cosine taper was applied to reduce the time history amplitude to zero.

For the RB/FB H1 component shown on Figure 3.7.1-252, the PSD for the windowed time histories are similar to the PSD computed using the full duration time history. There is a decrease in amplitude at frequencies above 30 Hz and below 1 Hz. The observed decreases reflect the fact that some of the energy content at these frequencies occurs outside of the selected T_D time window. For the shortest T_D of 30 seconds, a narrow dip in power occurs in the low frequency range near 0.4 Hz. However, the PSD for the windowed time histories are generally similar to the PSD using the full duration time history and show no significant gaps in power.

Figure 3.7.1-253 shows the results for the RB/FB H2 component. The PSD for the windowed time histories are also similar to the PSD computed using the full duration time history. There is a decrease in amplitude at frequencies above 25 Hz, and between about 0.7 and 1 Hz, again reflecting that some of the energy content at these frequencies occurs outside of the selected T_D time window. As was the case for the H1 component, the PSD for the windowed time histories are generally similar to the PSD using the full duration time history and show no significant gaps in power.

Figure 3.7.1-254 and Figure 3.7.1-255 show the corresponding comparisons for the CB H1 and CB H2 components, respectively. The results are similar to those shown for the corresponding RB/FB components.

In summary, the PSDs computed using the full duration, spectrally matched time histories show that there are no significant gaps in power over the frequency range of 0.3 to 50 Hz. PSDs computed using the windowed portion of the spectrally matched time histories corresponding to T_D also show no significant gaps in power. There is a narrow dip in power near 0.4 Hz using the window corresponding to a T_D of 30 seconds for the H1 component for both the RB/FB and CB. However, extending TD to 32, 34, or 36 seconds eliminates this narrow dip. The PSD computed using the windowed time histories show a decrease in power compared to PSD computed using the full duration time histories above 25 Hz. This difference indicates a degree of non-stationarity in the time histories, but does not produce significant gaps in the frequency range of 0.3 to 50 Hz.

In accordance with Interim Staff Guidance DC/COL-ISG-017 and the NEI developed white paper (Reference 3.7.1-201), the spectrally-matched time histories compatible with the RB/FB and CB enhanced SCOR FIRS were then input as outcropping motions at the foundation level into the LB, BE, and UB deterministic profiles without engineered granular backfill above the top of the Bass Islands Group bedrock to compute the resulting in-column motions at the RB/FB and CB foundation levels using the program SHAKE (Reference 3.7.1-222). A total of 18 SHAKE analyses were performed using combinations of the LB, BE, and UB deterministic profiles without engineered granular backfill above the top of the Bass Islands Group bedrock, the three time history components (two horizontal and one vertical components) and the two foundation levels (RB/FB and CB). The SHAKE analyses were performed using the LB, BE, and UB deterministic profiles in Table 3.7.1-209, Table 3.7.1-210, and Table 3.7.1-211 without iteration of soil properties to generate in-column motions at the foundation levels for input into the Fermi 3 site specific SSI analysis without engineered granular backfill above the top of the Bass Islands Group bedrock.

In-column motions at the foundation levels were also generated for the LB, BE, and UB deterministic profiles with engineered granular backfill above the top of the Bass Islands Group bedrock in Table 3.7.1-206, Table 3.7.1-207, and Table 3.7.1-208. The SHAKE analyses were performed using the spectrally-matched time histories compatible with the RB/FB and CB enhanced SCOR FIRS and without iteration of soil properties to generate 18 additional in-column motions at the foundation levels for the Fermi 3 site specific SSI analysis with engineered granular backfill above the top of the Bass Islands Group bedrock.

To evaluate the energy present at different frequencies in the 36 in-column acceleration time histories, power spectra were computed for each of the time histories. The cumulative power was then calculated from 0 to 100 Hz to determine what percentage of power is below 50 Hz in the in-column acceleration time histories. As an example, Figure ~~3.7.1-254~~ 3.7.1-256 presents the power spectrum and cumulative power plots for the horizontal (H1 and H2) in-column acceleration time history compatible with the BE deterministic profile without engineered granular backfill above the top of the Bass Islands Group bedrock. Table 3.7.1-220 presents the percentage of the cumulative power below 50 Hz for each in-column acceleration time history. The horizontal components include

Insert Figure 3.7.1-251 to Figure 3.7.1-255

~~**Figure 3.7.1-251 Slope of Near Constant Power used to Estimate Durations of 30 and 31.5 Seconds for Calculating the PSD for the Spectrally Matched Horizontal (H1 and H2) Components Compatible with the Fermi 3 RB/FB Enhanced SCOR FIRS**~~ **[EF3 SUP 3.7-1]**

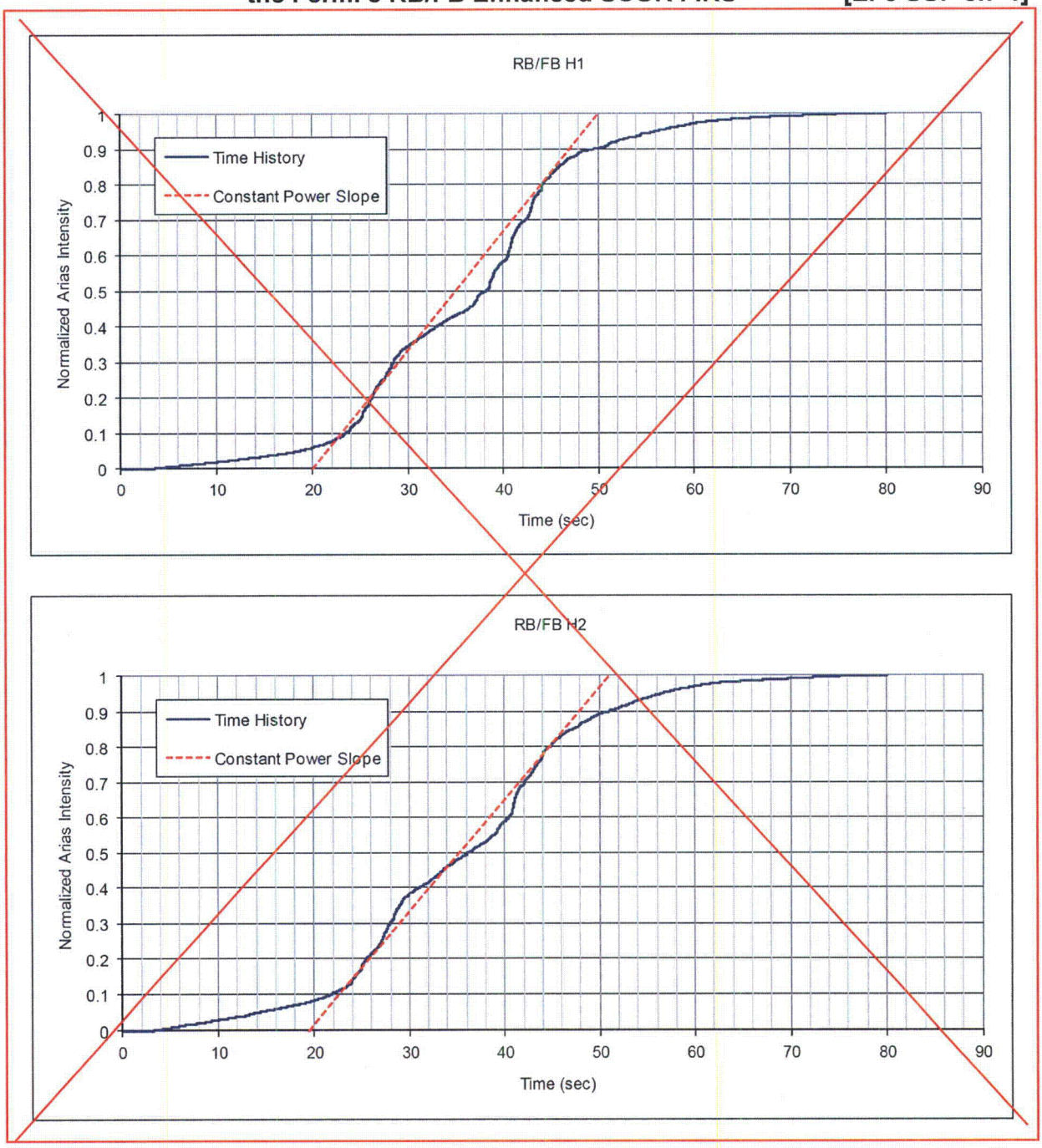

~~**Figure 3.7.1-252 PSD for Spectrally Matched Time History Components (H1 and H2) Compatible with the Fermi 3 RB/FB Enhanced SCOR FIRS and Target PSD Based on Appendix B of SRP 3.7.1**~~

[EF3 SUP 3.7-1]

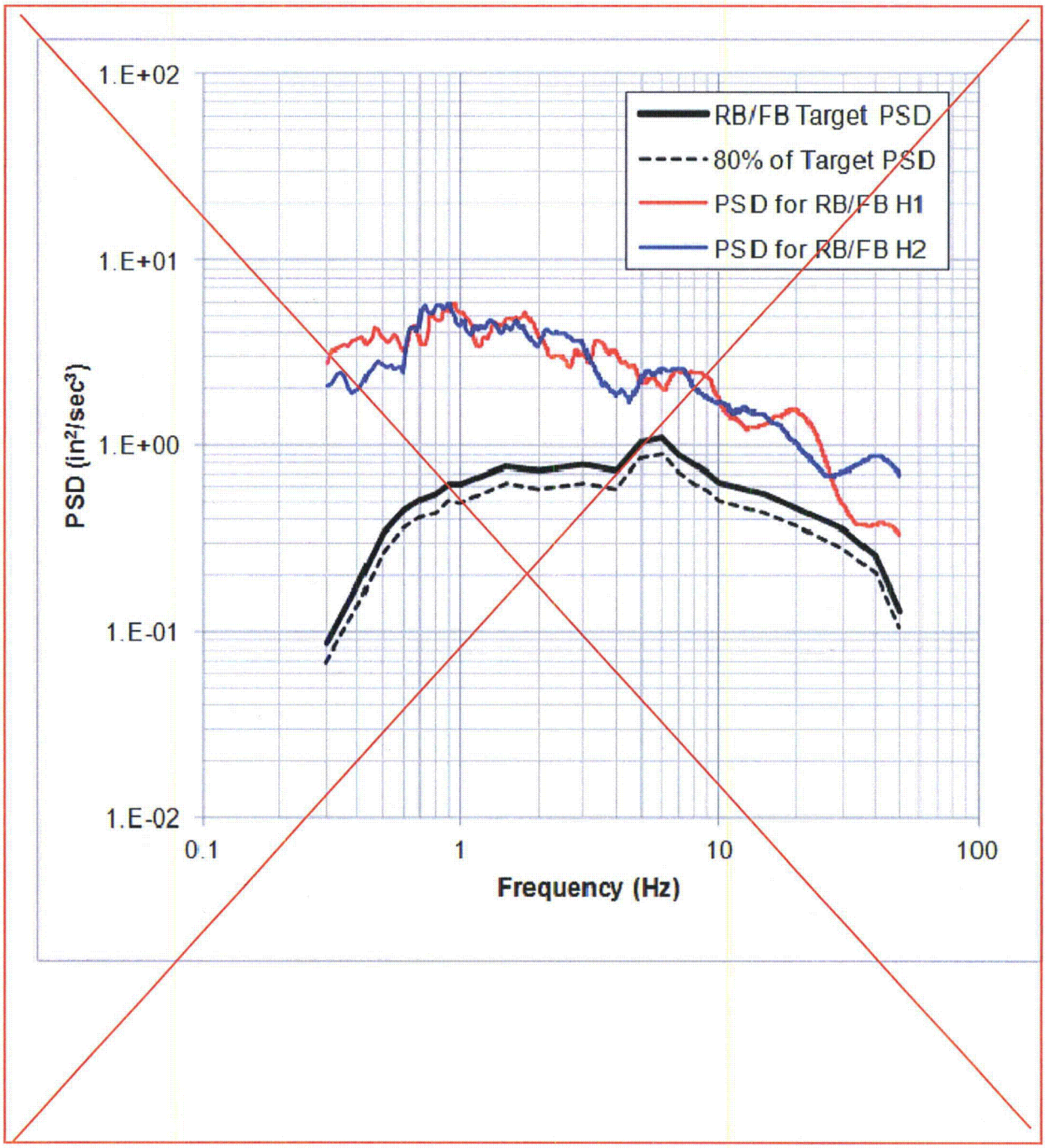

~~**Figure 3.7.1-253 PSD for Spectrally Matched Time History Components (H1 and H2) Compatible with the Fermi 3 CBEnhanced SCOR FIRS and Target PSD Based on Appendix B of SRP 3.7.1**~~

[EF3 SUP 3.7-1]

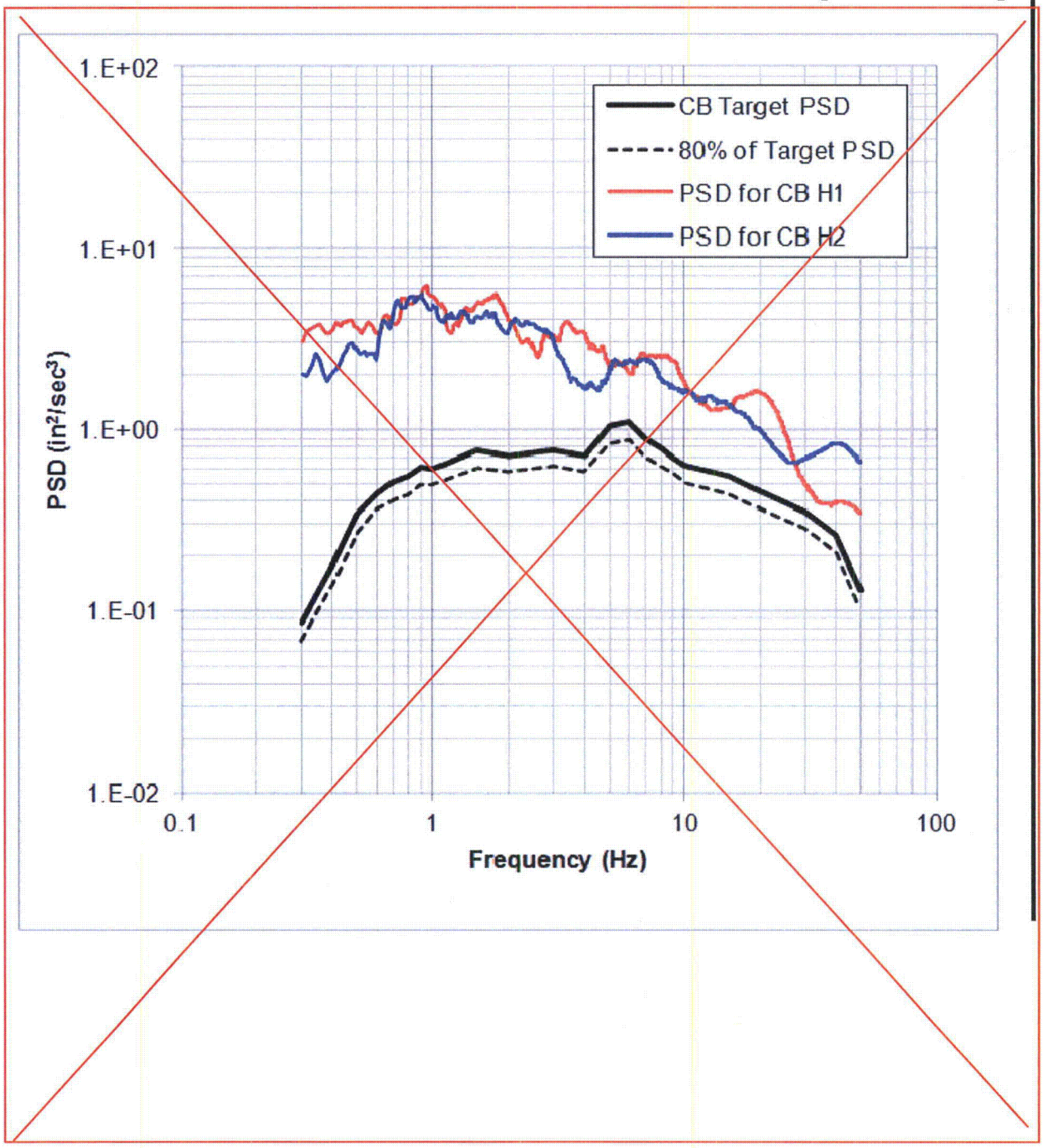

Insert Figure 3.7.1-251 to Figure 3.7.1-255

Figure 3.7.1-251 Normalized Arias Intensity and Estimates of Equivalent Stationary Duration for Calculating the PSD for the Spectrally Matched Horizontal (H1 and H2) Components Compatible with the Fermi 3 RB/FB Enhanced SCOR FIRS

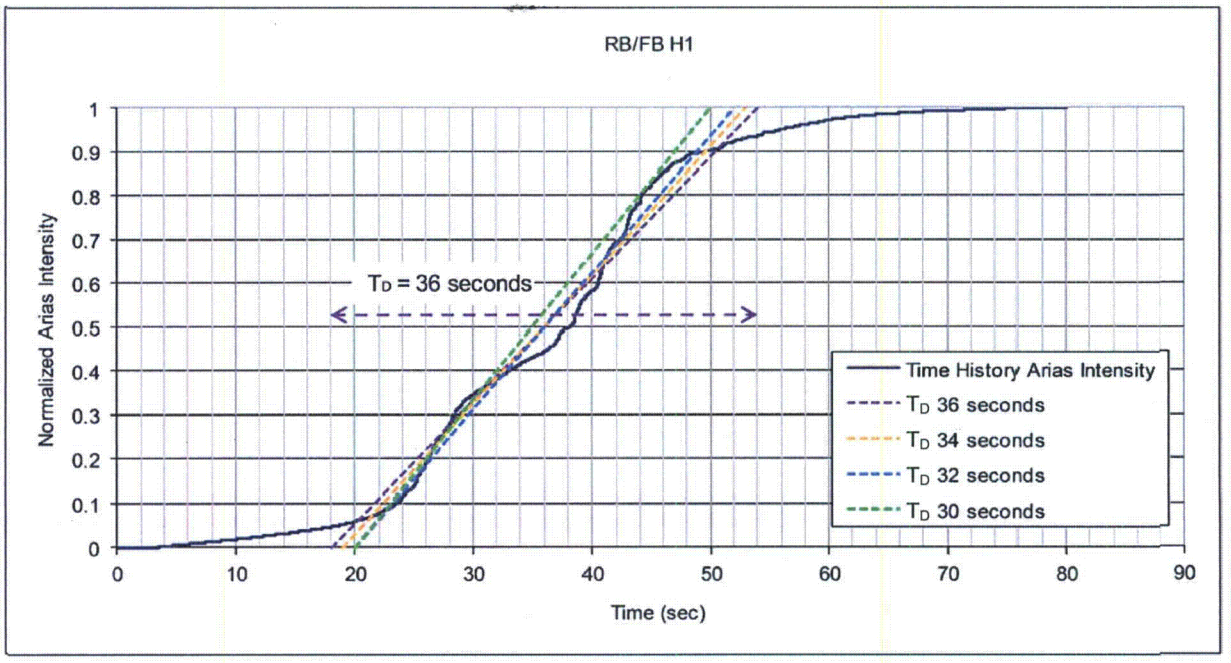

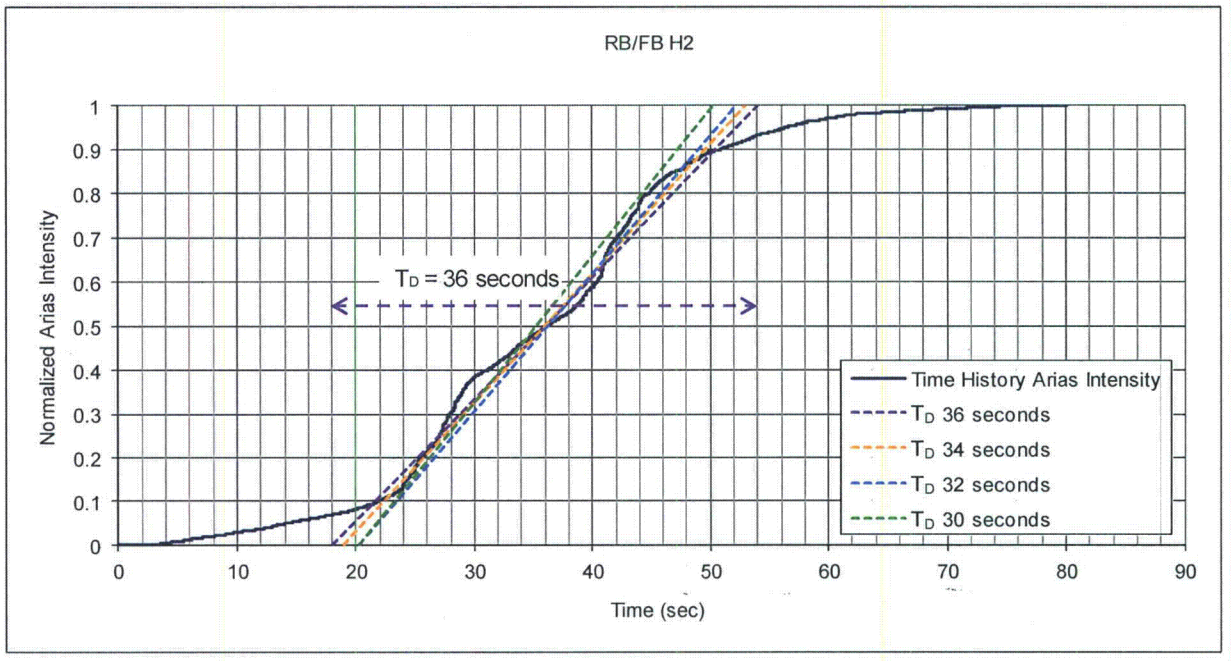

Insert Figure 3.7.1-251 to Figure 3.7.1-255
(Continued)

Figure 3.7.1-252 PSD Computed for the RB/FB H1 Component Spectrally Matched Time History (Enhanced SCOR FIRS) Using Full Duration Time Histories and Time Histories Windowed to an Equivalent Stationary Duration, T_D

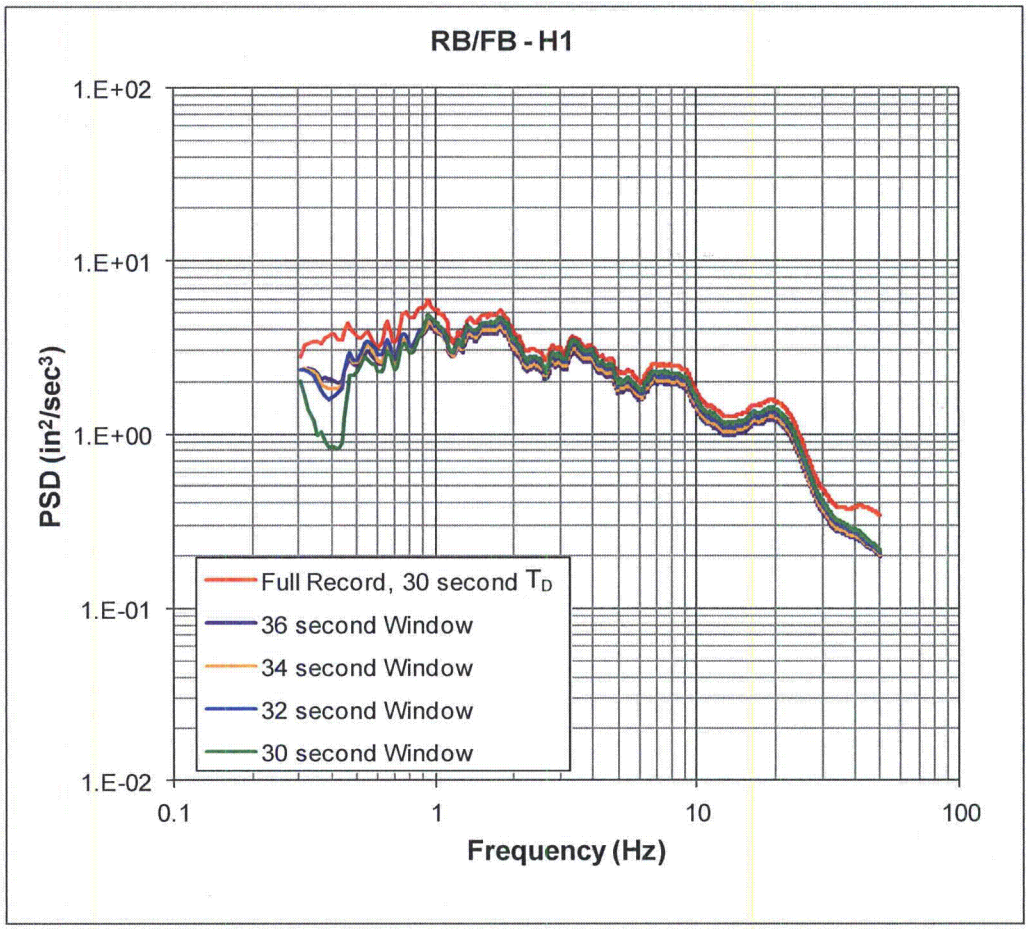

Insert Figure 3.7.1-251 to Figure 3.7.1-255
(Continued)

Figure 3.7.1-253 PSD Computed for the RB/FB H2 Component Spectrally Matched Time History (Enhanced SCOR FIRS) Using Full Duration Time Histories and Time Histories Windowed to an Equivalent Stationary Duration, T_D

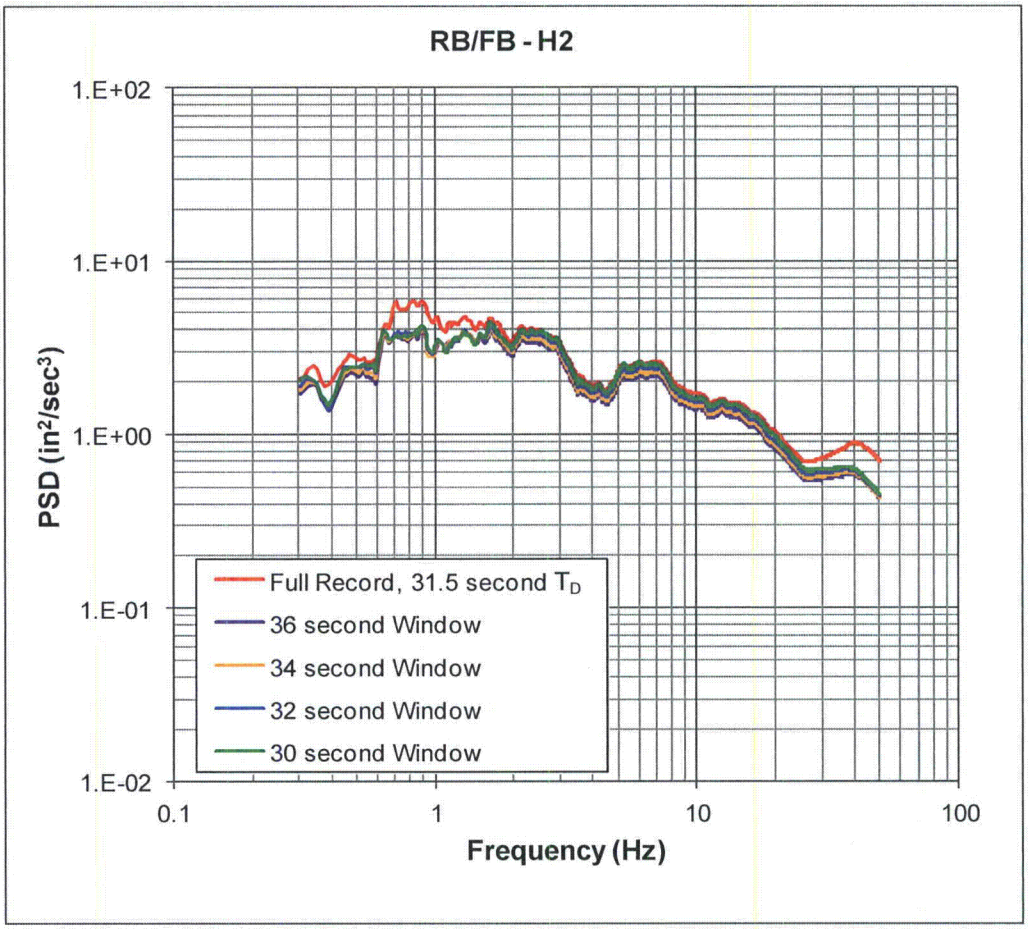

Insert Figure 3.7.1-251 to Figure 3.7.1-255
(Continued)

Figure 3.7.1-254 PSD Computed for the CB H1 Component Spectrally Matched Time History (Enhanced SCOR FIRS) Using Full Duration Time Histories and Time Histories Windowed to an Equivalent Stationary Duration, T_D

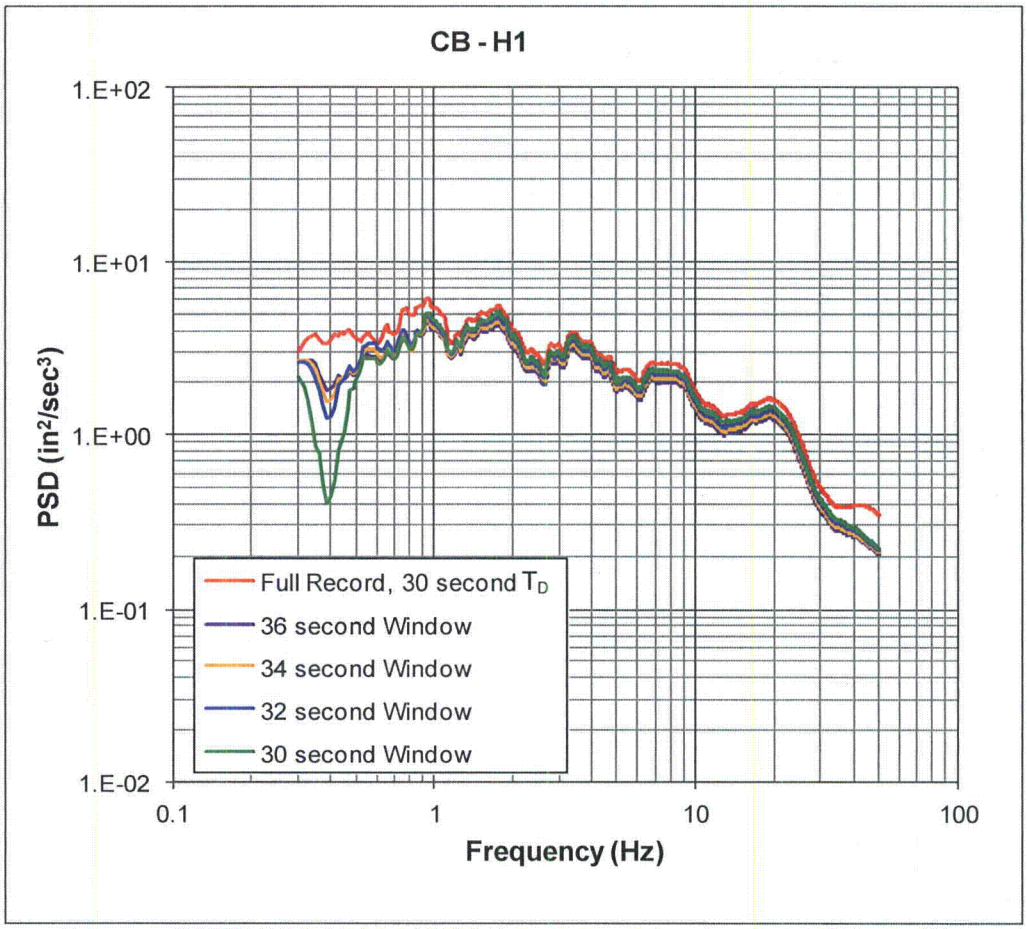

Insert Figure 3.7.1-251 to Figure 3.7.1-255
(Continued)

Figure 3.7.1-255 PSD Computed for the CB H2 Component Spectrally Matched Time History (Enhanced SCOR FIRS) Using Full Duration Time Histories and Time Histories Windowed to an Equivalent Stationary Duration, T_D

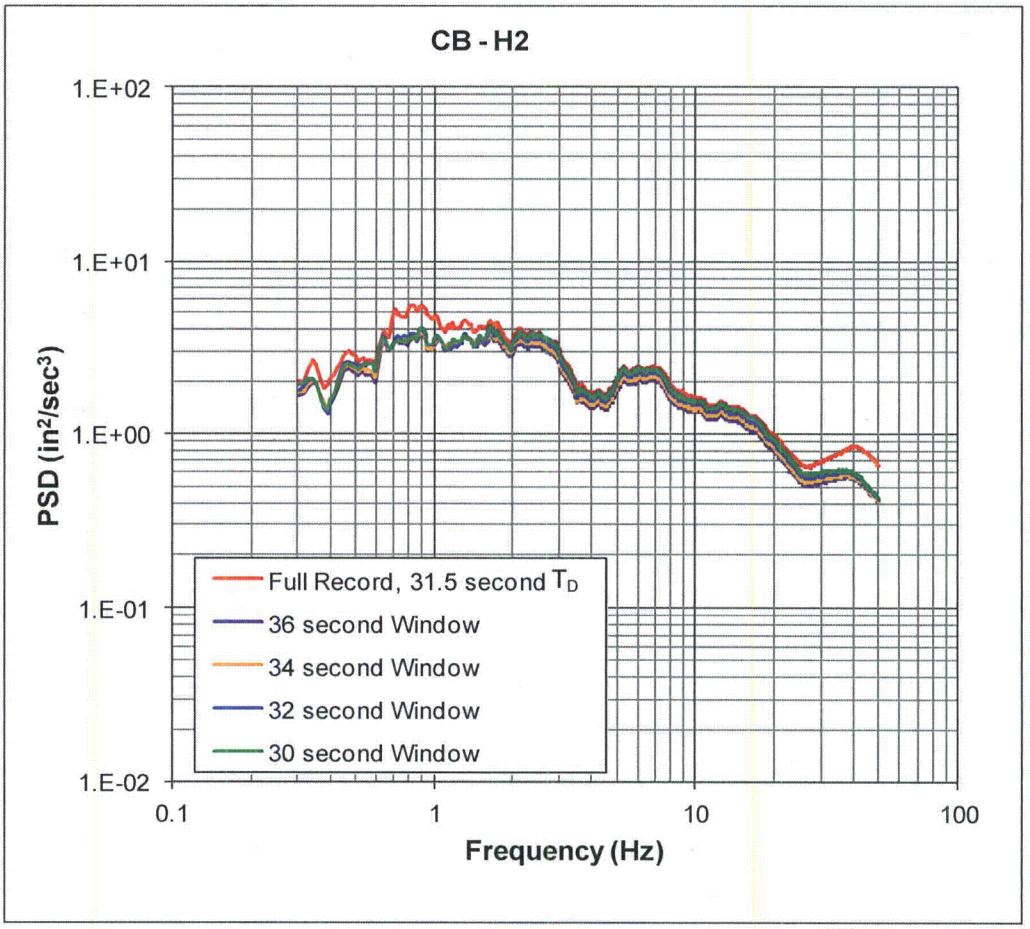

256

Figure 3.7.1-~~254~~ Power Spectra and Cumulative Power Plots for the Horizontal In-Column Acceleration Time Histories (H1 and H2) Compatible with the BE Deterministic Profile without Engineered Granular Backfill above the Top of the Bass Islands Group Bedrock [EF3 SUP 3.7-1]

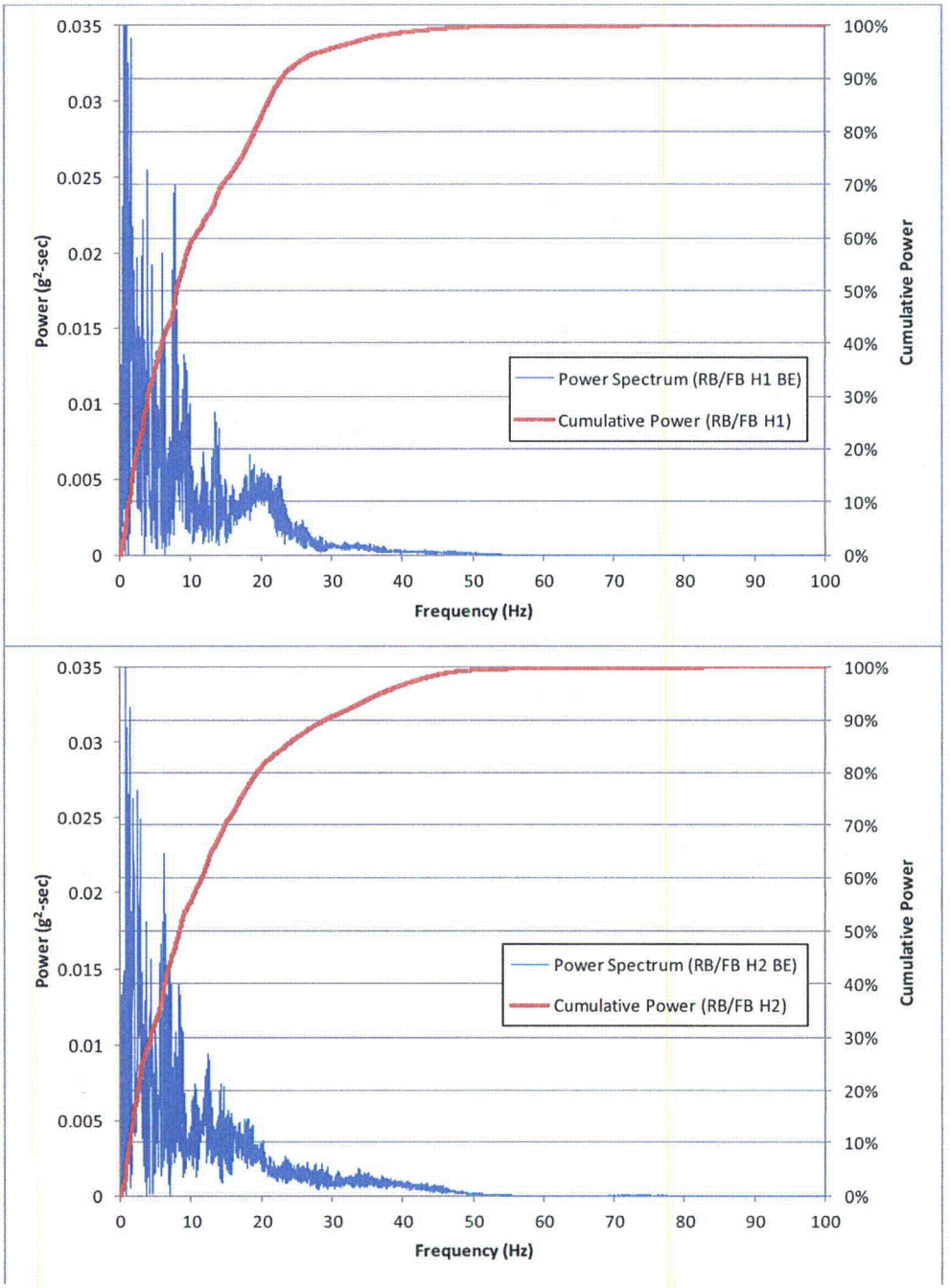

Attachment 8
NRC3-13-0036

Action Item 3.7-24
(4 pages)

NRC Action Item 3.7-24

RAI 03.07.02-9 discusses results for vertical oscillators. Provide a discussion for horizontal oscillators.

Response

The revised response to RAI 03.07.02-9 (Attachment 15) discusses both horizontal and vertical oscillators and provides discussion of how site specific results are bounded by the DCD results for the horizontal oscillators.

The discussion includes comparison of Fermi 3 floor response spectra and those from DCD.

For one conservative case a developed horizontal oscillator response based on floor input motion is compared to the DCD oscillator response.

Proposed COLA Markup

See Proposed FSAR Markup to Section 3.7.2.4.1.6.1.

Attachment 8
NRC3-13-0036
(following 1 page)

Markup of Fermi 3 COLA

The following markup represents how DTE Electric intends to reflect this RAI response in the next submittal of the Fermi 3 COLA. However, the same COLA content may be impacted by responses to other COLA RAIs, other COLA changes, plant design changes, editorial or typographical corrections, etc. As a result, the final COLA content that appears in a future submittal may be different than presented here.

The COLA markups were made to Draft Revision 6 of the Fermi 3 FSAR. Draft Revision 6 of the FSAR incorporates the proposed FSAR changes submitted in DTE Electric correspondence since the submittal of Revision 5 in February 2013 until the NRC audit in November 2013. Thus, the markups represent proposed FSAR changes since the conclusion of the NRC audit.

accelerations are compared with the Referenced DCD enveloping maximum vertical accelerations provided in Referenced DCD Table 3A.9-3e for the RB/FB Flexible Slab Oscillators. Table 3.7.2-205e also presents the percentage ratio of the Fermi 3 site-specific SSI enveloping maximum vertical accelerations to the Referenced DCD enveloping maximum vertical accelerations for the RB/FB Flexible Slab Oscillators. Table 3.7.2-205e shows that the Fermi 3 site-specific SSI enveloping maximum vertical accelerations for the RB/FB Flexible Slab Oscillators are lower than the Referenced DCD enveloping maximum vertical accelerations, with a maximum percentage ratio of approximately 75 percent. This indicates that the greatest Fermi 3 site-specific SSI enveloping maximum vertical acceleration is approximately 75 percent of the enveloping maximum vertical acceleration used in the ESBWR Standard Plant for the RB/FB Flexible Slab Oscillators.

A conservative assessment of the responses for RB/FB horizontal oscillators showed that the Fermi3 response spectra for these oscillators would be bounded by the DCD response spectra used for design.

For the CB ~~stick model~~, the Fermi 3 site-specific SSI enveloping maximum vertical accelerations are presented in Table 3.7.2-206. The Fermi 3 site-specific SSI enveloping maximum vertical accelerations for the CB stick model are presented in Table 3.7.2-206. The SSI enveloping maximum vertical accelerations are compared with the Referenced DCD enveloping maximum vertical accelerations provided in Referenced DCD Table 3A.9-3g for the CB stick model. Table 3.7.2-206 also presents the percentage ratio of the Fermi 3 site-specific SSI enveloping maximum vertical accelerations to the Referenced DCD enveloping maximum vertical accelerations for the CB stick model. Table 3.7.2-206 shows that the Fermi 3 site-specific SSI enveloping maximum vertical accelerations for the CB stick model are lower than the Referenced DCD enveloping maximum vertical accelerations, with a maximum percentage ratio of approximately 75 percent. This indicates that the greatest Fermi 3 site-specific SSI enveloping maximum vertical acceleration is approximately 75 percent of the enveloping maximum vertical acceleration used in the ESBWR Standard Plant for the CB.

3.7.2.4.1.6.2 Comparison of the Site-Specific SSI Floor Response Spectra

The site-specific floor response spectra for the BE, LB, and UB subsurface profiles are compared with the enveloping floor response spectra at 5 percent damping in Referenced DCD Subsection 3A.9.2.

For the RB/FB model, the floor response spectra at 5 percent damping obtained from Fermi 3 site-specific SSI analyses (herein called Fermi 3

Attachment 9
NRC3-13-0036

Action Item 3.7-25
(9 pages)

NRC Action Item 3.7-25

Confirm that the toes pressure used for the DCD concrete foundation design envelops the toe pressures from the site specific stability evaluation.

Response

The revised response to RAI 03.07.02-9 (Attachment 15) has been updated to state that the site specific toe pressures are bounded by the DCD toe pressures.

Sargent & Lundy Report SL-012018, "Evaluation of Reactor Building/Fuel Building and Control Building Dynamic Bearing Capacity, Foundation Stability, and Wall Seismic Soil Pressures Summary Report", Revision 1, December 10, 2013 (Attachment 18) has been revised to provide the basis for these values and conclusions.

See Proposed COLA Markup.

Proposed COLA Markup

See Proposed FSAR Markup to Section 3.7.2.4.1.7, Section 3.8.5.5.2, and Table 3.8.5-203.

Attachment 9
NRC3-13-0036
(following 6 pages)

Markup of Fermi 3 COLA

The following markup represents how DTE Electric intends to reflect this RAI response in the next submittal of the Fermi 3 COLA. However, the same COLA content may be impacted by responses to other COLA RAIs, other COLA changes, plant design changes, editorial or typographical corrections, etc. As a result, the final COLA content that appears in a future submittal may be different than presented here.

The COLA markups were made to Draft Revision 6 of the Fermi 3 FSAR. Draft Revision 6 of the FSAR incorporates the proposed FSAR changes submitted in DTE Electric correspondence since the submittal of Revision 5 in February 2013 until the NRC audit in November 2013. Thus, the markups represent proposed FSAR changes since the conclusion of the NRC audit.

site-specific SSI floor response spectra at 5 percent damping) are shown on Figure 3.7.2-207a through Figure 3.7.2-207f for the X-direction, on Figure 3.7.2-208a through Figure 3.7.2-208f for the Y-direction, and on Figure 3.7.2-209a through Figure 3.7.2-209f for the vertical direction. The Fermi 3 site-specific SSI floor response spectra at 5 percent damping are compared with the Referenced DCD Subsection 3A.9.2 enveloping floor response spectra at 5 percent damping on Figure 3.7.2-207a through Figure 3.7.2-209f (solid black lines). The Fermi 3 site-specific SSI floor response spectra at 5 percent damping at the locations presented in the Referenced DCD, Subsection 3A.9.2 for the RB/FB model are considerably lower than the DCD enveloping floor response spectra at 5 percent damping, indicating that the ESBWR Standard Plant for the RB/FB is acceptable at the Fermi 3 site.

For the CB model, Fermi 3 site-specific SSI floor response spectra at 5 percent damping are shown on Figure 3.7.2-210a and Figure 3.7.2-210b for the X-direction, on Figure 3.7.2-211a and Figure 3.7.2-211b for the Y-direction, and on Figure 3.7.2-212a and Figure 3.7.2-212b for the vertical direction. The Fermi 3 site-specific SSI floor response spectra at 5 percent damping are compared with the Referenced DCD Subsection 3A.9.2 enveloping floor response spectra at 5 percent damping as shown on Figure 3.7.2-210a through Figure 3.7.2-212b (solid black lines). The Fermi 3 site-specific SSI floor response spectra at 5 percent damping at the locations presented in the Referenced DCD, Subsection 3A.9.2 in the CB model are considerably lower than the DCD enveloping floor response spectra at 5 percent damping, indicating that the ESBWR Standard Plant design for the CB is acceptable at the Fermi 3 site.

3.7.2.4.1.7 Conclusions

The Fermi 3 site-specific SSI analyses for the RB/FB and CB consider partial embedment into the Bass Islands Group bedrock. Cases both with and without taking credit for the lateral support of the backfill located above the top of Bass Islands Group bedrock (Elevation 168.2 m [552 ft] NAVD 88, Table 2.5.4-201) have been analyzed. These results show the following:

- That seismic forces, floor response spectra, and accelerations are significantly less than for the Referenced DCD design values for the ESBWR Standard Plant based on the CSDRS.

- That the factors of safety for sliding and overturning are significantly greater than the required factor of safety of 1.1 in SRP 3.8.5.
- That the dynamic bearing demands are much smaller than the allowable dynamic bearing capacity on the Bass Islands Group dolomite presented in Table 2.5.4-227.

The results from the Fermi 3 site-specific SSI analyses show that the seismic forces in members, floor response spectra, and acceleration are bounded by values presented in the Referenced DCD for both the RB/FB and CB. In addition, Subsection 3.8.5 demonstrates that the actual factors of safety for overturning and sliding are greater than the required factors of safety.

~~The Fermi 3 site-specific SSI soil dynamic bearing demands for the RB/FB and CB are greater than the Referenced DCD maximum dynamic bearing demands for the material properties consistent with the BE, LB, and UB subsurface profiles (Subsection 3.8.5). However, the Fermi 3 site-specific SSI dynamic bearing demands for the RB/FB and CB are less than the allowable dynamic bearing capacity in Subsection 2.5.4.10, Table 2.5.4-227.~~

The Fermi 3 site-specific SSI maximum soil dynamic bearing demands for the RB/FB and CB are less than the Referenced DCD maximum dynamic bearing demands (Subsection 3.8.5).Thus, the DCD foundation design is not impacted and is adequate.

The Fermi 3 site-specific lateral seismic soil pressures from SSI and SSSI analyses for the RB/FB and the CB are shown on Figure 3.8.4-201a through Figure 3.8.4-201h, Figure 3.8.4-202a through Figure 3.8.4-202d, and Figure 3.8.4-203a and Figure 3.8.4-203b. The lateral seismic soil pressures on embedded portions of the exterior walls exceed the lateral seismic soil pressures reported in the DCD at some locations. The wall pressures are within the capacity of ESBWR DCD wall designs (Presented in Subsection 3.8.4).

Based on the Fermi 3 site-specific SSI analyses, the following conclusions apply to the Fermi 3 site:

- The Referenced DCD standard plant design (ESBWR Standard Plant) is applicable to the RB/FB and CB Seismic Category I structures at the Fermi 3 site with partial embedment into bedrock, considering cases that include and neglect the contribution of the surrounding backfill.
- The DCD backfill requirements for the backfill above the top of the Bass Islands Group bedrock (Elevation 168.2 m [552 ft] NAVD 88) that surrounds the embedded walls of the Fermi 3 Seismic Category I structures are shown to be unnecessary. Therefore, the backfill above

The resulting factor of safety against sliding is greater than 15, which is greater than the minimum factor of safety of 1.1 as required by SRP 3.8.5. During detailed design, the amount of shear-friction reinforcement in the fill concrete is selected to provide a minimum factor of safety of 1.1 against sliding for the FWSC, which provides a minimum 10 percent design margin for the shear-friction reinforcement.

The calculated Fermi 3 site-specific factors of safety against floatation for the RB/FB and CB are shown in Table 3.8.5-201 and Table 3.8.5-202, respectively. It is shown that the Fermi 3 site-specific factors of safety against floatation for the RB/FB and CB are 3.50 and 1.86 (greater than minimum factor of safety of 1.1 as required by SRP 3.8.5), respectively. These factors of safety indicate that the Fermi 3 RB/FB and CB are stable against floatation.

3.8.5.5.2 Soil Bearing Pressures

The maximum soil dynamic bearing pressure demand at the Fermi 3 site for the BE, UB, and LB subsurface profiles, based on the results from the Fermi 3 site-specific SSI analyses for the RB/FB and CB presented in Subsection 3.7.2.4.1, are evaluated using the Modified Energy Balance Method according to the Referenced DCD Section 3G.1.5.5.

The Fermi 3 site-specific SSI maximum soil bearing pressure (maximum toe pressure) demands are all less than the Referenced DCD maximum dynamic bearing demands for both the RB/FB and the CB in Referenced DCD, Tables 3G.1-58 and 3G.2-27, respectively.

The Fermi 3 site-specific SSI maximum dynamic soil bearing pressure demands are summarized in Table 3.8.5-203 for the RB/FB and CB. ~~As described in Section 3.7.2.4.1.6, the Fermi 3 site specific enveloping SSI seismic loads are lower than the Referenced DCD enveloping seismic loads. However, the Fermi 3 site specific SSI maximum soil bearing pressure demands for the BE, LB, and UB subsurface profile cases are all larger than the Referenced DCD maximum dynamic bearing demands for both the RB/FB and the CB in Referenced DCD, Table 2.0-1 for the hard soil site (Table 3.8.5-203). This is because the Referenced DCD SSI analyses were performed considering full embedment up to the finished ground level grade, while the Fermi 3 site specific SSI analyses were performed considering partial embedment condition without taking credit for the backfill above the top of the Bass Islands Group bedrock at Elevation 168.2 m (552.0 ft) NAVD 88. Therefore, the Fermi 3 site specific structure overturning moments resulting from the Fermi 3 site specific SSI analyses become larger than the structure overturning moments resulting from the Referenced DCD SSI analyses. As a result, the Fermi 3 site-specific dynamic soil bearing pressure demands~~

~~calculated based on the Fermi 3 site specific SSI analyses are larger compared to the Referenced DCD hard soil site dynamic soil bearing pressure demands.~~

The Fermi 3 site-specific SSI maximum dynamic soil bearing pressure demands presented in Table 3.8.5-203 for the RB/FB and the CB are compared with the Fermi 3 site-specific allowable bearing capacity under the dynamic condition in Table 2.5.4-227 in Subsection 2.5.4.10. It is confirmed that the Fermi 3 site-specific maximum dynamic soil bearing pressure demands for the RB/FB and CB are less than the allowable bearing capacity under dynamic condition presented in Table 2.5.4-227 in Subsection 2.5.4.10.

Table 3.8.5-203 Maximum Soil Dynamic Bearing Pressure Demand for RB/FB and CB [EF3 SUP 3.8-1]

	Dynamic Bearing Pressure Demand			
	RB/FB		CB	
Subsurface Condition	Fermi 3 Site-Specific SSI (Static + FIRS (1))	Referenced DCD (Static + SSE (2))	Fermi 3 Site-Specific SSI (Static + FIRS (1))	Referenced DCD (Static + SSE (2))
Fermi 3 Lower Bound Subsurface Profile	1913 KPa (39954 lbf/ft^2)	NA	791 KPa (16520 lbf/ft^2)	NA
Fermi 3 Best Estimate Subsurface Profile	1970 KPa (41144 lbf/ft^2)	NA	823 KPa (17189 lbf/ft^2)	NA
Fermi 3 Upper Bound Subsurface Profile	2053 KPa (42878 lbf/ft^2)	NA	853 KPa (17815 lbf/ft^2)	NA
Referenced DCD, Hard Soil Site	NA	1,100 KPa (23,000 lbf/ft^2)	NA	420 KPa (8,800 lbf/ft^2)

Notes:
(1) FIRS is the Enhanced SCOR FIRS developed in Subsection 3.7.1
(2) SSE is the Referenced DCD CSDRS

KPa = kilopascal
NA = Not applicable

Insert Table 3.8.5-203

Table 3.8.5-203 Maximum Soil Dynamic Bearing Pressure Demand for RB/FB and CB [EF3 SUP 3.8-1]

	Dynamic Bearing Pressure Demand	
	RB/FB	CB
Subsurface Condition	**Fermi 3 Site-Specific SSI (Static + FIRS [1])**	**Fermi 3 Site-Specific SSI (Static + FIRS [1])**
Fermi 3 Lower Bound Subsurface Profile	1,913 KPa (39,954 lbf/ft^2)	791 KPa (16,520 lbf/ft^2)
Fermi 3 Best Estimate Subsurface Profile	1,970 KPa (41,144 lbf/ft^2)	823 KPa (17,189 lbf/ft^2)
Fermi 3 Upper Bound Subsurface Profile	2,053 KPa (42,878 lbf/ft^2)	853 KPa (17,815 lbf/ft^2)

Notes:

(1) FIRS is the SSI FIRS developed in Subsection 3.7.1

KPa = kilopascal

Attachment 10
NRC3-13-0036

Action Item 3.7-28
(5 pages)

NRC Action Item 3.7-28

Confirm that the sliding forces from the Control Building are transferred to the rock and describe the transfer mechanism.

Response

The revised responses to RAI 03.07.02-9 (Attachment 15) and RAI 03.08.05-3 (Attachment 16) have been revised to reflect (1) that lateral loads on the concrete fill from the sliding evaluation are transferred through the concrete to the rock below by friction, (2) the rock around the CB is capable of resisting the bearing pressure, and (3) the reference to rock anchors has been removed.

Sargent & Lundy Report SL-012018, "Evaluation of Reactor Building/Fuel Building and Control Building Dynamic Bearing Capacity, Foundation Stability, and Wall Seismic Soil Pressures Summary Report", Revision 1, December 10, 2013 (Attachment 18) has been revised to provide the basis for these values and conclusions.

The revision to S&L Report SL012018 includes a clarification to the definition of F_r.

See Proposed COLA Markup.

Proposed COLA Markup

See Proposed FSAR Markup to Subsection 3.8.5.5.1.

Attachment 10
NRC3-13-0036
(following 2 pages)

Markup of Fermi 3 COLA

The following markup represents how DTE Electric intends to reflect this RAI response in the next submittal of the Fermi 3 COLA. However, the same COLA content may be impacted by responses to other COLA RAIs, other COLA changes, plant design changes, editorial or typographical corrections, etc. As a result, the final COLA content that appears in a future submittal may be different than presented here.

The COLA markups were made to Draft Revision 6 of the Fermi 3 FSAR. Draft Revision 6 of the FSAR incorporates the proposed FSAR changes submitted in DTE Electric correspondence since the submittal of Revision 5 in February 2013 until the NRC audit in November 2013. Thus, the markups represent proposed FSAR changes since the conclusion of the NRC audit.

Islands Group bedrock at Elevation 168.2 m (552.0 ft) NAVD 88. The gap between the RB/FB and CB up to the top of the Bass Islands Group bedrock at Elevation 168.2 m (552.0 ft) NAVD 88 is also filled with fill concrete. As the Fermi 3 site-specific SSI neglects the backfill above the top of the bedrock, forces associated with the backfill are not included in the sliding analysis; therefore, the bedrock alone supplies the resistance to sliding of both the RB/FB and the CB. In the sliding evaluation for the Fermi 3 RB/FB and CB, the following skin friction resistance forces are neglected:

1. F_{us} = Skin friction resistance force provided by basemat side parallel to the direction of motion (i.e., $F_{us} = 0$)
2. F_{us}' = Skin friction resistance force provided by shear key side parallel to the direction of motion (when shear keys are used (i.e., $F_{us}' = 0$).

The calculated Fermi 3 site-specific factors of safety against sliding for the RB/FB and CB are shown in Table 3.8.5-201 and Table 3.8.5-202, respectively. The Fermi 3 site-specific factors of safety against sliding for the RB/FB and CB are ~~1.22 and 1.10 (equal to or greater than minimum factor of safety of 1.1 as required by SRP 3.8.5), respectively.~~ These factors of safety indicate that the Fermi 3 RB/FB and CB are stable against sliding.

Insert 3.8.5.5.1

The sliding of the FWSC was evaluated using the driving forces (the base shear time history forces) based on the governing factor of safety cases from the Referenced DCD SSI analysis results without crediting the backfill surrounding the basemat. The sliding evaluation also includes the fill concrete below the FWSC in which the shear keys are embedded. The presence of the shear keys results in potential failure occurring within the fill concrete. The fill concrete was evaluated in accordance with ACI 318 and the corresponding portions of ACI 349 considering the following:

- Failure of the fill concrete in compression from lateral pressure applied by the shear keys. This potential failure condition is checked using the ACI 318 Section 22.5.5.
- Failure through the fill concrete at or below the base of the shear keys considering the maximum amount of shear resistance from shear-friction reinforcement allowed in ACI 318, Section 11.6 and the corresponding portions of ACI 349, Section 11.7.

Insert 3.8.5.5.1

With the exception of the CB with no engineered backfill above the top of the Bass Islands Group bedrock, the sliding stability safety factors are based on available friction at the bottom of the foundation. For CB with no engineered backfill, in addition to the base friction, lateral bearing resistance along the CB foundation sides by the in-situ rock or concrete fill between the CB and RB/FB is required to meet the minimum required sliding safety factor of 1.10. The concrete fill between the CB and the RB/FB is capable of providing the required lateral bearing resistance through the friction between the bottom of the concrete fill and the top of the in-situ rock below. The in-situ Bass Islands Group bedrock is also found capable of providing the required lateral bearing resistance.

Attachment 11
NRC3-13-0036

Action Item 3.7-29
(2 pages)

NRC Action Item 3.7-29

Review the conclusions in the summary reports to assure that the margins between site specific accelerations and maximum moments and the respective DCD values are correctly stated.

Response

Sargent & Lundy Report SL-011956, "SSI Analyses of Reactor Building/Fuel Building and Control Building with Engineered Backfill Summary Report", Revision 1, December 10, 2013 (Attachment 17) has been revised to correct typographical errors in the text. The values in the calculation and the tables in the Report are correct. There are no changes to the conclusions of the Report.

The response to RAI 03.07.02-9 (Attachment 15) has been revised to refer to the current revision of Report SL-011956.

Proposed COLA Markup

None.

Attachment 12
NRC3-13-0036

Action Item 3.7-30
(5 pages)

NRC Action Item 3.7-30

Update FSAR Subsection 3A.5 to reflect use of SASSI2010 and method of analysis.

Response

See Proposed COLA Markup.

Proposed COLA Markup

See Proposed FSAR Markup to Appendix 3A.5.3.

Attachment 12
NRC3-13-0036
(following 2 pages)

Markup of Fermi 3 COLA

The following markup represents how DTE Electric intends to reflect this RAI response in the next submittal of the Fermi 3 COLA. However, the same COLA content may be impacted by responses to other COLA RAIs, other COLA changes, plant design changes, editorial or typographical corrections, etc. As a result, the final COLA content that appears in a future submittal may be different than presented here.

The COLA markups were made to Draft Revision 6 of the Fermi 3 FSAR. Draft Revision 6 of the FSAR incorporates the proposed FSAR changes submitted in DTE Electric correspondence since the submittal of Revision 5 in February 2013 until the NRC audit in November 2013. Thus, the markups represent proposed FSAR changes since the conclusion of the NRC audit.

Appendix 3A Seismic Soil-Structure Interaction Analysis

This section of the referenced DCD is incorporated by reference with the following departures and/or supplements.

3A.1 Introduction

Replace the last sentence in the second paragraph with the following.

EF3 CDI

Site-specific geotechnical data is described in Chapter 2. This data is compatible with the site enveloping parameters considered in the standard design.

3A.2 ESBWR Standard Plant Site Plan

Replace the first two sentences of the first paragraph with the following.

EF3 CDI

The site plan is shown in Figure 2.1-204. The plan orientation is denoted on the figure.

3A.5 SOIL-STRUCTURE INTERACTION ANALYSIS METHOD

Insert 3A.5.3 →

~~3A.5.2 SASSI2000 Analysis Method~~

~~Replace the second sentence of the first paragraph with the following.~~

~~EF3 CDI~~

~~The program uses finite elements with complex moduli for modeling the structure and foundation properties and is based on the direct method and the frequency domain complex response method.~~

Appendix 3B Containment Hydrodynamic Load Definitions

This section of the referenced DCD is incorporated by reference with no departures or supplements.

Appendix 3C Computer Programs Used in the Design and Analysis of Seismic Category I Structures

This section of the referenced DCD is incorporated by reference with no departures or supplements.

Insert 3A.5.3

Add the following at the end of this section.

EF3 SUP 3A.5-1 3A.5.3 SASSI2010 Analysis Method

SASSI2010 computer program is used for all site-specific SSI and SSSI analyses using the direct method or modified subtraction method of analysis as detailed in Subsection 3.7.2.4.1.3.

Attachment 13
NRC3-13-0036

Action Item 3.7-31
(5 pages)

NRC Action Item 3.7-31

Clarify FSAR to indicate that the stick model used in SSI and SSSI analysis cases (Base Model) corresponds to uncracked properties.

Response

See Proposed COLA Markup.

Proposed COLA Markup

See Proposed FSAR Markup to Section 3.7.2.4.1

Attachment 13
NRC3-13-0036
(following 2 pages)

Markup of Fermi 3 COLA

The following markup represents how DTE Electric intends to reflect this RAI response in the next submittal of the Fermi 3 COLA. However, the same COLA content may be impacted by responses to other COLA RAIs, other COLA changes, plant design changes, editorial or typographical corrections, etc. As a result, the final COLA content that appears in a future submittal may be different than presented here.

The COLA markups were made to Draft Revision 6 of the Fermi 3 FSAR. Draft Revision 6 of the FSAR incorporates the proposed FSAR changes submitted in DTE Electric correspondence since the submittal of Revision 5 in February 2013 until the NRC audit in November 2013. Thus, the markups represent proposed FSAR changes since the conclusion of the NRC audit.

3.7.2 **Seismic System Analysis**

3.7.2.4 **Soil-Structure Interaction**

Add the following at the end of the first paragraph.

EF3 SUP 3.7-4

This subsection of the Referenced DCD, including associated Appendix 3A in its entirety, is incorporated by reference with the following supplement for the Fermi 3 site-specific soil-structure interaction (SSI) analyses for the RB/FB and CB. The site-specific SSI analyses for the RB/FB and CB were performed using the direct method of the SASSI2010 computer program. The SSI analysis approach and the structural models are the same as presented in Appendix 3A of the Referenced DCD.

The FWSC is essentially a surface founded structure in the Referenced DCD, Subsection 3.7.1.1 and there are no embedded walls for the FWSC. Therefore, the Referenced DCD backfill requirements surrounding Seismic Category I structures are not applicable to FWSC embedded basemat (embedded 2.35 m (7.7 feet)). The FWSC is founded on fill concrete which meets the Referenced DCD requirements for backfill underneath Seismic Category I structures. Therefore, there is no site-specific SSI analysis performed for the FWSC.

Add the following subsections following Subsection 3.7.2.4.

3.7.2.4.1 **Fermi 3 Site-Specific Soil-Structure Interaction Analysis**

This subsection presents the Fermi 3 site-specific SSI analyses performed in accordance with SRP 3.7.2 for the Seismic Category I RB/FB and CB. The Fermi 3 site-specific FIRS developed in Subsection 3.7.1 is in accordance with Regulatory Guide 1.208 and NRC Interim Staff Guidance (DC/COL-ISG-017) for ensuring hazard-consistent seismic input for site response and soil-structure interaction analyses. The Fermi 3 site-specific FIRS developed in and Subsection 3.7.1 are fully enveloped, in all cases, by the ESBWR CSDRS. Therefore, the Fermi 3 site-specific SSI analyses were not performed to address an exceedance of the CSDRS by the FIRS; rather, the Fermi 3 site-specific SSI analyses were performed to address the following Fermi 3 site-specific conditions:

- Partial embedment in the Bass Islands Group bedrock of the RB/FB and CB Seismic Catagory I structures, as shown on Figure 2.5.4-202

and Figure 2.5.4-203, to confirm that the Referenced DCD design is applicable for this case.

- To demonstrate that the Referenced DCD requirements for the backfill surrounding Seismic Catagory I structures can be neglected for RB/FB and CB with the RB/FB and CB partially embedded in the bedrock at the Fermi 3 site.

The Fermi 3 site-specific SSI analyses follow the same methodology used in the Referenced DCD for SSI analyses for the ESBWR Standard Plant using the SASSI2010 computer program. The SASSI2010 structural models are developed from the Referenced DCD lumped-mass stick models coupled with the Fermi 3 site-specific strain compatible dynamic subsurface properties developed in Subsection 3.7.1. In the SASSI2010 model for the Fermi 3 site-specific SSI analyses, the RB/FB and CB are modeled as partially embedded into the Bass Islands Group bedrock. Cases with and without backfill above the top of the Bass Islands Group bedrock at Elevation 168.2 m (552.0 ft) NAVD 88 surrounding the RB/FB and CB have been considered. Fill concrete is used to backfill the gap between the RB/FB and CB and excavated bedrock up to the top of Bass Islands Group bedrock at Elevation 168.2 m (552.0 ft) NAVD 88, as shown on Figure 2.5.4-202 and Figure 2.5.4-203.

As shown in the Referenced DCD, Table 3A.6-1, there are some models with minor modifications to evaluate the modeling effects. For the Fermi 3 SSI analyses, the most basic model, "Base" is applied. The Base Model is for uncracked concrete.

The site-specific SSI analyses results are presented and compared with the Referenced DCD seismic responses in the following subsections to confirm the applicability of the ESBWR Standard Plant for the RB/FB and CB. Lateral wall pressures due to seismic loadings are evaluated in Subsection 3.8.4. In addition, the foundation stability and the dynamic bearing pressure demands are evaluated in Subsection 3.8.5 for the RB/FB and CB based on the Fermi 3 site-specific SSI analyses results.

3.7.2.4.1.1 Strain Compatible Dynamic Subsurface Material Properties

The geology of the Fermi 3 site is discussed in detail in Subsection 2.5.1. The subsurface materials encountered and the engineering properties of subsurface materials at Fermi 3 site are discussed in detail in Subsection 2.5.4.

In accordance with SRP 3.7.2, three subsurface material profiles, a best estimate (BE) profile, a lower bound (LB) profile, and an upper bound (UB) profile, were developed and used in the SSI analyses to account for

Attachment 14
NRC3-13-0036

One CD Containing Requested Electronic Files
(2 pages)

Directory of D:\

12/04/2013	09:37AM	32,475 bytes	Digitalized_Data_for_FSAR_ Figures_3.7.1- 230 _and_3.7.1-231.xlsx

1 File(s) 32,474 bytes
0 Dir(s) 0 bytes free

Attachment 15
NRC3-13-0036
(113 Pages)

Supplemental Response to RAI Letter No. 79
(eRAI Tracking No. 6605)

RAI Question No. 03.07.02-9

NRC RAI 03.07.02-9

10CFR50, Appendix S requires that evaluation for SSE must take into account soil-structure interaction (SSI) effects. To address RAIs 03.07.02-6, 03.07.02-7, 03.07.02-8, 03.08.05-2, 03.08.05-3, and 03.08.05-4, DTE has performed a site-specific SSI analysis of the Control Building (CB) for the Fermi 3 site conditions using the SASSI2000 code, with the backfill material surrounding the CB as well as the bedrock layers included in the analysis. Report SER-DTF-009, Revision 0 submitted by DTE on June 15, 2012, documents the results of this SSI analysis. The staff has reviewed this report and has some concerns. In order to determine that the Fermi 3 analysis has appropriately taken into account the SSI effects, the applicant is requested to address the following issues, including supplementing the responses to the RAIs identified above as necessary.

1. SSI Analysis Methodology and Modeling Issues

Regarding the SSI model of the CB with the surrounding backfill material, the staff has a concern with the horizontal dimension of the FE mesh used to model the excavated soil volume in the SSI analyses documented in the report SER-DTF-009, Revision 0.

The SASSI2000 code User's Manual (Rev. 1, pg. 4-10) indicates that the maximum horizontal mesh dimension should be no more than 20percent of the shear wave length of the subsurface material at the highest frequency of interest. This implies that the SSI model cannot capture frequencies higher than f = 0.2Vs/d, where Vs is the shear wave velocity of the material and d is the horizontal mesh dimension. Section 4.3 of the report indicates that, in the bedrock, the maximum vertical mesh dimension is 1.0 m and the typical horizontal mesh dimension is 4.0 m. In the backfill, the maximum vertical mesh dimension is 1.5 m but the horizontal mesh dimension is not mentioned (however, Figs. 4.3-1 through 4.3-3 appear to indicate that the latter dimension is also 4.0 m). Therefore, assuming a horizontal dimension of 4.0 m for the entire FE mesh, the limiting frequency of the SSI model could be as low as f = (0.2)(170)/(4.0) = 8.5 Hz, if based on the shear wave velocity at the top of the backfill, or f = (0.2)(240)/(4.0) = 12.1 Hz, if based on the shear wave velocity at the bottom of the backfill. Backfill properties are taken from Table 3.1-1 of the report.

Section 4.3 of the report explains that the limiting frequency is considered to be f=(0.2)(240)/(1.5) = 31 Hz; however, this is based on the maximum vertical mesh dimension in the backfill, 1.5m, and the shear wave velocity at the bottom of the backfill, 240 m/s. This is not consistent with the recommendations of the SASSI2000 User's Manual, and also ignores the vertical variation of the backfill properties.

In Section 4.3 of the report it was concluded that "since the dominant frequency of the backfill above the bedrock is estimated to be about f = Vs/(4h) = 240/4/11.3 = 5.3 Hz, the higher frequency range of input motion energy will be reduced in nature." The staff however needs further quantitative assessment demonstrating that the results using the existing soil mesh size will be conservative when compared to an analysis using a more refined soil mesh size (meeting the element thickness and horizontal

element dimension criteria) adequate for transmitting up to the maximum frequency of interest.

In Section 4.3 of the report it is indicated that: "the DCD mesh sensitivity study (for the excavated volume) provided by GEH in MFN 06.252 Dated September 13.2006 (ML0627202441) can be applied to the Fermi site-specific conditions." However, the soil profile assumed in the DCD study differs significantly from the soil profile at the Fermi 3 site. In the DCD study, the backfill has a shear wave velocity of 300 m/s and extends to a depth of 5.1 m below the bottom of the CB foundation; the soil underlying the backfill has a shear wave velocity of 800 m/s. At the Fermi 3 site, the CB is partially embedded in bedrock with shear wave velocity in the order of 2000 m/s. As a result, the transfer functions obtained in the DCD study differ significantly from those at the Fermi 3 site (as reported in SER-DTF-009 Revision 0, Appendix A). The conclusions of the DCD study depend on the shape of the computed transfer functions. As such, the staff could not determine the applicability of the DCD mesh sensitivity study to the Fermi 3 site-specific SSI analyses with backfill included.

Since the maximum frequency that can be captured with fidelity by the SSI model is significantly less than the minimum requirement of 50 Hz set in ISG-1, and the FE mesh of the SSI model deviates from the guidance in SRP Section 3.7.2, which indicates that element mesh size should be selected on the basis that further refinement has negligible effect on the solution results, the applicant is requested to provide a quantitative technical justification to demonstrate that the SSI model used is acceptable. This technical justification should take into account the energy content of the input motions, which is known to be substantial at frequencies above 8.5 Hz and non-negligible between 25 Hz and 50 Hz. The staff needs this information to ensure that the existing soil mesh size used in the SSI analysis adequately accounts for the SSE frequencies of interest in the evaluation of SSI effects.

2. *Comparison of SASSI2000 Direct Method (DM) versus Subtraction Method (SM) – Transfer Functions and FRS*

Appendix of A of SER-DTF-009 Revision 0 describes a comparative study of SSI response performed using the DM (denoted case CFB1a) and the SM (denoted case CFB1). A limitation of the study is that the same input motions and bedrock properties were not used in both cases. Case CFB1 a used the revised (i.e., "enhanced") input motions and bedrock properties described in the response to RAI 03.07.01-6, while case CFB1 did not. Therefore, it is not always clear whether the identified discrepancies are due to methodology (SM vs. DM), input motions, or bedrock properties.

The discussion in Appendix A is predicated on the assumption that the SSI analysis results for the DM can be used as the basis for comparing transfer functions and FRS at frequencies above 8.5 Hz. However, as indicated in item 1 of this RAI, it is not clear whether the SSI model can capture frequencies higher than 8.5 Hz with sufficient fidelity.

As such, the staff cannot determine the acceptability of the comparative study until the SSI modeling issues are resolved, and until it is demonstrated that the SSI analysis results using both the DM and SM are valid for the frequency range of interest. Therefore, in light of the issues raised in item 1 of this RAI, the applicant is requested to reevaluate the information presented in Appendix A of SER-DTF-009 Revision 0 using an acceptable SSI model, and using the same revised input motions and bedrock properties for both cases CFB1a and CFB1.

The applicant is also requested to provide the following additional information regarding Appendix A of SER-DTF-009 Revision 0:

(a) Quantify the differences in FRS computed using the DM and SM, currently depicted in Figs. A-1 through A-3 (but may need to be reevaluated). It appears that differences at certain frequencies are in the order of 100 percent (e.g., Fig. A-1a at 10 Hz).

(b) Provide additional comparisons of transfer functions and response spectra computed using the DM and SM, for the critical SDOF oscillators representing out-of-plane slab response. In the response spectra comparisons, include the licensing-basis SSI analysis case (which ignores the backfill).

(c) Explain the ESBWR DCD seismic design process for obtaining seismic input (amplified spectra) for piping and equipment supported on flexible floor slabs and walls. Provide an example of the seismic input that is used at the locations identified in item (b) above.

(d) Explain how the ESBWR DCD seismic design process for piping and equipment supported on flexible floor slabs and walls takes into account the following site-specific issues identified at the Fermi 3 site: (i) potential increases in vertical seismic input due to the backfill surrounding the structure (relative to the licensing-basis SSI analysis which ignores the backfill), and (ii) uncertainties in results computed using the SM vs. DM. This information should be provided in conjunction with item 4, sub-item (d), below.

(e) Explain why it is considered appropriate to extrapolate the conclusions of Appendix A to the Reactor Building (RB).

3. Comparison of SASSI2000 Direct Method (DM) versus Subtraction Method (SM) – Lateral Soil Pressures

The comparative study of SSI response performed using the DM (denoted case CFB1a) and the SM (denoted case CFB1), described in Appendix of A of SER-DTF-009 Revision 0, also includes a comparison of seismic lateral soil pressures.

From comparisons of computed seismic lateral soil pressures for cases CFB1a and CFB1, Appendix A concludes that soil pressures computed using the DM and SM are similar in trend and magnitude but do not correspond exactly; both cases are bounded by the DCD design pressures. Appendix A also indicates that some of the discrepancies may be due to differences in input motions and bedrock properties

considered for cases CFB1a and CFB1, which is a limitation of the comparative study identified in Item 2 of this RAI.

As indicated in Item 2 of this RAI, the staff cannot determine the acceptability of the comparative study until the SSI modeling issues are resolved, and until it is demonstrated that the SSI analysis results using both the DM and SM are valid for the frequency range of interest Therefore, in light of the issues raised in Item 1 of this RAI, the applicant is requested to reevaluate the information presented in Appendix A of SER-DTF-009 Revision 0, including seismic lateral soil pressures, using an acceptable SSI model and using the same revised input motions and bedrock properties for both cases CFB1a and CFB1.

The soil pressures listed in Appendix A, Table A-2, used for comparison to DCD design pressures, represent averages over the height of each wall segment. It is not acceptable to the staff to average computed lateral soil pressures over the height of the wall segments because this underestimates the soil pressures at elevations close to the backfill-to-bedrock transition. The sharp increase in lateral soil pressures at these elevations reflects a physical discontinuity in the site conditions at these elevations, which should be accounted for in the design. Therefore, the applicant is requested to provide a quantitative assessment of the sidewall design (bending moments and shears) at the locations where the DCD design pressures are exceeded. Provide technical justifications for the use of any averaging.

For the SSI analyses of the RB and CB that ignore the backfill (i.e., the licensing-basis analysis), the applicant is also requested to provide a quantitative assessment of the sidewall design (bending moments and shears) at the locations where the DCD design pressures are exceeded. Provide technical justifications for the use of any averaging.

4. Effect of Assumed Structural Damping Ratios

Section 5.1 of SER-DTF-009 Revision 0 evaluates the impact of considering a 4 percent structural damping ratio, in accordance with the guidance in RG 1.61 (for reinforced concrete when computed stress levels significantly below code limits), compared to the 7 percent value considered in the site-specific SSI analyses performed previously. The SASSI2000 DM was used in this evaluation.

From comparisons of FRS computed using the two damping ratios, Section 5.1 concludes that the SSI analyses of the RB and CB, performed previously, are not significantly impacted by using either 7 percent or 4 percent damping ratios, and are within the DCD envelope by a substantial margin. This conclusion, however, is predicated on the assumption that the reported SSI analysis results can be used to compute FRS at frequencies between 8 Hz and 40 Hz. As indicated in item 1 of this RAI, it is not clear whether the SSI model can capture frequencies higher than 8.5 Hz with sufficient fidelity. Therefore, the staff cannot determine the acceptability of the applicant's conclusion until the SSI modeling issues are resolved, and until it is demonstrated that the SSI analysis results are valid in the frequency range of

interest. The applicant is requested to reevaluate the information presented in Section 5.1 of SER-DTF-009, Revision 0 in light of the issues raised in item 1 of this RAI.

The applicant is also requested to provide the following additional information regarding Section 5.1 of SER-DTF-009 Revision 0:

(a) Quantify the differences in FRS between the 4 percent damping case and the 7 percent damping case, currently depicted in Figs. 5.1-1 through 5.1-3 (but may need to be reevaluated).

(b) Clarify whether the SSI analyses used the revised (i.e., "enhanced") input motions and bedrock properties described in the response to RAI 03.07.01-6.

(c) Since it appears that the vertical response of the SDOF oscillators is more sensitive to differences in damping ratios, provide comparisons of response spectra for the critical SDOF oscillator representing out-of-plane slab response.

(d) Explain how the ESBWR DCD seismic design process for piping and equipment supported on flexible floor slabs takes into account the following site-specific issues identified at the Fermi 3 site: (i) increases in vertical seismic input due to 4 percent damping ratios in the structure (relative to the licensing-basis SSI analysis which assumes 7 percent ratio). This information should be provided in conjunction with item 2, sub-item (d), above.

(e) Explain why it is considered appropriate to extrapolate the conclusions of Section 5.1 to the RB.

5. Response Spectra in Adjacent Nodes Used to Assess SSSI Effects

Section 5.2 of SER-DTF-009, Revision 0 describes a comparative study of seismic response of a soil point adjacent to the CB, which is used to assess structure-soil-structure interaction (SSSI) effects. The SSI analysis was performed using the DM (denoted case CFB1a) and the SM (denoted case CFB1c).

The applicant is requested to reevaluate the information presented in Section 5.2 of SER-DTF-009, Revision 0 in light of the issues raised in item 1 of this RAI. The applicant is also requested to clarify whether the SSI analyses used the revised (i.e., "enhanced") input motions and bedrock properties described in the response to RAI 03.07.01-6.

6. Relative Lateral Wall Deflections

Appendix C of SER-DTF-009 Revision 0 summarizes lateral wall deflections of the RB and CB toward each other, to assess potential SSSI effects. The reference point in each case is at the top of the basemat for each building. The SSI analyses cases considered were those reported in Shimizu Engineering Reports SER-DTF-006, Revision 1 and SER-DTF-008, Revision 0.

To complete the staff's evaluation, the applicant is requested to provide the maximum displacement of each reference point relative to a fixed reference system, for all the SSI analyses cases considered. This information is necessary to quantify the relative motions of the basemats toward each other.

Response

The response to this RAI was provided in DTE letter NRC3-13-0032, September 12, 2013 (ML 13259A244).

This response replaces the previous response in its entirety. The changes are identified with revision bars.

This RAI identifies issues with various aspects of the Fermi 3 soil-structure interaction (SSI) analyses, primarily that the current analyses are not capable of capturing frequencies of at least 50 Hz, as recommended by Interim Staff Guidance DC/COL-ISG-1, in order to sufficiently capture the high frequency content of the horizontal and vertical Foundation Input Response Spectra (FIRS). Limitations on the size of the model that can be analyzed with the seismic analysis software used for the previous analyses (SASSI2000) make it difficult to perform analyses that satisfy all available guidance for the Fermi site.

To address these issues, DTE has re-performed the Fermi 3 site-specific SSI analyses using SASSI2010 with sufficiently fine mesh such that frequencies of up to about 50 Hz are captured (except for SSI models with engineered backfill and LB subsurface profile), OBE damping, and input acceleration time histories considering the impact of the Central and Eastern United States (CEUS) Seismic Source Characterization (SSC) model for Fermi 3 site. In addition, the rock-engineered backfill profiles consider the impact of acceleration time histories based on CEUS SSC model. SASSI2010 is a newer version of SASSI2000 that addresses some of the limitations on the size of the model that can be analyzed.

The individual analyses and results are discussed in detail in Sargent & Lundy Reports SL-011864, SL-011956, and SL-011960 (References 4, 5, and 6). The site-specific SSI analysis cases are shown in Tables 1 and 2. The Fermi 3 site-specific SSI analyses for the Reactor Building/Fuel Building (RB/FB) and Control Building (CB) consider partial embedment into the Bass Islands Group bedrock. Cases with and without engineered backfill located above the top of Bass Islands Group bedrock (Elevation 168.2 m [552 ft] NAVD 88, FSAR Table 2.5.4-201) have been analyzed.

Frequencies of up to about 50 Hz are captured, except for SSI models with engineered backfill and LB subsurface profile. As shown in Tables 1 and 2 the SSI analysis models with engineered backfill have considered only UB and LB subsurface profiles. To keep the LB model within SASSI2010 computer code capability, the LB model layer thicknesses and mesh dimensions are kept the same as those for the corresponding UB model. For the LB models, frequencies of up to about 19 Hz are captured.

The results from the Fermi 3 site-specific SSI and structure-soil-structure interaction (SSSI) analyses using the Best Estimate (BE), Lower Bound (LB), and Upper Bound (UB) subsurface profiles show that the seismic forces in members, floor response spectra, and accelerations are bounded by values presented in the Referenced DCD for both the RB/FB and CB.

Based on the Fermi 3 site-specific SSI and SSSI analyses, the following conclusions apply to the Fermi 3 site:

- The Referenced DCD standard plant design (ESBWR Standard Plant) is applicable to the RB/FB and CB Seismic Category I structures at the Fermi 3 site with partial embedment into bedrock.
- The DCD backfill requirements for the backfill above the top of the Bass Islands Group bedrock (Elevation 168.2 m [552 ft] NAVD 88) that surrounds the embedded walls of the Fermi 3 Seismic Category I structures are shown to be unnecessary. Therefore, the backfill above the top of the Bass Islands Group bedrock is not Seismic Category I backfill.
- The following Fermi 3 site-specific SSI dynamic responses using the SSI FIRS and the BE, LB, and UB subsurface profiles are less than the corresponding dynamic responses in the referenced DCD using the Certified Seismic Design Response Spectra (CSDRS):
    - Fermi 3 site-specific SSI enveloping seismic loads are less than the Referenced DCD enveloping seismic loads. The Fermi 3 site-specific SSI enveloping seismic loads are a maximum of 86 and 72 percent of the Referenced DCD values for the RB/FB and CB, respectively (Refer to Tables 3 through 8).
    - Fermi 3 site-specific SSI enveloping maximum vertical accelerations are less than the Referenced DCD enveloping maximum vertical accelerations. The Fermi 3 site-specific SSI enveloping maximum vertical accelerations are a maximum of 75 percent of the Referenced DCD values for the RB/FB and CB, respectively (Refer to Tables 9 through 15).
    - Fermi 3 site-specific SSI floor response spectra are considerably less than the Referenced DCD enveloping floor response spectra at the same locations (Refer to Figures 1 through 24).

The Fermi 3 site-specific lateral wall evaluations were performed as detailed in Sargent & Lundy Report SL-012018 (Reference 7). Lateral soil pressure on embedded portions of the exterior walls exceeds the lateral soil pressures reported in the DCD at some locations (Refer to Figures 25 through 38). The adequacy of the wall designs for lateral soil pressures have been evaluated. The wall soil pressures are within the capacity of ESBWR DCD wall designs.

The Fermi 3 site-specific foundation stability (sliding, overturning, and flotation) evaluations, and dynamic bearing capacity evaluations, were performed as detailed in Sargent & Lundy Report SL-012018 (Reference 7).

- The Fermi 3 site-specific foundation stability evaluations demonstrated that the minimum Fermi 3 site-specific factors of safety for sliding and overturning for the RB/FB and CB are 1.1 for sliding and 1,733 for overturning (Refer to Tables 16 and

17). With the exception of CB Licensing Basis case (i.e., with no engineered backfill), both the CB and RB/FB are stable against sliding using only the available friction force at the bottom of their respective basemats. For CB with no engineered backfill, in addition to the base friction, lateral bearing resistance along the CB foundation sides by the in-situ rock or concrete fill between the CB and RB/FB is required to meet the minimum required sliding safety factor of 1.10. The concrete fill between the CB and the RB/FB is capable of providing the required lateral bearing resistance through the friction between the bottom of the concrete fill and the top of the in-situ rock below. The in-situ Bass Islands Group bedrock is also found capable of providing the required lateral bearing resistance.

- The Fermi 3 RB/FB and CB are stable against flotation with a minimum factor of safety of 1.86 (Refer to Tables 16 and 17).
- The Fermi 3 site-specific SSI maximum soil bearing pressure demands (toe pressures) are all less than the Referenced DCD maximum dynamic bearing demands for both the RB/FB and the CB in Referenced DCD, Tables 3G.1-58 and 3G.2-27, respectively.

The above describes a wholesale replacement of the Fermi 3 SSI analyses submitted to date. Supplementary responses to RAIs 03.07.02-6, 03.07.02-7, 03.07.02-8, 03.08.05-2, 03.08.05-3, and 03.08.05-4 were included as Attachments 2, 3, 4, 5, 6, and 7in DTE letter NRC3-13-0032, September 12, 2013 (ML 13259A244). The Supplemental response to RAI 03.08.05-3 provided with this letter replaces the response in Attachment 6 of DTE letter NRC3-13-0032 in its entirety.

References

1. Sargent & Lundy Report SL-011814, "Modified Subtraction Method (MSM) Reactor Building/Fuel Building Benchmark Summary Report", Revision 0, May 2, 2013, enclosed with DTE Letter NRC3-13-0017, May 3, 2013 (ML13127A033).
2. Sargent & Lundy Report SL-011863, "Modified Subtraction Method (MSM) Firewater Service Complex Benchmark Summary Report", Revision 0, May 21, 2013, enclosed with DTE Letter NRC3-13-0021, June 19, 2013 (ML13175A262).
3. Sargent & Lundy Report SL-011874, "Modified Subtraction Method (MSM) Control Building Benchmark Summary Report", Revision 0, June 10, 2013, enclosed with DTE Letter NRC3-13-0021, June 19, 2013 (ML13175A262).
4. Sargent & Lundy Report SL-011864, "Licensing Basis SSI Analyses of Reactor Building/Fuel Building and Control Building Summary Report", Revision 1, July 24, 2013, enclosed with DTE Letter NRC3-13-0026, July 25, 2013 (ML13210A145).
5. Sargent & Lundy Report SL-011956, "SSI Analyses of Reactor Building/Fuel Building and Control Building with Engineered Backfill Summary Report", Revision 1, December 10, 2013, (Attachment 17).

6. Sargent & Lundy Report SL-011960, "SSSI Sensitivity Studies of CB and FWSC with Engineered Backfill Summary Report", Revision 0, August 13, 2013, enclosed with DTE Letter NRC3-13-0028, August 14, 2013 (ML13232A005).
7. Sargent & Lundy Report SL-012018, "Evaluation of Reactor Building/Fuel Building and Control Building Dynamic Bearing Capacity, Foundation Stability, and Wall Seismic Soil Pressures Summary Report", Revision 1, December 10, 2013 (Attachment 18).

1. SSI Analysis Methodology and Modeling Issues

Regarding the SSI model of the CB with the surrounding backfill material, the staff has a concern with the horizontal dimension of the FE mesh used to model the excavated soil volume in the SSI analyses documented in the report SER-DTF-009, Revision 0.

The SASSI2000 code User's Manual (Rev. 1, pg. 4-10) indicates that the maximum horizontal mesh dimension should be no more than 20percent of the shear wave length of the subsurface material at the highest frequency of interest. This implies that the SSI model cannot capture frequencies higher than f = 0.2Vs/d, where Vs is the shear wave velocity of the material and d is the horizontal mesh dimension. Section 4.3 of the report indicates that, in the bedrock, the maximum vertical mesh dimension is 1.0 m and the typical horizontal mesh dimension is 4.0 m. In the backfill, the maximum vertical mesh dimension is 1.5 m but the horizontal mesh dimension is not mentioned (however, Figs. 4.3-1 through 4.3-3 appear to indicate that the latter dimension is also 4.0 m). Therefore, assuming a horizontal dimension of 4.0 m for the entire FE mesh, the limiting frequency of the SSI model could be as low as f = (0.2)(170)/(4.0) = 8.5 Hz, if based on the shear wave velocity at the top of the backfill, or f = (0.2)(240)/(4.0) = 12.1 Hz, if based on the shear wave velocity at the bottom of the backfill. Backfill properties are taken from Table 3.1-1 of the report.

Section 4.3 of the report explains that the limiting frequency is considered to be f=(0.2)(240)/(1.5) = 31 Hz; however, this is based on the maximum vertical mesh dimension in the backfill, 1.5m, and the shear wave velocity at the bottom of the backfill, 240 m/s. This is not consistent with the recommendations of the SASSI2000 User's Manual, and also ignores the vertical variation of the backfill properties.

In Section 4.3 of the report it was concluded that "since the dominant frequency of the backfill above the bedrock is estimated to be about f = Vs/(4h) = 240/4/11.3 = 5.3 Hz, the higher frequency range of input motion energy will be reduced in nature." The staff however needs further quantitative assessment demonstrating that the results using the existing soil mesh size will be conservative when compared to an analysis using a more refined soil mesh size (meeting the element thickness and horizontal element dimension criteria) adequate for transmitting up to the maximum frequency of interest.

In Section 4.3 of the report it is indicated that: "the DCD mesh sensitivity study (for the excavated volume) provided by GEH in MFN 06.252 Dated September 13.2006 (ML0627202441) can be applied to the Fermi site-specific conditions." However, the soil profile assumed in the DCD study differs significantly from the soil profile at the Fermi 3 site. In the DCD study, the backfill has a shear wave velocity of 300 m/s and extends to a depth of 5.1 m below the bottom of the CB foundation; the soil underlying the backfill has a shear wave velocity of 800 m/s. At the Fermi 3 site, the CB is partially embedded in bedrock with shear wave velocity in the order of 2000 m/s. As a result, the transfer functions obtained in the DCD study differ significantly from those at the Fermi 3 site (as reported in SER-DTF-009 Revision 0, Appendix A).

The conclusions of the DCD study depend on the shape of the computed transfer functions. As such, the staff could not determine the applicability of the DCD mesh sensitivity study to the Fermi 3 site-specific SSI analyses with backfill included.

Since the maximum frequency that can be captured with fidelity by the SSI model is significantly less than the minimum requirement of 50 Hz set in ISG-1, and the FE mesh of the SSI model deviates from the guidance in SRP Section 3.7.2, which indicates that element mesh size should be selected on the basis that further refinement has negligible effect on the solution results, the applicant is requested to provide a quantitative technical justification to demonstrate that the SSI model used is acceptable. This technical justification should take into account the energy content of the input motions, which is known to be substantial at frequencies above 8.5 Hz and non-negligible between 25 Hz and 50 Hz. The staff needs this information to ensure that the existing soil mesh size used in the SSI analysis adequately accounts for the SSE frequencies of interest in the evaluation of SSI effects.

The licensing basis case analyses (i.e., without backfill) have been re-performed with the Central and Eastern United States (CEUS) seismic inputs and a sufficiently fine mesh such that frequencies of up to about 50 Hz are captured. These analyses, described in detail in Sargent & Lundy Report SL-011864 (Reference 4), utilize the direct method (DM), also called the flexible volume method, of the SASSI software.

In order to evaluate both the effect of engineered backfill and the effect of nearby structures, analyses that include engineered backfill have been re-performed with the CEUS seismic inputs. Because a sufficiently fine mesh must be utilized such that frequencies up to about 50 Hz can be captured, the DM cannot be utilized for all of the cases where backfill is considered. In order to address this issue, the modified subtraction method (MSM) for RB/FB analyses and the DM for CB analyses were used. These analyses are described in detail in Sargent & Lundy Report SL-011956 (Reference 5).

To justify use of the MSM, it was benchmarked against the DM, demonstrating that the MSM and DM provide acceptably close results for the Fermi site. These analyses are described in detail in Sargent & Lundy Reports SL-011814, SL-011863, and SL-011874 (References 1, 2, and 3).

In order to determine structure-soil-structure interaction (SSSI) effects, DTE has re-performed the SSSI analyses with the MSM. These analyses were made with the CEUS seismic inputs and a sufficiently fine mesh such that frequencies of up to about 50 Hz could be captured, except for SSI models with engineered backfill and LB subsurface profile. As shown in Tables 1 and 2, the SSI and SSSI analysis models with engineered backfill have considered only UB and LB subsurface profiles. To keep the LB model within SASSI2010 computer code capability, the LB model layer thicknesses and mesh dimensions are kept the same as those for the corresponding UB model. In the LB

models, frequencies of up to about 19 Hz can be captured. These analyses are described in detail in Sargent & Lundy Report SL-011960 (Reference 6).

2. *Comparison of SASSI2000 Direct Method (DM) versus Subtraction Method (SM) – Transfer Functions and FRS*

Appendix of A of SER-DTF-009 Revision 0 describes a comparative study of SSI response performed using the DM (denoted case CFB1a) and the SM (denoted case CFB1). A limitation of the study is that the same input motions and bedrock properties were not used in both cases. Case CFB1 a used the revised (i.e., "enhanced") input motions and bedrock properties described in the response to RAI 03.07.01-6, while case CFB1 did not. Therefore, it is not always clear whether the identified discrepancies are due to methodology (SM vs. DM), input motions, or bedrock properties.

The discussion in Appendix A is predicated on the assumption that the SSI analysis results for the DM can be used as the basis for comparing transfer functions and FRS at frequencies above 8.5 Hz. However, as indicated in item 1 of this RAI, it is not clear whether the SSI model can capture frequencies higher than 8.5 Hz with sufficient fidelity.

As such, the staff cannot determine the acceptability of the comparative study until the SSI modeling issues are resolved, and until it is demonstrated that the SSI analysis results using both the DM and SM are valid for the frequency range of interest. Therefore, in light of the issues raised in item 1 of this RAI, the applicant is requested to reevaluate the information presented in Appendix A of SER-DTF-009 Revision 0 using an acceptable SSI model, and using the same revised input motions and bedrock properties for both cases CFB1a and CFB1.

The applicant is also requested to provide the following additional information regarding Appendix A of SER-DTF-009 Revision 0:

(a) Quantify the differences in FRS computed using the DM and SM, currently depicted in Figs. A-1 through A-3 (but may need to be reevaluated). It appears that differences at certain frequencies are in the order of 100 percent (e.g., Fig. A-1a at 10 Hz).

(b) Provide additional comparisons of transfer functions and response spectra computed using the DM and SM, for the critical SDOF oscillators representing out-of-plane slab response. In the response spectra comparisons, include the licensing-basis SSI analysis case (which ignores the backfill).

(c) Explain the ESBWR DCD seismic design process for obtaining seismic input (amplified spectra) for piping and equipment supported on flexible floor slabs and walls. Provide an example of the seismic input that is used at the locations identified in item (b) above.

(d) Explain how the ESBWR DCD seismic design process for piping and equipment supported on flexible floor slabs and walls takes into account the following site-specific issues identified at the Fermi 3 site: (i) potential increases in vertical seismic input due to the backfill surrounding the structure (relative to the

licensing-basis SSI analysis which ignores the backfill), and (ii) uncertainties in results computed using the SM vs. DM. This information should be provided in conjunction with item 4, sub-item (d), below.

(e) Explain why it is considered appropriate to extrapolate the conclusions of Appendix A to the Reactor Building (RB).

In order to evaluate the effect of engineered backfill, analyses that include engineered backfill have been re-performed with the CEUS seismic inputs. The DM was utilized for all of the Control Building (CB) cases where engineered backfill is considered. Operating Basis Earthquake (OBE) damping values have been used for the structural elements.

These analyses are described in detail in Sargent & Lundy Report SL-011956 (Reference 5), which supersedes SER-DTF-009.

RB/FB and CB Floor Oscillators

Some of the RB/FB and CB floors have out-of-plane frequencies lower than 50 Hz. The SSI models of the RB/FB and the CB include oscillators to represent these lower out-of plane frequencies. These oscillators are shown in ESBWR DCD Figures 3A.7-4 and 3A.7-6 for RB/FB and CB respectively. The ESBWR standard plant design documents provide response spectra at these oscillators, which are used in the design process for piping and equipment supported on the respective flexible floors. The SSI analyses discussed in Sargent & Lundy Report SL-011864 (References 4) and Sargent & Lundy Report SL-011956 (References 5) are used to develop response spectra at these oscillators. The maximum vertical accelerations and the response spectra at the oscillators from the SSI analyses discussed in References 4 and 5 are bounded by the corresponding ESBWR standard plant design maximum vertical accelerations and response spectra.

Attached Figures 39 through 47 show the comparisons between the 5% damped response spectra at the floor slab oscillators from the Fermi 3 SSI models and the corresponding standard plant enveloping oscillators response spectra for the CB.

Attached Figures 48 through 91 show the comparisons between the 5% damped response spectra at the floor slab oscillators from the Fermi 3 SSI models and the corresponding standard plant enveloping oscillators response spectra for the RB/FB.

The spectra comparisons show that the standard plant enveloping oscillators response spectra bound the site specific Fermi 3 oscillators response spectra.

RB/FB Wall Oscillators

Some of the RB/FB walls have out-of-plane frequencies lower than 50 Hz. ESBWR DCD. Figure 3A.7-4 shows horizontal wall oscillators to represent these lower out-of-plane wall frequencies. In ESBWR DCD Figure 3A.7-4, the horizontal wall oscillators are attached to

Node 105 (Elevation 13.57m) and to the walls between Node 109 (Elevation 34.00m) and Node 110 (Elevation 52.40m). The ESBWR standard plant design documents provide response spectra at these oscillators which are used in the design process for piping and equipment supported on the respective flexible wall regions.

For the Fermi 3 SSI analyses, the most basic model, "Base" was applied. The base model is for uncracked concrete. The base structural models discussed in Sargent & Lundy Report SL-011864 (References 4) and Sargent & Lundy Report SL-011956 (References 5), do not include the RB/FB wall oscillators. Hence, the response spectra at the wall oscillators are not developed in the SSI analyses discussed in References 4 and 5.

For assessing response spectra at the wall oscillators, decoupled seismic analyses of the oscillators (without considering interaction between the oscillators and the RB/FB) with the respective input motion at the oscillator's attachment location in the RB/FB SSI models are analyzed. The decoupled model approach generally produces conservative results. For the oscillators at walls located between Nodes 109 and 110, the oscillators' response spectra are developed using the input motions from Node 109 and Node 110, separately. Thus, the response spectra of these oscillators will be in-between the response spectra from Node 109 input and Node 110 input.

Attached Figures 92 through 96 show the comparisons between the 5% damped oscillators' response spectra from Node 109 input and the corresponding Standard Plant enveloping response spectra for the applicable wall region. Attached Figures 97 through 101 show the comparisons between the 5% damped oscillators' response spectra from Node 110 and the corresponding Standard Plant enveloping response spectra for the applicable wall region. Since for the layered soil conditions, ESBWR DCD has used Case RL-6 with cracked wall out-of-plane (ESBWR DCD Table 3A.6-1), layered Fermi 3 (with engineered granular backfill described in Reference 5) is used in developing these oscillator spectra. The oscillator damping used is 7%, consistent with the DCD damping for the concrete cracked case. The input motions for the oscillators are from building a model with 4% structural damping (analyses described in Reference 5), resulting in conservative oscillator response spectra.

The spectra comparisons in Figures 92 through 101 show that the standard plant enveloping oscillator response spectra bound the site specific Fermi 3 oscillator response spectra by a large margin, except in Figure 93, where the seismic input from Node 109 produces Node 99982 oscillator spectral value almost same as the standard plant enveloping oscillator response spectra. Since Node 99982 oscillator is located between Node 109 and Node 110, the response spectra at Node 99982 will be in-between the response spectra from Node 109 input and Node 110 input. Thus the spectra for this oscillator will also be bounded by the standard plant enveloping oscillator response spectra. Figures 102 and 103 on which response spectra at node 99982 from Node 109 input and Node 110 input are plotted on the same sheet (one sheet for LB case and one sheet for UB case) are provided to help visualize where the actual response would lie.

3. Comparison of SASSI2000 Direct Method (DM) versus Subtraction Method (SM) – Lateral Soil Pressures

The comparative study of SSI response performed using the DM (denoted case CFB1a) and the SM (denoted case CFB1), described in Appendix A of SER-DTF-009, Revision 0, also includes a comparison of seismic lateral soil pressures.

From comparisons of computed seismic lateral soil pressures for cases CFB1a and CFB1, Appendix A concludes that soil pressures computed using the DM and SM are similar in trend and magnitude but do not correspond exactly; both cases are bounded by the DCD design pressures. Appendix A also indicates that some of the discrepancies may be due to differences in input motions and bedrock properties considered for cases CFB1a and CFB1, which is a limitation of the comparative study identified in Item 2 of this RAI.

As indicated in Item 2 of this RAI, the staff cannot determine the acceptability of the comparative study until the SSI modeling issues are resolved, and until it is demonstrated that the SSI analysis results using both the DM and SM are valid for the frequency range of interest Therefore, in light of the issues raised in Item 1 of this RAI, the applicant is requested to reevaluate the information presented in Appendix A of SER-DTF-009 Revision 0, including seismic lateral soil pressures, using an acceptable SSI model and using the same revised input motions and bedrock properties for both cases CFB1a and CFB1.

The soil pressures listed in Appendix A, Table A-2, used for comparison to DCD design pressures, represent averages over the height of each wall segment. It is not acceptable to the staff to average computed lateral soil pressures over the height of the wall segments because this underestimates the soil pressures at elevations close to the backfill-to-bedrock transition. The sharp increase in lateral soil pressures at these elevations reflects a physical discontinuity in the site conditions at these elevations, which should be accounted for in the design. Therefore, the applicant is requested to provide a quantitative assessment of the sidewall design (bending moments and shears) at the locations where the DCD design pressures are exceeded. Provide technical justifications for the use of any averaging.

For the SSI analyses of the RB and CB that ignore the backfill (i.e., the licensing-basis analysis), the applicant is also requested to provide a quantitative assessment of the sidewall design (bending moments and shears) at the locations where the DCD design pressures are exceeded. Provide technical justifications for the use of any averaging.

As indicated in Item 1, the SSI (with and without engineered backfill) and SSSI analyses have been re-performed with the CEUS seismic inputs. The SSI and SSSI analyses that

include the engineered backfill are described in detail in Sargent & Lundy Reports SL-011956 and SL-011960 (References 5 and 6).

Because a sufficiently fine mesh must be utilized such that frequencies up to about 50 Hz can be captured, the DM cannot be utilized for all of the cases where engineered backfill is considered. In order to address this issue, for SSI analyses, the modified subtraction method (MSM) for RB/FB analyses and the DM for CB analyses were used. The SSSI models have been reanalyzed using DM or MSM. To justify use of the MSM, it was benchmarked against the DM, demonstrating that the MSM and DM provide acceptably close results for the Fermi site. These benchmark analyses are described in detail in Sargent & Lundy Reports SL-011814, SL-011863, and SL-011874 (References 1, 2, and 3).

The lateral soil pressures on embedded portions of the exterior walls exceed the lateral soil pressures reported in the DCD at some locations. The adequacy of the wall designs for lateral soil pressures have been evaluated and summarized in Sargent & Lundy Report SL-012018 (Reference 7). The soil pressure evaluations described in this report do not rely upon averages over the height of each wall segment and do not take any credit for reduced Fermi 3 seismic in-plane loads due to horizontal and vertical accelerations. Soil pressures at elevations close to the backfill-to-bedrock transition, including the sharp increase in lateral soil pressures at elevations close to the backfill-to-bedrock transition are evaluated. A quantitative assessment of the sidewall design (out-of-plane bending moments and shears due to lateral soil pressure) at the locations where the DCD design pressures are exceeded has been provided. The induced out-of-plane bending moments and shear forces in the walls due to the seismic soil pressures from the Fermi 3 SSI and SSSI analyses are bounded by either the corresponding induced out-of-plane bending moments and shear forces due to ESBWR DCD design soil pressures or the corresponding induced out-of-plane bending moments and shear forces in the walls due to the \ESBWR DCD wall capacity passive pressures. Note that in the DCD design of RB/FB exterior walls, the DCD wall capacity passive pressures were in addition to the at-rest soil pressures and were applied as seismic loads. At-rest soil pressures were applied separately and were considered concurrent with the seismic loads. Thus, the above comparisons of induced out-of-plane shears and moments are appropriate comparisons. Therefore, the Fermi 3 wall pressures are within the capacity of ESBWR DCD wall designs.

4. Effect of Assumed Structural Damping Ratios

Section 5.1 of SER-DTF-009 Revision 0 evaluates the impact of considering a 4 percent structural damping ratio, in accordance with the guidance in RG 1.61 (for reinforced concrete when computed stress levels significantly below code limits), compared to the 7 percent value considered in the site-specific SSI analyses performed previously. The SASSI2000 DM was used in this evaluation.

From comparisons of FRS computed using the two damping ratios, Section 5.1 concludes that the SSI analyses of the RB and CB, performed previously, are not significantly impacted by using either 7 percent or 4 percent damping ratios, and are within the DCD envelope by a substantial margin. This conclusion, however, is predicated on the assumption that the reported SSI analysis results can be used to compute FRS at frequencies between 8 Hz and 40 Hz. As indicated in item 1 of this RAI, it is not clear whether the SSI model can capture frequencies higher than 8.5 Hz with sufficient fidelity. Therefore, the staff cannot determine the acceptability of the applicant's conclusion until the SSI modeling issues are resolved, and until it is demonstrated that the SSI analysis results are valid in the frequency range of interest. The applicant is requested to reevaluate the information presented in Section 5.1 of SER-DTF-009, Revision 0 in light of the issues raised in item 1 of this RAI.

The applicant is also requested to provide the following additional information regarding Section 5.1 of SER-DTF-009 Revision 0:

(a) Quantify the differences in FRS between the 4 percent damping case and the 7 percent damping case, currently depicted in Figs. 5.1-1 through 5.1-3 (but may need to be reevaluated).

(b) Clarify whether the SSI analyses used the revised (i.e., "enhanced") input motions and bedrock properties described in the response to RAI 03.07.01-6.

(c) Since it appears that the vertical response of the SDOF oscillators is more sensitive to differences in damping ratios, provide comparisons of response spectra for the critical SDOF oscillator representing out-of-plane slab response.

(d) Explain how the ESBWR DCD seismic design process for piping and equipment supported on flexible floor slabs takes into account the following site-specific issues identified at the Fermi 3 site: (i) increases in vertical seismic input due to 4 percent damping ratios in the structure (relative to the licensing-basis SSI analysis which assumes 7 percent ratio). This information should be provided in conjunction with item 2, sub-item (d), above.

(e) Explain why it is considered appropriate to extrapolate the conclusions of Section 5.1 to the RB.

In all SSI and SSSI re-analyses, OBE damping values have been used for the structural elements. In the RB/FB model OBE damping values of 4% and 3% are used for reinforced concrete elements and welded steel elements, respectively. In the CB model OBE damping of 4% has been used for the reinforced concrete elements.

5. Response Spectra in Adjacent Nodes Used to Assess SSSI Effects

Section 5.2 of SER-DTF-009, Revision 0 describes a comparative study of seismic response of a soil point adjacent to the CB, which is used to assess structure-soil-structure interaction (SSSI) effects. The SSI analysis was performed using the DM (denoted case CFB1a) and the SM (denoted case CFB1c).

The applicant is requested to reevaluate the information presented in Section 5.2 of SER-DTF-009, Revision 0 in light of the issues raised in item 1 of this RAI. The applicant is also requested to clarify whether the SSI analyses used the revised (i.e., "enhanced") input motions and bedrock properties described in the response to RAI 03.07.01-6.

As explained in Items 1 and 2 above, Fermi 3 SSI and SSSI analyses have been re-performed using refined models and OBE damping. In these analyses, the input acceleration time histories consider the impact of the CEUS Seismic Source Characterization (SSC) model for the Fermi 3 site. In addition, the rock-engineered backfill profiles consider the impact of acceleration time histories based on CEUS SSC model.

6. Relative Lateral Wall Deflections

Appendix C of SER-DTF-009 Revision 0 summarizes lateral wall deflections of the RB and CB toward each other, to assess potential SSSI effects. The reference point in each case is at the top of the basemat for each building. The SSI analyses cases considered were those reported in Shimizu Engineering Reports SER-DTF-006, Revision 1 and SER-DTF-008, Revision 0.

To complete the staff's evaluation, the applicant is requested to provide the maximum displacement of each reference point relative to a fixed reference system, for all the SSI analyses cases considered. This information is necessary to quantify the relative motions of the basemats toward each other.

The maximum east-west (CB is on the east side of the RB/FB) displacements of the RB/FB and the CB along the embedment heights of the buildings are conservatively calculated with reference to a common reference point. The common reference point is the FIRS at the RB/FB basemat bottom elevation. The RB/FB and CB SSSI analyses with engineered backfill (Sargent and Lundy Report SL-011960, Rev. 0, Reference 6) are used for calculating the displacements. The procedure to calculate the displacements with reference to the common reference point is as follows:

Step 1: In the RB/FB and CB SSSI analyses described in Sargent & Lundy Report SL-011960, relative displacements at the RB/FB basement; at nodes along the height of the embedment, and at the location of the center of the CB basemat are calculated with reference to the free-field (FIRS) motion at the RB/FB basemat bottom elevation (input in the SASSI2010 analysis). From this analysis, the ground motions at the basemat location, in the free-field are also calculated.

Step 2: The CB SSI analysis described in Sargent & Lundy Report SL-011960 is performed using the ground motion response at the center of CB basemat location in the free-field (input motion) as obtained in Step 1 above

Step 3: From the CB SSI analysis described in Step 2 above, the relative displacements at the CB basemat and at nodes along the height of the embedment of the CB are calculated with reference to the input motion in the free-field at CB basemat elevation.

Step 4: The CB displacements calculated in Step 3 are added to the displacement at the CB basemat location calculated in Step 1. Thus the displacements calculated in Step 4 are with reference to the RB/FB free-field (FIRS) motion. These displacements in CB and the displacements calculated in Step 1 have the common reference point, i.e. RB/FB free-field (FIRS) motion.

Using the above procedure, the maximum relative displacement between the embedded portions of the RB/FB and CB walls is 3.6 mm. This small relative displacement is not considered to impose any significant interaction between the two structures.

Proposed COLA Revision

Proposed COLA revisions were previously provided in Attachment 9 to DTE letter NRC3-13-0032, September 12, 2013 (ML 13259A245).

Table 1 RB/FB Soil-Structure Interaction Analysis Cases

Building	Case ID No.	Model* (DCD)	Model	SASSI2010 Method of Analysis	Input Motion	Subsurface Profile		
						UB	BE	LB
RB/FB	RBFB1UB-DM	Base	SSI Without Engineered Backfill	DM	FIRS	✓	--	--
	RBFB1BE-DM		SSI Without Engineered Backfill	DM		--	✓	--
	RBFB1LB-DM		SSI Without Engineered Backfill	DM		--	--	✓
	RBFB2UB-MSM		SSI With Engineered Backfill	MSM		✓	--	--
	RBFB2LB-MSM		SSI With Engineered Backfill	MSM		--	--	✓

Note *: As shown in the DCD Table 3A.6-1, there are some models with minor modifications to evaluate the modeling effects. For the Fermi 3 SSI analyses, the most basic model, "Base" is applied.
BE = Best estimate
LB = Lower bound
UB = Upper bound

Table 2 CB Soil-Structure Interaction Analysis

Building	Case ID No.	Model* (DCD)	Model	SASSI2010 Method of Analysis	Input Motion	Subsurface Profile		
						UB	BE	LB
CB	CB1UB-DM	Base	SSI Without Engineered Backfill	DM	FIRS	✓	--	--
	CB1BE-DM		SSI Without Engineered Backfill	DM		--	✓	--
	CB1LB-DM		SSI Without Engineered Backfill	DM		--	--	✓
	CB2UB-DM		SSI With Engineered Backfill	DM		✓	--	--
	CB2LB-DM		SSI With Engineered Backfill	DM		--	--	✓
	CB3UB-DM		SSSI With Engineered Backfill	DM		✓	--	--
	CB3LB-DM		SSSI With Engineered Backfill	DM		--	--	✓
	CB4-FWSC1UB-MSM		SSSI With Engineered Backfill	MSM		✓	--	--
	CB4-FWSC1LB-MSM		SSSI With Engineered Backfill	MSM		--	--	✓

Note *: As shown in the DCD Table 3A.6-1, there are some models with minor modifications to evaluate the modeling effects. For the Fermi 3 SSI analyses, the most basic model, "Base" is applied.
BE = Best estimate
LB = Lower bound
UB = Upper bound

Table 3 Ratio with DCD Enveloping Seismic Loads: RB/FB Stick

Elevation (m)	Element No.	Node No.	Fermi 3 enveloping SSI seismic load					Enveloping seismic load ratio (SSI / DCD)				
			Shear force (MN)		Bending moment (MN-m)		Torsion (MN-m)	Shear force		Bending moment		Torsion
			X-Dir	Y-Dir	X-Dir	Y-Dir		X-Dir	Y-Dir	X-Dir	Y-Dir	
52.4	1110	110			994.4	975.3				61%	54%	
		109	89.5	97.4	2235.4	2547.8	670.9	59%	62%	52%	57%	49%
34.0	1109	109			2929.2	3357.8				52%	61%	
		108	105.8	97.2	3644.5	3978.3	1130.5	55%	64%	56%	63%	47%
27.0	1108	108			3760.4	4589.9				49%	65%	
		107	250.4	221.9	4880.2	5536.1	2127.3	59%	55%	54%	64%	64%
22.5	1107	107			5069.2	5904.2				51%	64%	
		106	279.6	251.4	6448.9	7043.4	4091.1	58%	54%	56%	62%	67%
17.5	1106	106			6968.1	7337.7				56%	61%	
		105	300.5	297.0	8149.6	8342.5	3353.8	56%	53%	59%	60%	66%
13.57	1105	105			8406.8	8597.5				59%	60%	
		104	319.2	314.8	9846.0	9785.6	3535.9	56%	52%	59%	58%	67%
9.06	1104	104			10062.8	10000.2				59%	58%	
		103	339.9	327.3	11477.1	11199.3	3819.4	56%	50%	59%	57%	64%
4.65	1103	103			7412.4	6390.9				39%	32%	
		102	390.9	283.8	9408.5	7788.9	4794.1	47%	33%	41%	32%	42%
-1.00	1102	102			9925.3	8280.6				42%	33%	
		101	420.2	292.3	12033.1	9724.1	5238.7	48%	31%	44%	33%	45%
-6.40	1101	101			7529.3	6445.1				27%	21%	
		2	223.7	165.0	8536.2	6850.0	3453.9	24%	16%	26%	19%	30%

Table 4 Ratio with DCD Enveloping Seismic Loads: RCCV Stick

			Fermi 3 enveloping SSI seismic load					Enveloping seismic load ratio (SSI / DCD)				
			Shear force (MN)		Bending moment (MN-m)		Torsion (MN-m)	Shear force		Bending moment		Torsion
Elevation (m)	Element No.	Node No.	X-Dir	Y-Dir	X-Dir	Y-Dir		X-Dir	Y-Dir	X-Dir	Y-Dir	
34.0	1209	209			94.4	222.8				48%	38%	
		208	87.7	106.5	606.5	949.1	16.9	64%	58%	57%	63%	47%
27.0	1208	208			828.9	1427.5				49%	56%	
		206	102.1	128.7	1516.5	2630.7	1236.3	62%	52%	51%	60%	68%
17.5	1206	206			1599.7	2824.7				48%	60%	
		205	134.1	135.0	2111.6	3327.8	1326.7	58%	47%	51%	58%	67%
13.57	1205	205			2182.8	3434.9				50%	58%	
		204	147.0	149.6	2772.8	4035.4	1479.5	56%	46%	51%	56%	68%
9.06	1204	204			2903.0	4161.4				52%	55%	
		203	162.2	162.2	3605.5	4781.9	1678.0	53%	44%	53%	54%	64%
4.65	1203	203			3737.8	4931.4				53%	54%	
		202	83.9	83.9	4213.6	5407.1	1295.8	37%	29%	53%	51%	45%
-1.00	1202	202			4361.6	5574.3				54%	52%	
		201	114.0	104.4	4978.5	6126.1	1328.3	42%	32%	53%	49%	45%
-6.40	1201	201			5070.2	6222.6				53%	49%	
		2	60.8	45.6	5309.2	6374.5	579.6	23%	15%	49%	45%	30%

Table 5 Ratio with DCD Enveloping Seismic Loads: Vent Wall/Pedestal Stick

			Fermi 3 enveloping SSI seismic load					Enveloping seismic load ratio (SSI / DCD)				
			Shear force (MN)		Bending moment (MN-m)		Torsion (MN-m)	Shear force		Bending moment		Torsion
Elevation (m)	Element No.	Node No.	X-Dir	Y-Dir	X-Dir	Y-Dir		X-Dir	Y-Dir	X-Dir	Y-Dir	
17.50	701	701			27.2	26.8				35%	32%	
		702	8.8	10.6	38.4	29.7	21.1	25%	29%	34%	22%	18%
14.50	702	702			39.5	40.1				33%	27%	
		703	9.7	10.4	53.2	57.5	21.7	27%	26%	24%	22%	18%
11.50	703	703			51.8	59.0				23%	22%	
		704	11.2	12.2	66.2	92.6	22.3	30%	29%	19%	24%	19%
8.50	704	704			68.0	93.8				20%	24%	
		705	12.3	12.9	80.2	107.6	22.9	33%	29%	21%	25%	19%
7.4625	705	705			74.9	104.8				21%	24%	
		706	7.0	6.6	86.7	120.2	11.4	17%	16%	19%	23%	11%
4.65	1303	303			211.6	274.3				36%	44%	
		377	16.5	16.5	240.7	302.4	63.9	50%	37%	40%	45%	45%
2.4165	1377	377			297.2	372.2				41%	46%	
		302	24.3	23.8	359.1	430.8	77.7	51%	36%	46%	47%	45%
-1.00	1302	302			332.2	395.7				40%	41%	
		376	33.4	29.9	379.8	443.4	66.4	51%	37%	41%	42%	45%
-2.75	1376	376			380.0	443.5				41%	42%	
		301	33.5	30.0	497.3	544.7	66.4	51%	37%	45%	41%	45%
-6.40	1301	301			466.6	541.4				41%	40%	
		2	25.1	18.0	554.0	585.4	34.9	24%	15%	33%	30%	30%

Table 6 Ratio with DCD Enveloping Seismic Loads: RSW Stick

			Fermi 3 enveloping SSI seismic load					Enveloping seismic load ratio (SSI / DCD)				
			Shear force (MN)		Bending moment (MN-m)		Torsion (MN-m)	Shear force		Bending moment		Torsion
Elevation (m)	Element No.	Node No.	X-Dir	Y-Dir	X-Dir	Y-Dir		X-Dir	Y-Dir	X-Dir	Y-Dir	
24.18	707	707			1.0	1.0				48%	59%	
		708	1.5	1.2	7.1	5.4	0.2	50%	44%	54%	44%	50%
20.2	708	708			10.4	8.1				57%	48%	
		709	7.1	4.6	40.5	24.0	0.7	49%	37%	51%	35%	50%
15.775	709	709			42.8	24.8				52%	35%	
		710	8.2	5.2	79.4	47.7	1.0	47%	36%	50%	36%	53%
11.35	710	710			79.9	48.0				50%	35%	
		711	8.7	6.3	114.8	72.6	1.0	44%	38%	49%	37%	42%
7.4625	711	711			74.6	98.1				38%	53%	
		712	18.0	17.0	103.9	140.3	12.1	44%	48%	36%	56%	52%
4.65	712	713			46.9	57.6				37%	43%	
		714	7.2	7.2	55.9	69.6	13.7	50%	37%	42%	46%	45%
2.4165	713	713			1.5	1.4				42%	44%	
		714	0.5	0.5	1.2	1.2	0.1	33%	38%	41%	44%	50%
1.96	714	714			1.1	1.0				41%	42%	
		715	0.3	0.3	0.3	0.2	0.05	33%	43%	60%	44%	50%

Table 7 Ratio with DCD Enveloping Seismic Loads: RPV Stick

Location	Element No.	Node No.	Fermi 3 enveloping SSI seismic load					Enveloping seismic load ratio (SSI / DCD)				
			Axial (MN)	Shear force (MN)		Bending moment (MN-m)		Axial	Shear force		Bending moment	
				X-Dir	Y-Dir	X-Dir	Y-Dir		X-Dir	Y-Dir	X-Dir	Y-Dir
Shroud Bottom	844	845	4.6			11.7	6.6	54%			72%	46%
		846	4.6	5.0	2.6	15.8	7.3	54%	70%	37%	74%	42%
RPV Support	871	815	10.7			83.6	57.2	42%			58%	42%
		711	10.7	16.0	10.4	74.5	54.3	42%	86%	58%	53%	40%

Table 8 Ratio with DCD Enveloping Seismic Loads: CB Stick

			Fermi 3 enveloping SSI seismic load					Enveloping seismic load ratio (SSI / DCD)				
			Shear force (MN)		Bending moment (MN-m)		Torsion (MN-m)	Shear force		Bending moment		Torsion
Elevation (m)	Element No.	Node No.	X-Dir	Y-Dir	X-Dir	Y-Dir		X-Dir	Y-Dir	X-Dir	Y-Dir	
13.80	6	6			78.9	68.1				49%	55%	
		5	19.0	20.8	127.7	126.7	20.1	57%	71%	51%	64%	27%
9.06	5	5			173.9	159.7				48%	58%	
		4	36.1	39.4	304.1	316.2	42.6	68%	72%	53%	71%	33%
4.65	4	4			183.8	109.8				25%	20%	
		3	49.8	50.4	476.6	427.8	79.8	66%	63%	42%	43%	45%
-2.00	3	3			384.4	426.0				31%	41%	
-7.40		2	58.9	64.7	679.0	678.2	148.1	47%	65%	43%	44%	60%

Table 9 Ratio with DCD Enveloping Maximum Vertical Acceleration: RB/FB

Elev. (m)	Node No.	Stick model	Fermi 3 enveloping SSI max. vertical acceleration (g)	Enveloping max. vertical acceleration ratio (SSI / DCD)
52.40	110	RB/FB	0.46	36%
34.00	109	RB/FB	0.36	43%
27.00	108	RB/FB	0.34	46%
22.50	107	RB/FB	0.29	40%
17.50	106	RB/FB	0.29	40%
13.57	105	RB/FB	0.28	38%
9.06	104	RB/FB	0.29	40%
4.65	103	RB/FB	0.28	36%
-1.00	102	RB/FB	0.26	34%
-6.40	101	RB/FB	0.25	37%
-11.50	2	RB/FB	0.23	36%
-15.50	1	RB/FB	0.23	45%

Table 10 Ratio with DCD Enveloping Maximum Vertical Acceleration: RCCV

Elev. (m)	Node No.	Stick model	Fermi 3 enveloping SSI max. vertical acceleration (g)	Enveloping max. vertical acceleration ratio (SSI / DCD)
34.00	209	RCCV	0.37	41%
27.00	208	RCCV	0.35	40%
17.50	206	RCCV	0.30	41%
13.57	205	RCCV	0.28	36%
9.06	204	RCCV	0.26	41%
4.65	203	RCCV	0.24	35%
-1.00	202	RCCV	0.21	36%
-6.40	201	RCCV	0.22	37%

Table 11 Ratio with DCD Enveloping Maximum Vertical Acceleration: VW/Pedestal

Elev. (m)	Node No.	Stick model	Fermi 3 enveloping SSI max. vertical acceleration (g)	Enveloping max. vertical acceleration ratio (SSI / DCD)
17.50	701	VW	0.33	30%
14.50	702	VW	0.32	31%
11.50	703	VW	0.32	35%
8.50	704	VW	0.31	40%
7.4625	705	VW	0.31	44%
4.65	706, 303	Pedestal	0.28	42%
2.4165	377	Pedestal	0.26	41%
-1.00	302	Pedestal	0.22	37%
-2.753	376	Pedestal	0.21	41%
-6.40	301	Pedestal	0.22	43%

Table 12 Ratio with DCD Enveloping Maximum Vertical Acceleration: RSW

Elev. (m)	Node No.	Stick model	Fermi 3 enveloping SSI max. vertical acceleration (g)	Enveloping max. vertical acceleration ratio (SSI / DCD)
24.18	707	RSW	0.40	41%
20.20	708	RSW	0.40	42%
15.775	709	RSW	0.37	45%
11.35	710	RSW	0.34	45%
7.4625	711	RSW	0.31	44%
4.65	712	RSW	0.28	42%
2.4615	713	RSW	0.26	41%
1.96	714	RSW	0.26	41%
-0.80	715	RSW	0.26	40%

Table 13 Ratio with DCD Enveloping Maximum Vertical Acceleration: RB/FB Flexible Slab Oscillators (Sheet 1 of 2)

Elev. (m)	Node No.	Stick model	Fermi 3 enveloping SSI max. vertical acceleration (g)	Enveloping max. vertical acceleration ratio (SSI / DCD)
52.40	9101	Oscillator	0.46	38%
	9102	Oscillator	0.84	46%
	9103	Oscillator	1.50	48%
	9104	Oscillator	1.15	47%
	9105	Oscillator	0.86	37%
	9106	Oscillator	1.46	49%
	9107	Oscillator	1.15	41%
	9108	Oscillator	0.93	36%
34.00	9091	Oscillator	0.51	39%
	9092	Oscillator	0.49	45%
27.00	9081	Oscillator	0.46	40%
	9082	Oscillator	0.45	45%
	9083	Oscillator	0.46	42%
	9084	Oscillator	0.50	38%
	9085	Oscillator	0.41	43%
22.50	9071	Oscillator	0.72	45%
	9072	Oscillator	0.98	75%
	9073	Oscillator	0.96	47%
	9074	Oscillator	0.59	45%
	9075	Oscillator	0.54	47%
17.50	9061	Oscillator	0.76	42%
	9062	Oscillator	0.96	65%
	9063	Oscillator	0.39	47%
	9064	Oscillator	0.86	47%
	9065	Oscillator	0.47	33%

Table 14 Ratio with DCD Enveloping Maximum Vertical Acceleration: RB/FB Flexible Slab Oscillators (Sheet 2 of 2)

Elev. (m)	Node No.	Stick model	Fermi 3 enveloping SSI max. vertical acceleration (g)	Enveloping max. vertical acceleration ratio (SSI / DCD)
13.57	9051	Oscillator	0.39	48%
	9052	Oscillator	0.50	34%
9.06	9041	Oscillator	0.37	42%
	9042	Oscillator	0.55	38%
4.65	9031	Oscillator	0.74	63%
	9032	Oscillator	0.41	42%
	9033	Oscillator	0.60	59%
	9034	Oscillator	0.74	49%
	9035	Oscillator	0.47	34%
-1.00	9021	Oscillator	0.58	52%
	9022	Oscillator	0.78	54%
	9023	Oscillator	0.50	50%
	9024	Oscillator	0.45	51%
	9025	Oscillator	0.53	40%
	9026	Oscillator	0.77	49%
	9027	Oscillator	0.36	41%
-6.40	9011	Oscillator	0.50	55%
	9012	Oscillator	0.51	55%
	9013	Oscillator	0.60	44%

Table 15 Ratio with DCD Enveloping Maximum Vertical Acceleration: CB

Elev. (m)	Node No.	Stick model	Fermi 3 enveloping SSI max. vertical acceleration (g)	Enveloping max. vertical acceleration ratio (SSI / DCD)
13.8	6	CB	0.37	37%
9.06	5	CB	0.34	40%
4.65	4	CB	0.30	41%
-2	3	CB	0.23	40%
-7.4	2	CB	0.21	40%
-10.4	1	CB	0.21	40%
13.8	9001	Oscillator	1.21	55%
	9002	Oscillator	0.76	56%
	9003	Oscillator	1.02	71%
9.06	9101	Oscillator	1.05	53%
	9102	Oscillator	0.71	56%
	9103	Oscillator	1.07	75%
4.65	9201	Oscillator	0.55	42%
	9202	Oscillator	0.84	59%
-2	9301	Oscillator	0.65	47%

Table 16 Factors of Safety for RB/FB Foundation Stability

Load Combination	Overturning		Sliding		Flotation	
	SRP 3.8.5 Minimum FS	Calculated FS	SRP 3.8.5 Minimum FS	Calculated FS	SRP 3.8.5 Minimum FS	Calculated FS
D+H+E'	1.1	2,262	1.1	1.22	--	--
D+F'	--	--	--	--	1.1	3.50

Where,
D=Dead Load
H=Lateral Soil Pressure
E'=Safe Shutdown Earthquake
F'=Buoyant forces of design basis flood
FS=Factor of Safety

Table 17 Factors of Safety for CB Foundation Stability

Load Combination	Overturning		Sliding		Flotation	
	SRP 3.8.5 Minimum FS	Calculated FS	SRP 3.8.5 Minimum FS	Calculated FS	SRP 3.8.5 Minimum FS	Calculated FS
D+H+E'	1.1	1,733	1.1	1.10	--	--
D+F'	--	--	--	--	1.1	1.86

Where,
D=Dead Load
H=Lateral Soil Pressure
E'=Safe Shutdown Earthquake
F'=Buoyant forces of design basis flood
FS=Factor of Safety

Table 18 Maximum Soil Dynamic Bearing Pressure Demand for RB/FB and CB

Subsurface Condition	Dynamic Bearing Pressure Demand			
	RB/FB		CB	
	Fermi 3 Site-Specific SSI (Static + FIRS [1])	Referenced DCD (Static + SSE[2])	Fermi 3 Site-Specific SSI (Static + FIRS [1])	Referenced DCD (Static + SSE[2])
Fermi 3 Lower Bound Subsurface Profile	1913 KPa (39954 lbf/ft^2)	NA	791 KPa (16520 lbf/ft^2)	NA
Fermi 3 Best Estimate Subsurface Profile	1970 KPa (41144 lbf/ft^2)	NA	823 KPa (17189 lbf/ft^2)	NA
Fermi 3 Upper Bound Subsurface Profile	2053 KPa (42878 lbf/ft^2)	NA	853 KPa (17815 lbf/ft^2)	NA
Referenced DCD, Hard Soil Site	NA	1,100 KPa (23,000 lbf/ft^2)	NA	420 KPa (8,800 lbf/ft^2)

Notes:

(1) FIRS is the SSI FIRS developed in Subsection 3.7.1

(2) SSE is the Referenced DCD CSDRS

KPa = kilopascal

NA = Not applicable

Figure 1 Comparison of Floor Response Spectra - RB/FB Refueling Floor in X-Direction

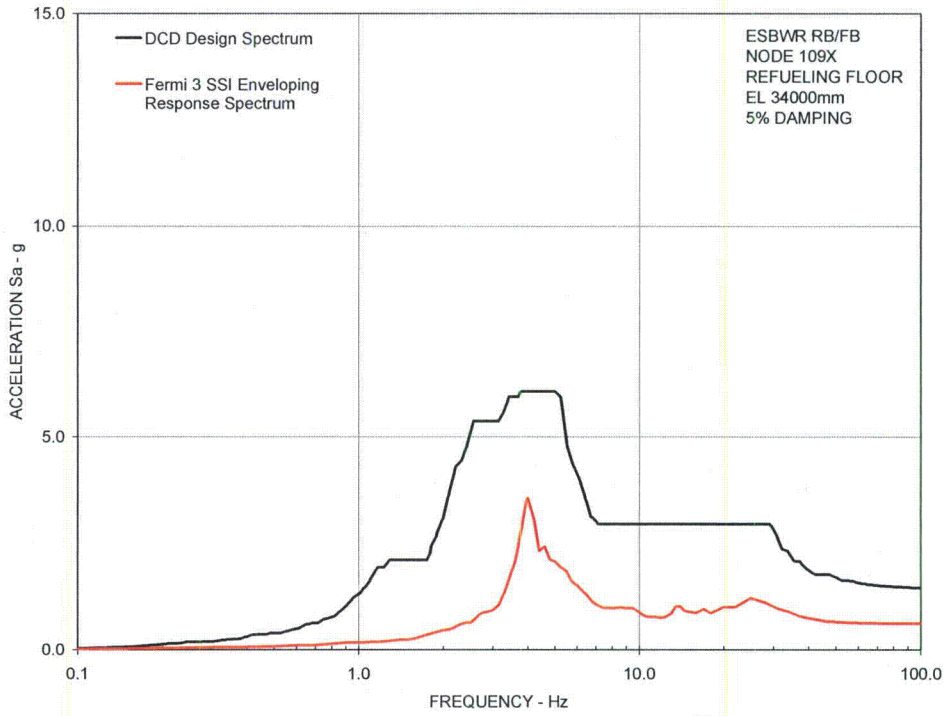

Figure 2 Comparison of Floor Response Spectra - RCCV Top Slab in X-Direction

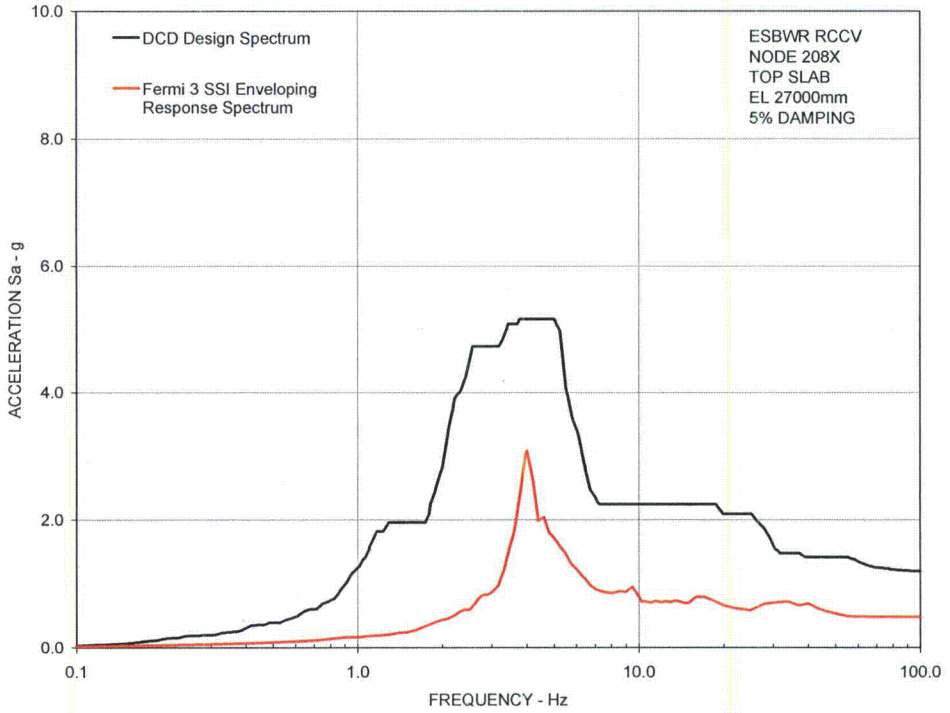

Figure 3 Comparison of Floor Response Spectra - Vent Wall Top in X-Direction

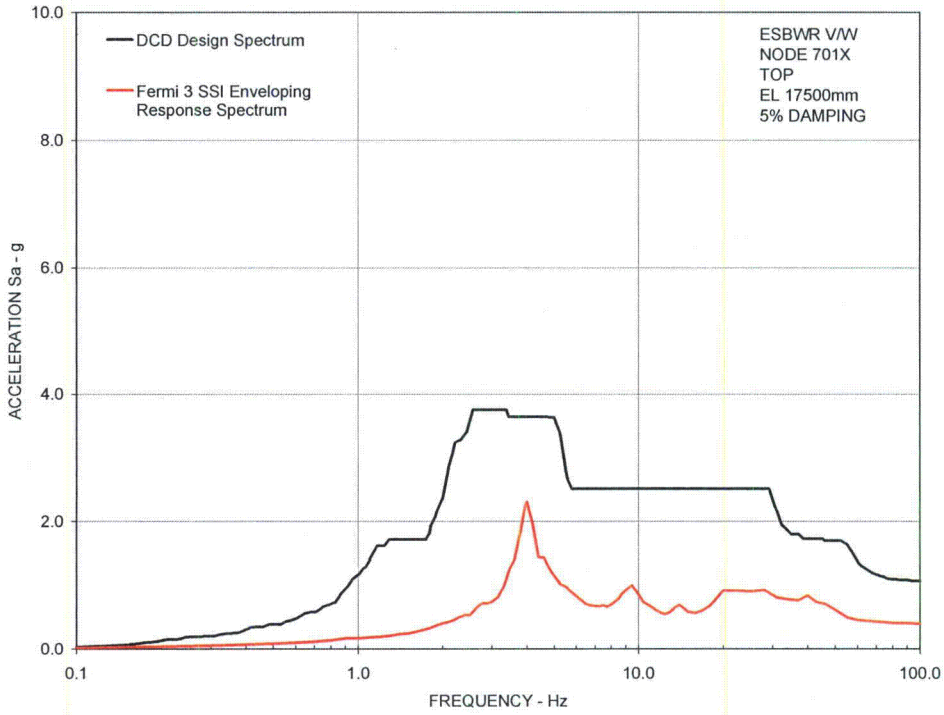

Figure 4 Comparison of Floor Response Spectra - RSW Top in X-Direction

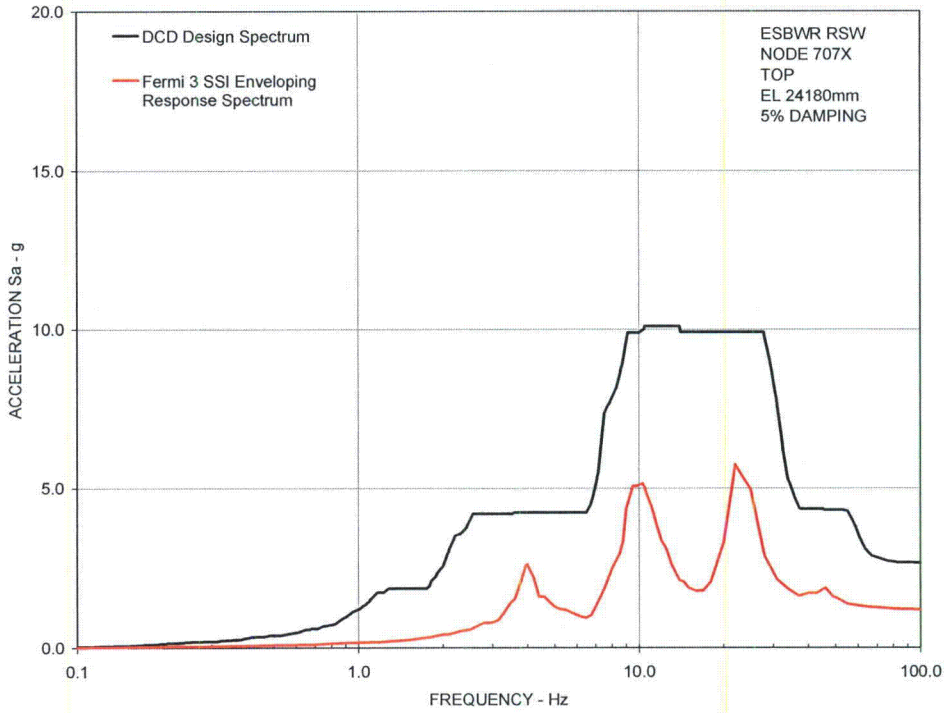

Figure 5 Comparison of Floor Response Spectra - RPV Top in X-Direction

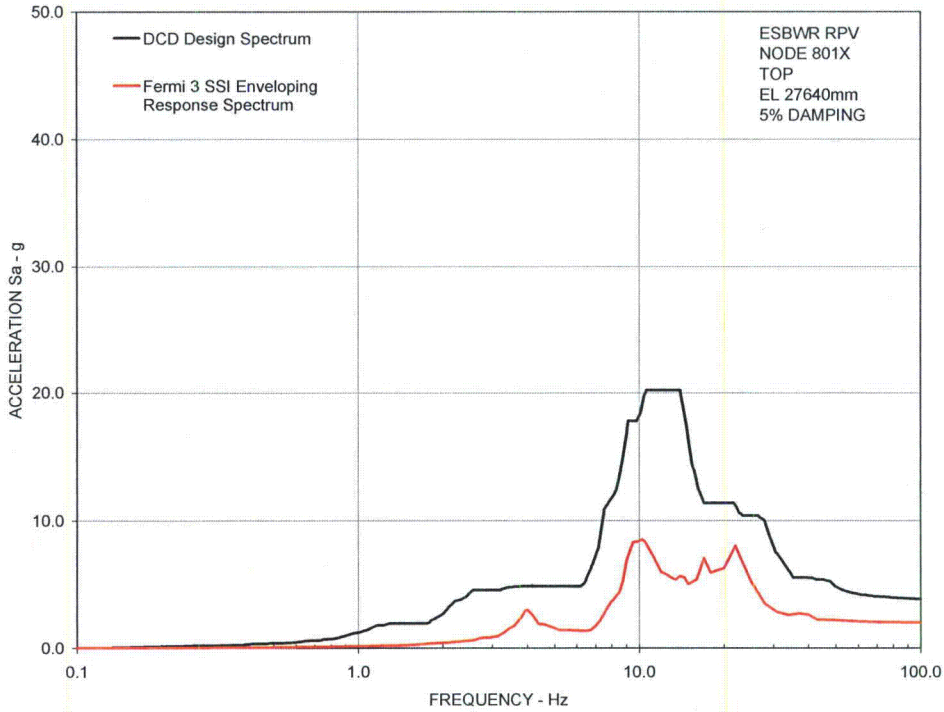

Figure 6 Comparison of Floor Response Spectra - RB/FB Basemat in X-Direction

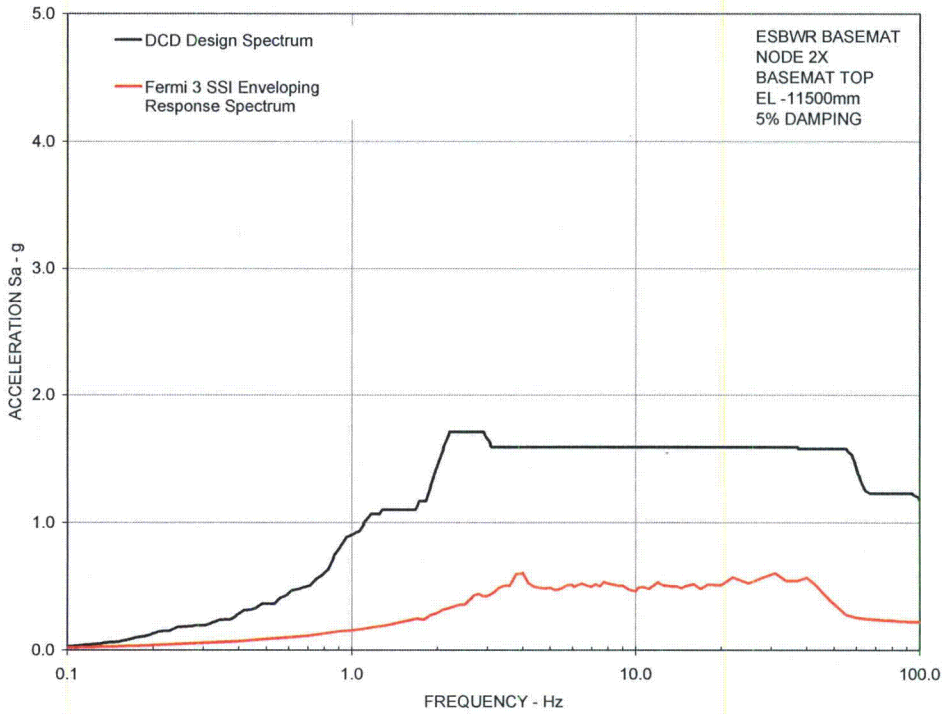

Figure 7 Comparison of Floor Response Spectra - RB/FB Refueling Floor in Y-Direction

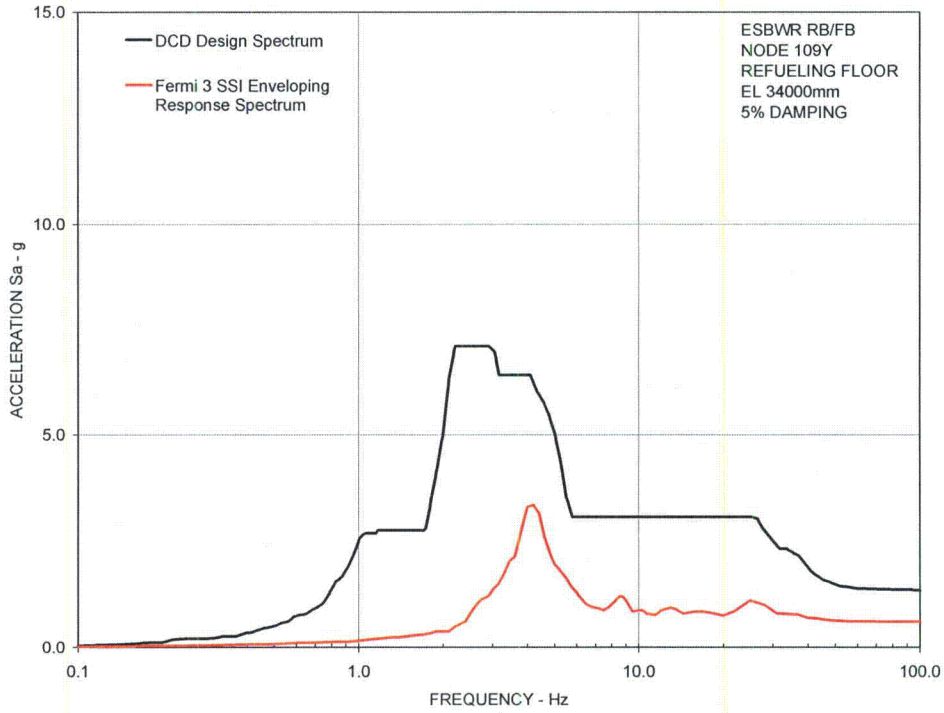

Figure 8 Comparison of Floor Response Spectra - RCCV Top Slab in Y-Direction

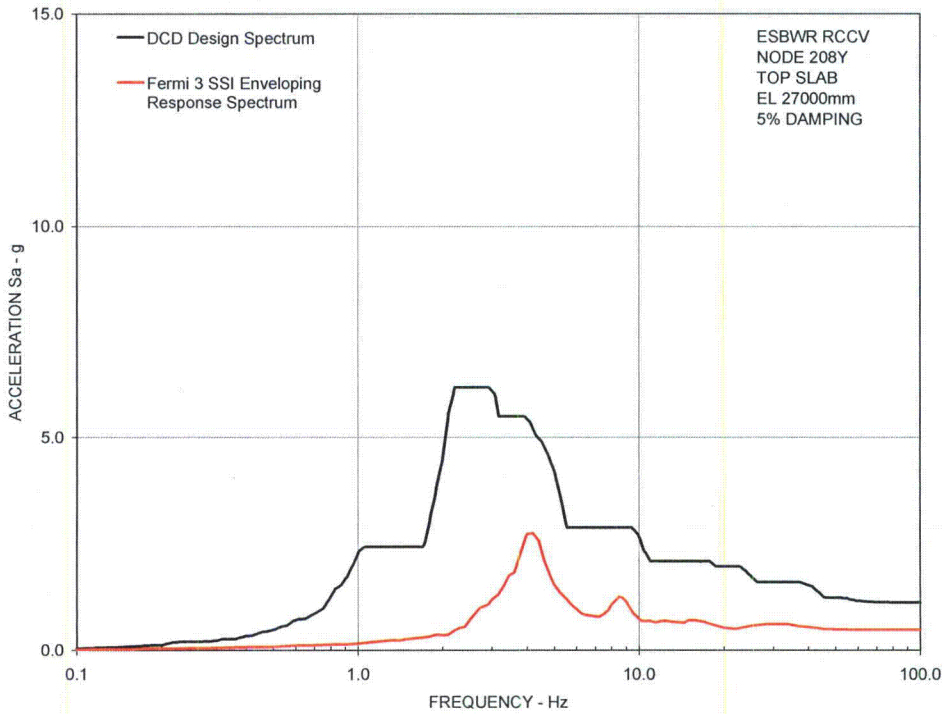

Figure 9 Comparison of Floor Response Spectra - Vent Wall Top in Y-Direction

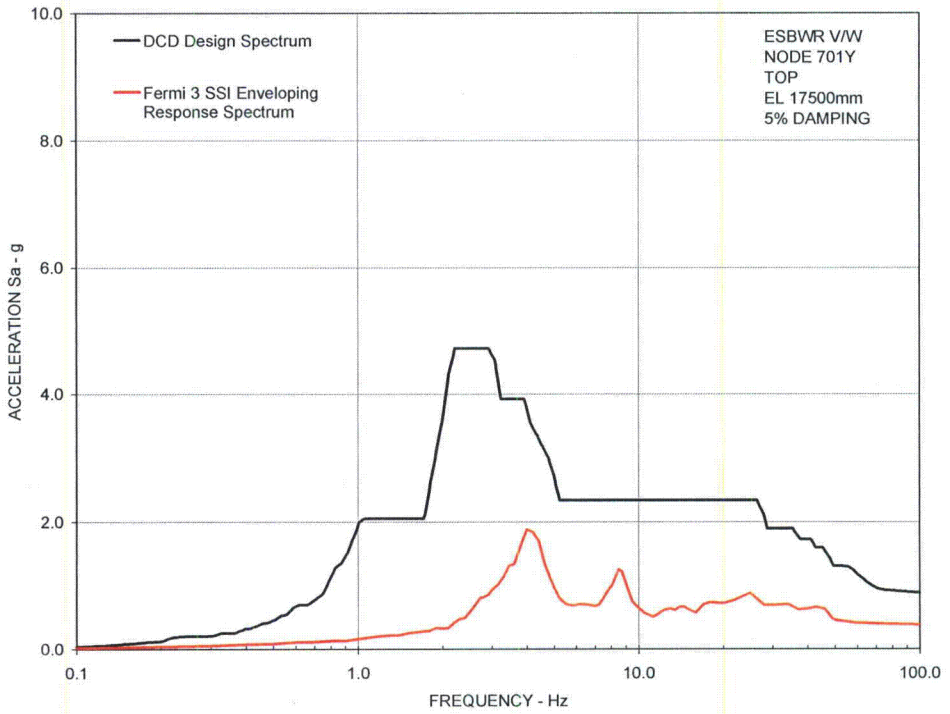

Figure 10 Comparison of Floor Response Spectra - RSW Top in Y-Direction

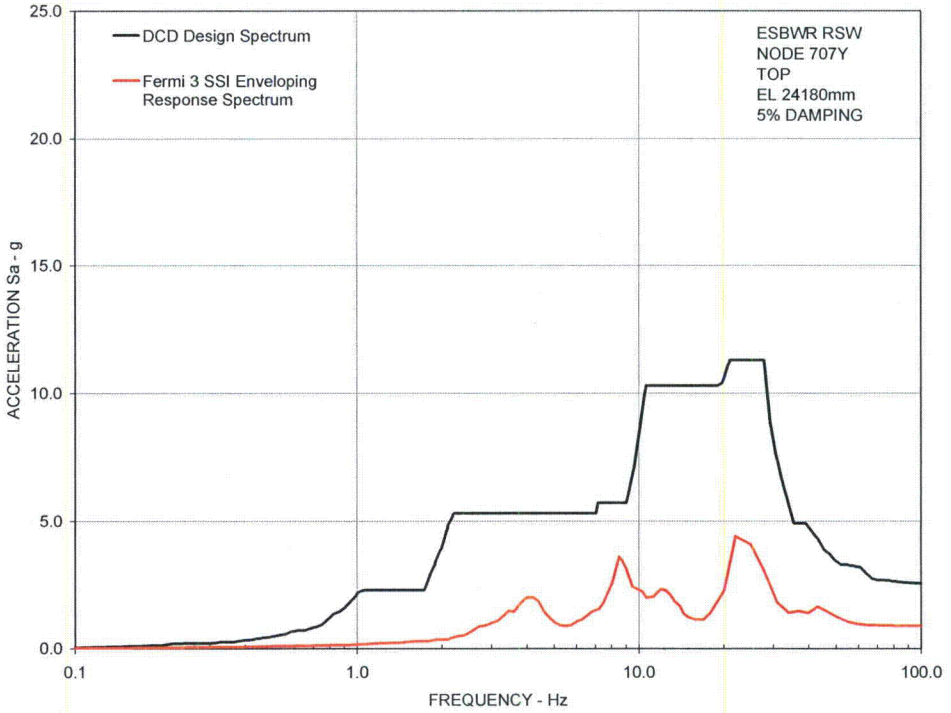

Figure 11 Comparison of Floor Response Spectra - RPV Top in Y-Direction

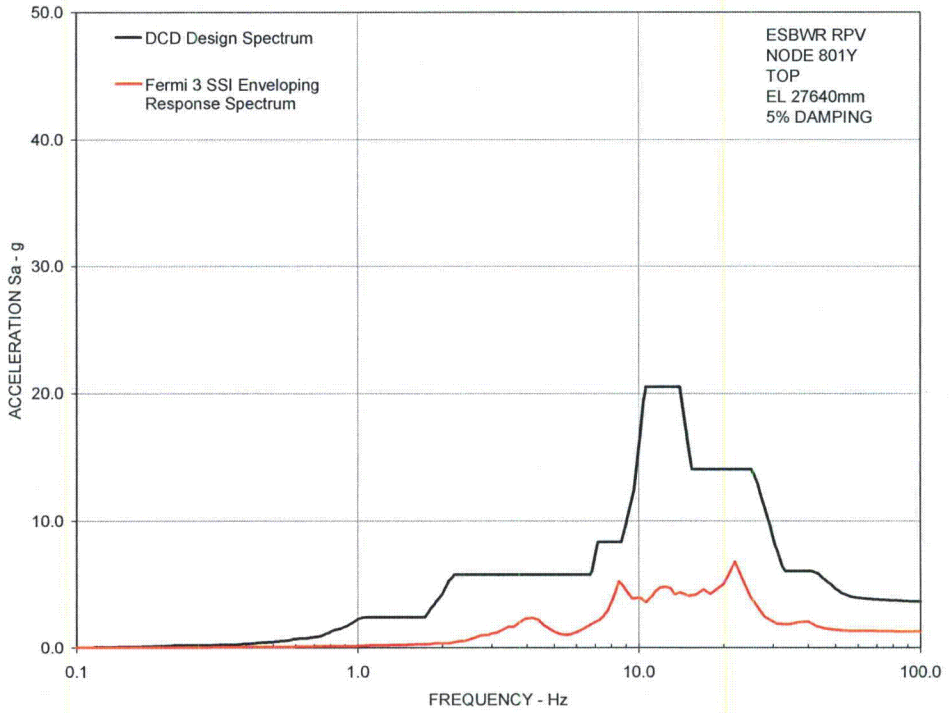

Figure 12 Comparison of Floor Response Spectra - RB/FB Basemat in Y-Direction

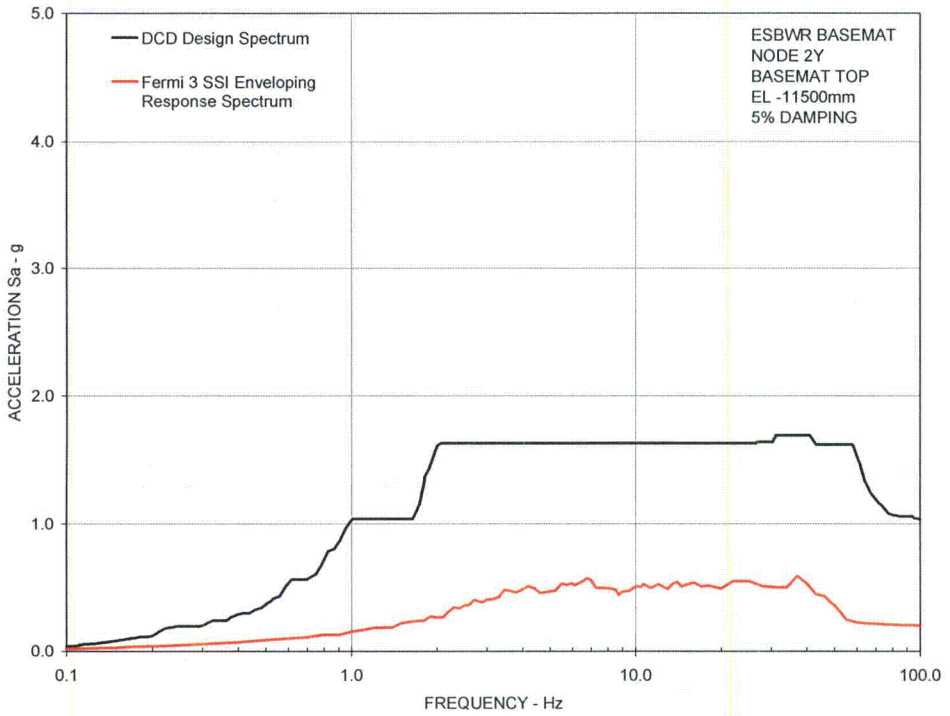

Figure 13 Comparison of Floor Response Spectra - RB/FB Refueling Floor in Z-Direction

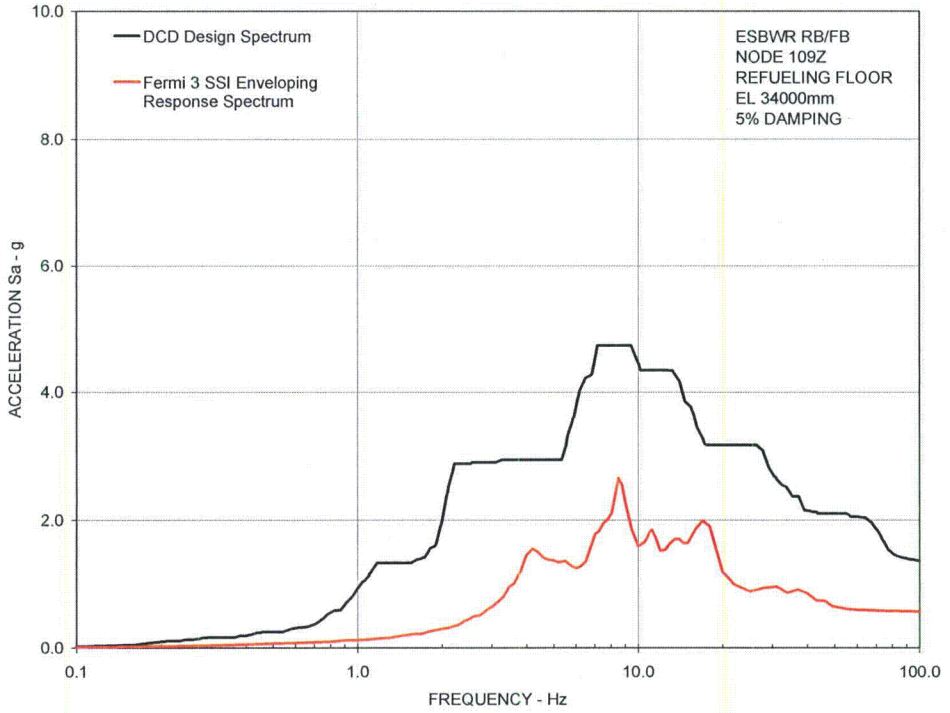

Figure 14 Comparison of Floor Response Spectra - RCCV Top Slab in Z-Direction

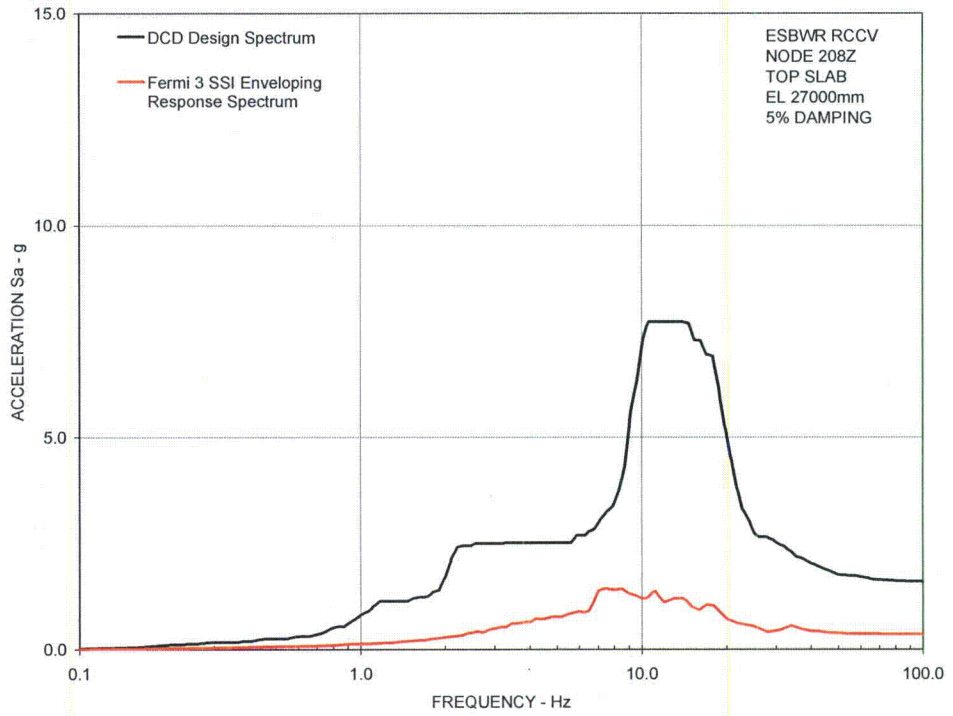

Figure 15 Comparison of Floor Response Spectra - Vent Wall Top in Z-Direction

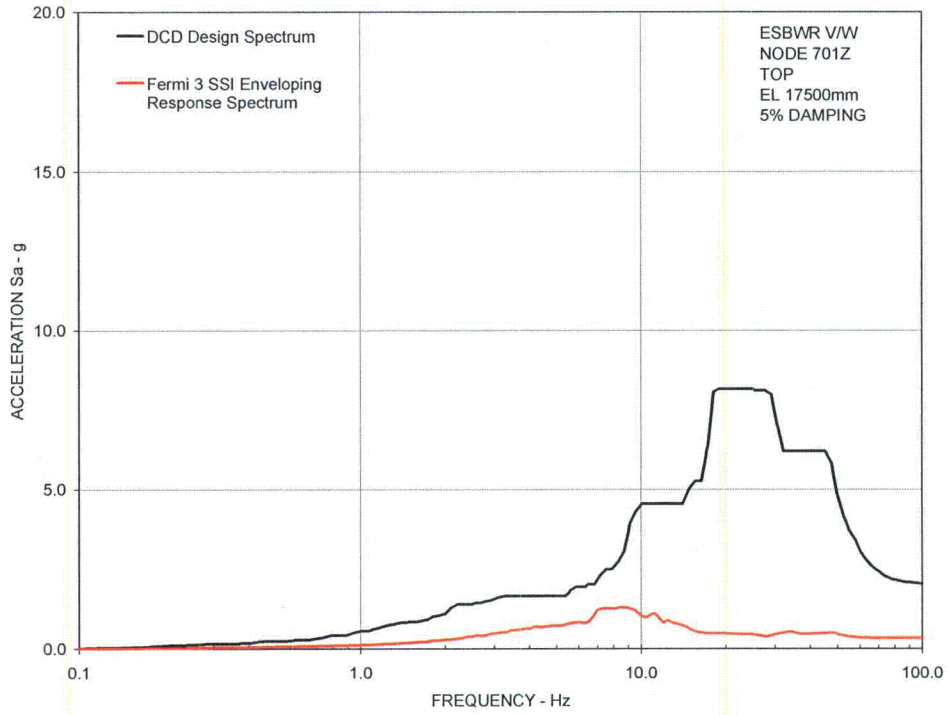

Figure 16 Comparison of Floor Response Spectra - RSW Top in Z-Direction

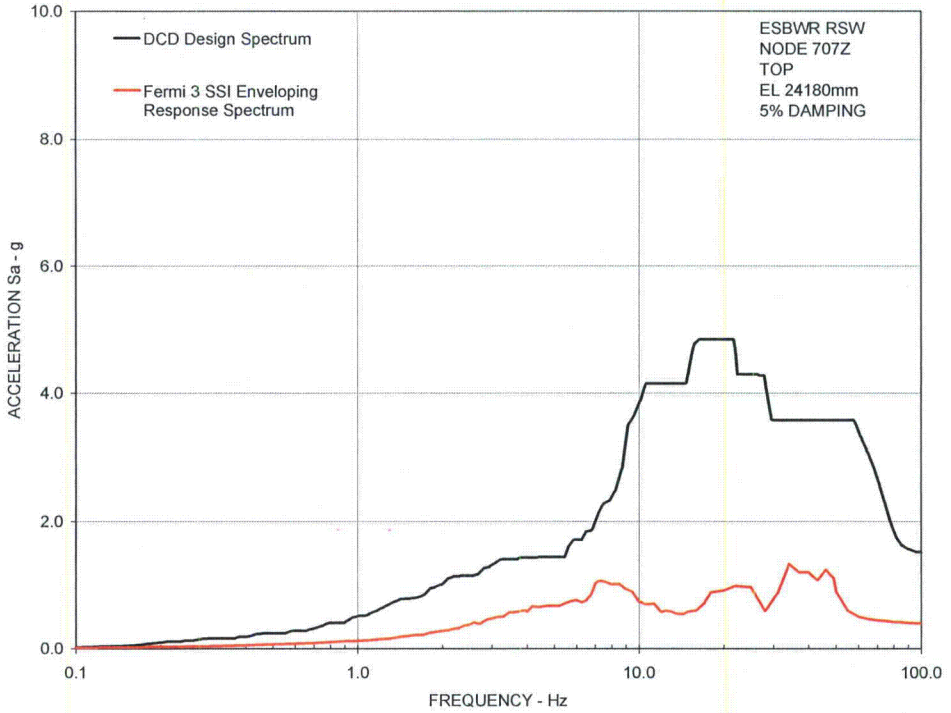

Figure 17 Comparison of Floor Response Spectra - RPV Top in Z-Direction

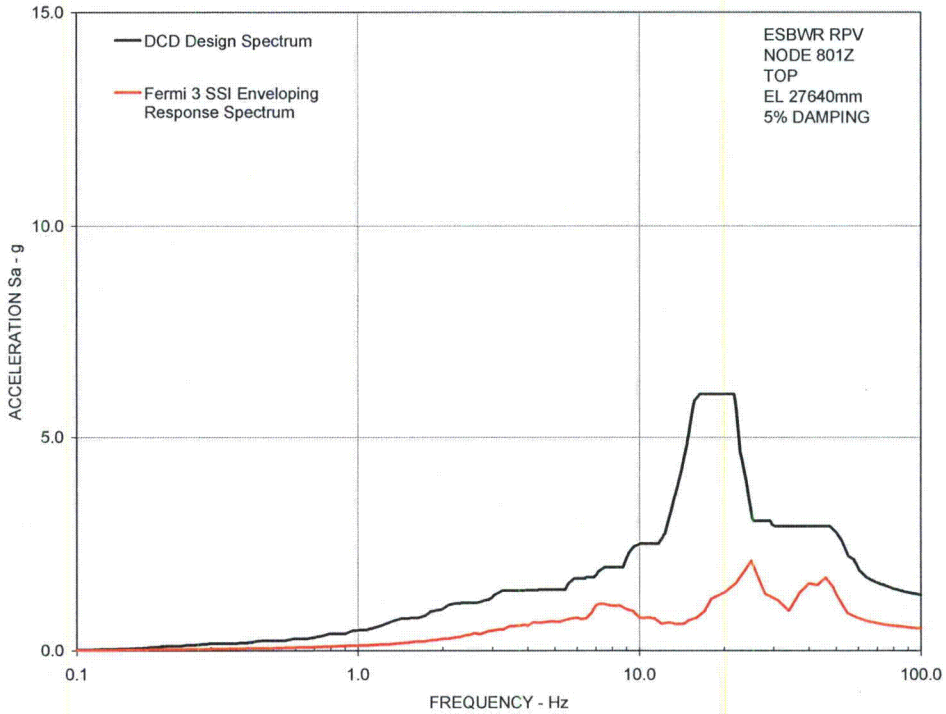

Figure 18 Comparison of Floor Response Spectra - RB/FB Basemat in Z-Direction

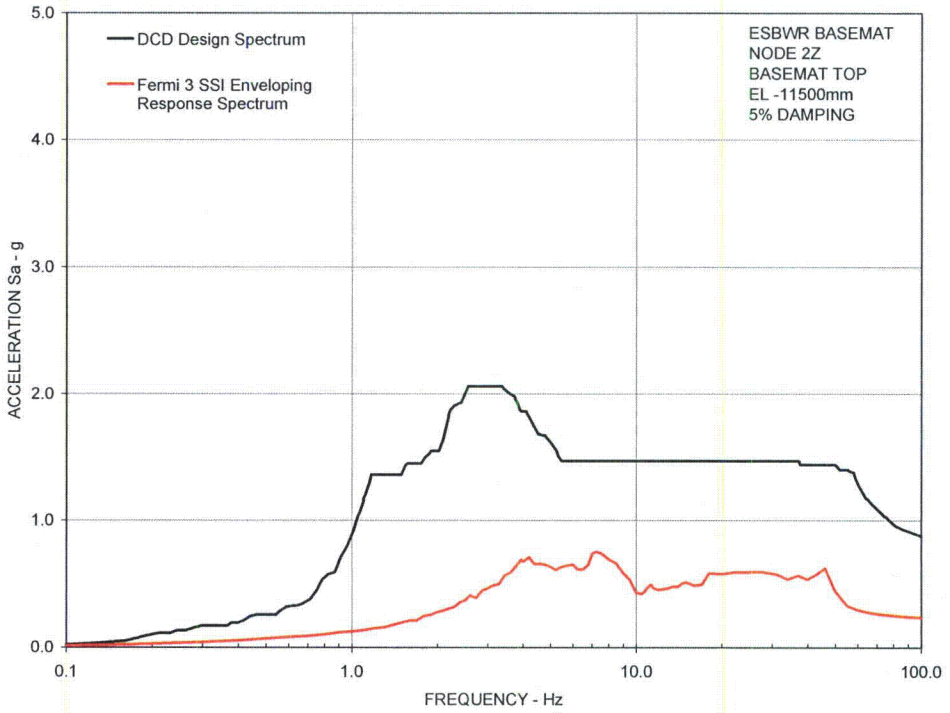

Figure 19 Comparison of Floor Response Spectra - CB Top in X-Direction

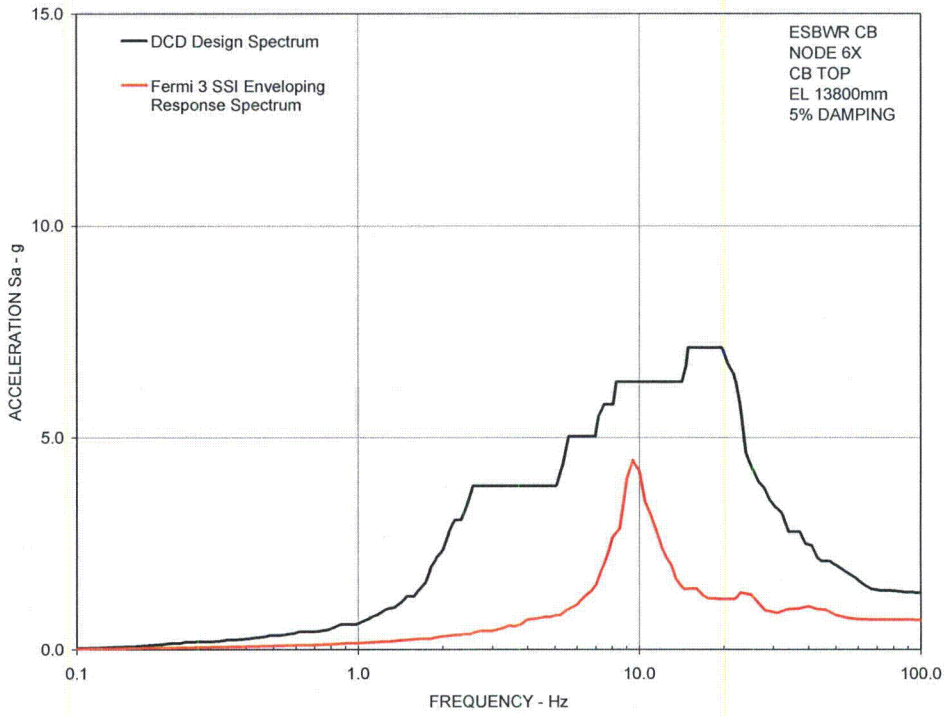

Figure 20 Comparison of Floor Response Spectra - CB Basemat in X-Direction

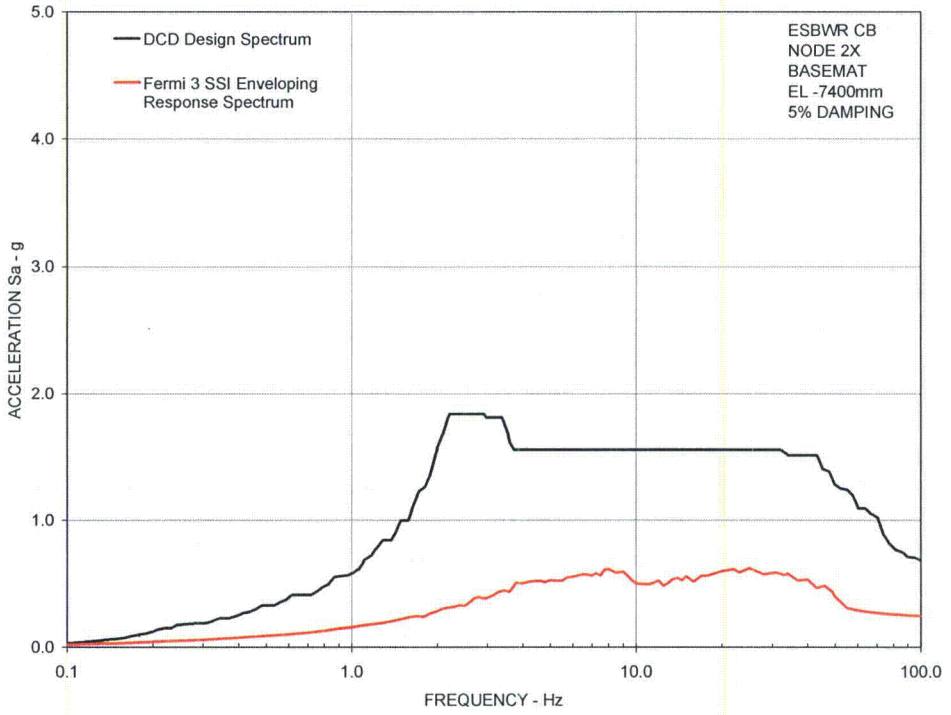

Figure 21 Comparison of Floor Response Spectra - CB Top in Y-Direction

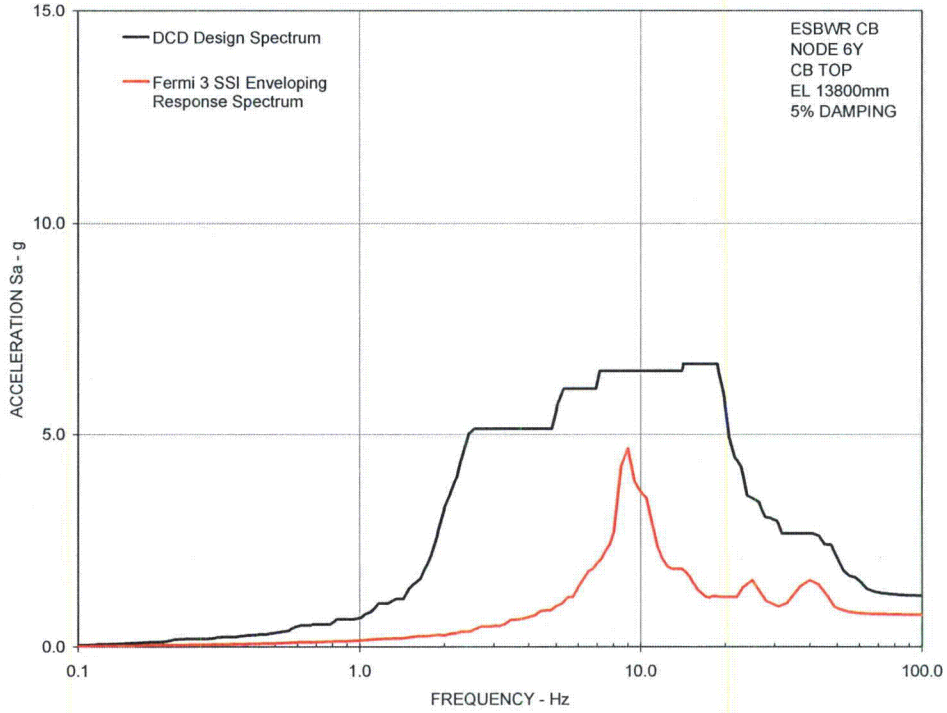

Figure 22 Comparison of Floor Response Spectra - CB Basemat in Y-Direction

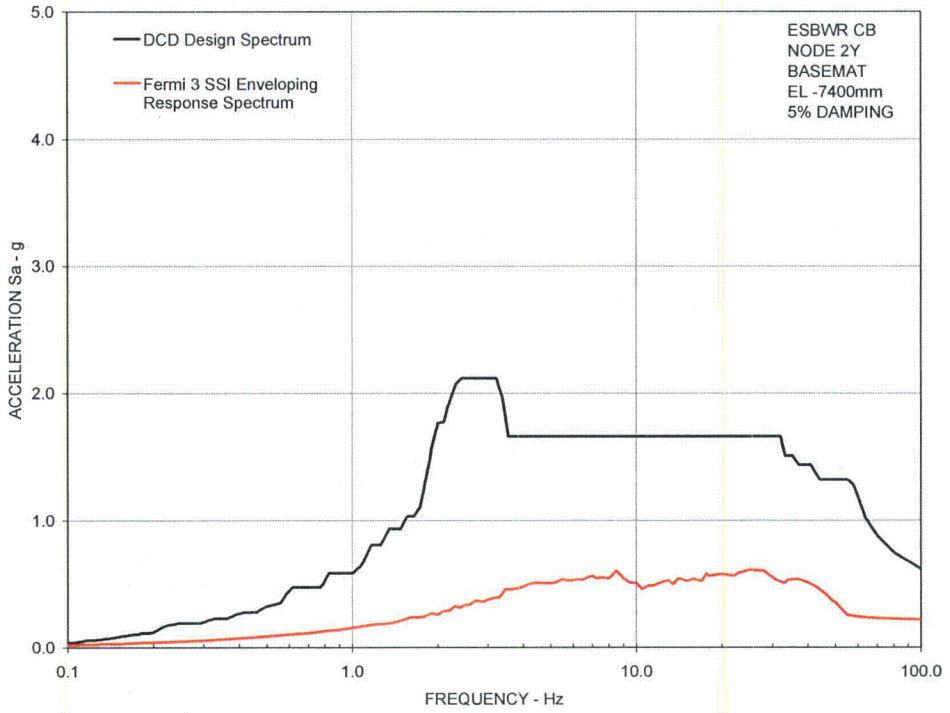

Figure 23 Comparison of Floor Response Spectra - CB Top in Z-Direction

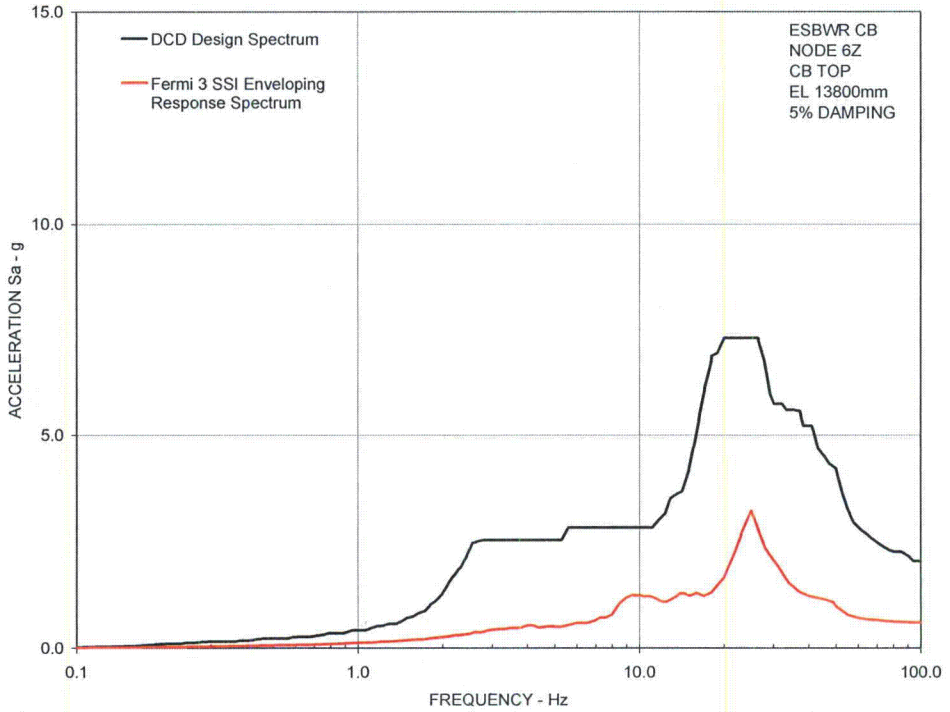

Figure 24 Comparison of Floor Response Spectra - CB Basemat in Z-Direction

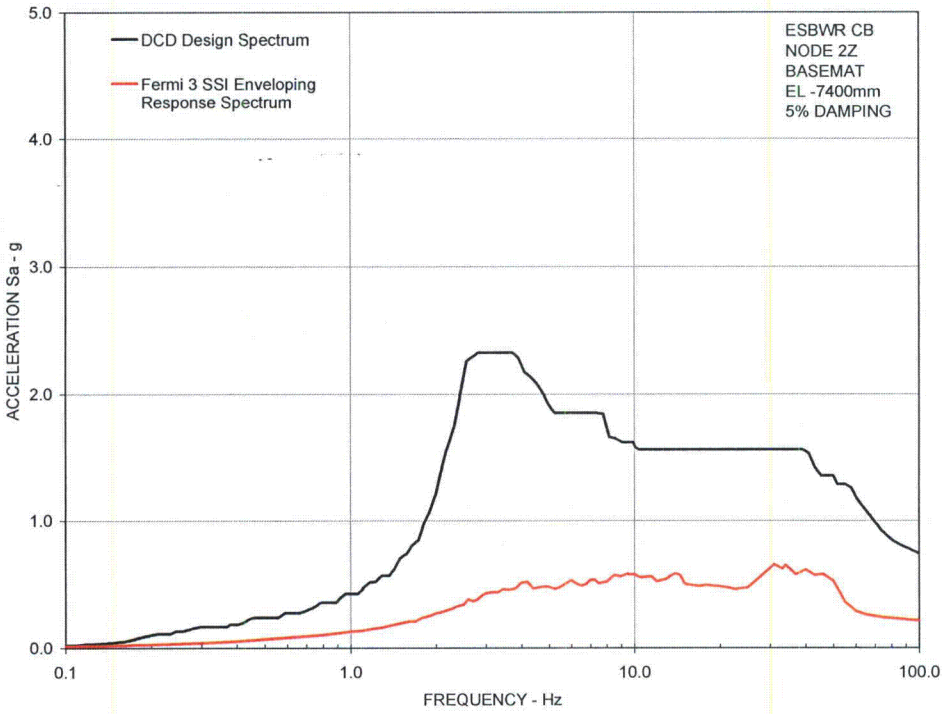

Figure 25 SSI Lateral Soil Pressure RB/FB

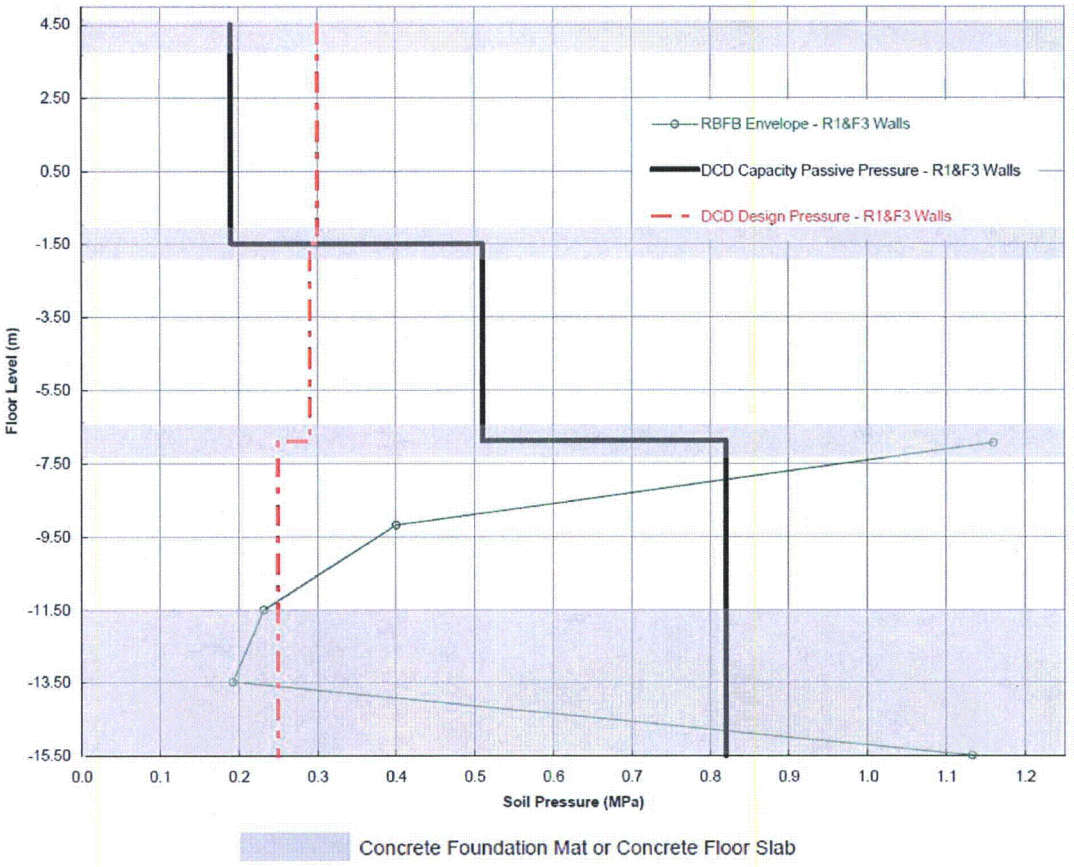

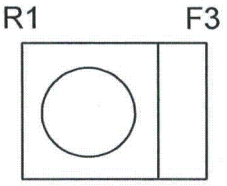

(a) Licensing Basis Envelope – Walls on Column Rows R1 and F3

Figure 26 SSI Lateral Soil Pressure RB/FB

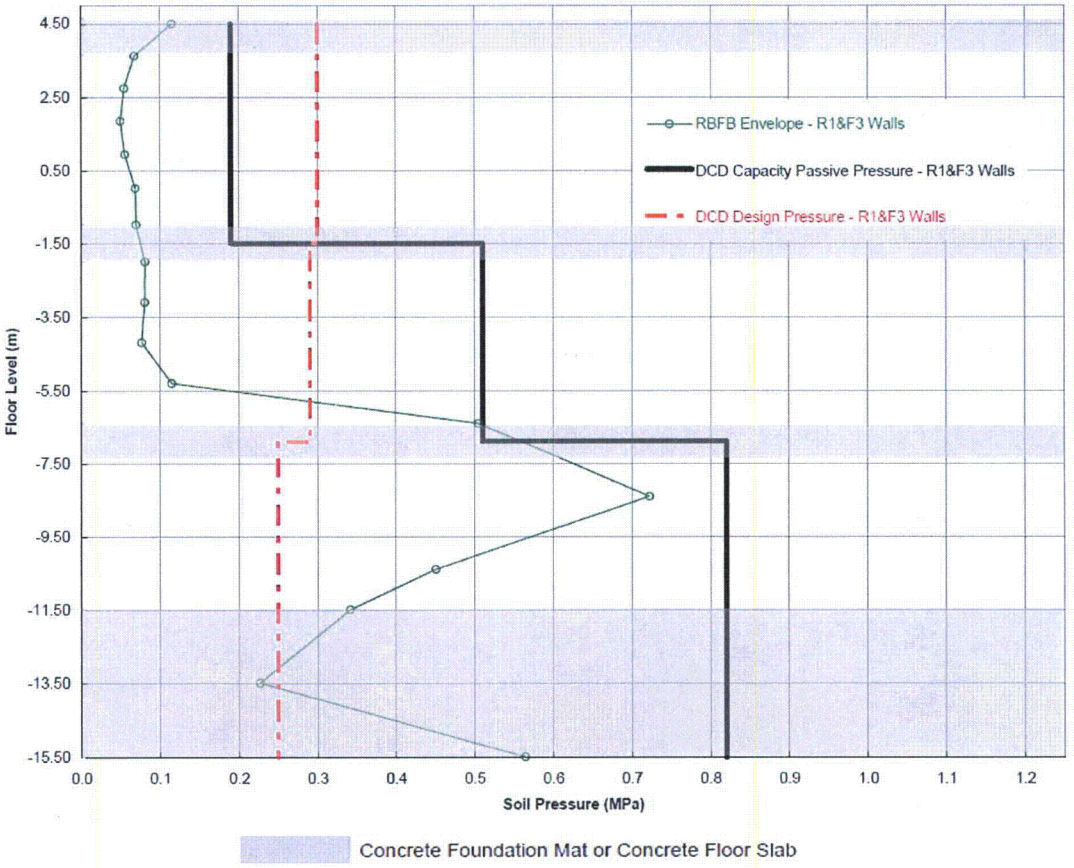

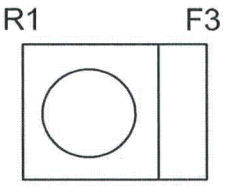

(b) Engineered Backfill Envelope – Walls on Column Rows R1 and F3

Figure 27 SSI Lateral Soil Pressure RB/FB

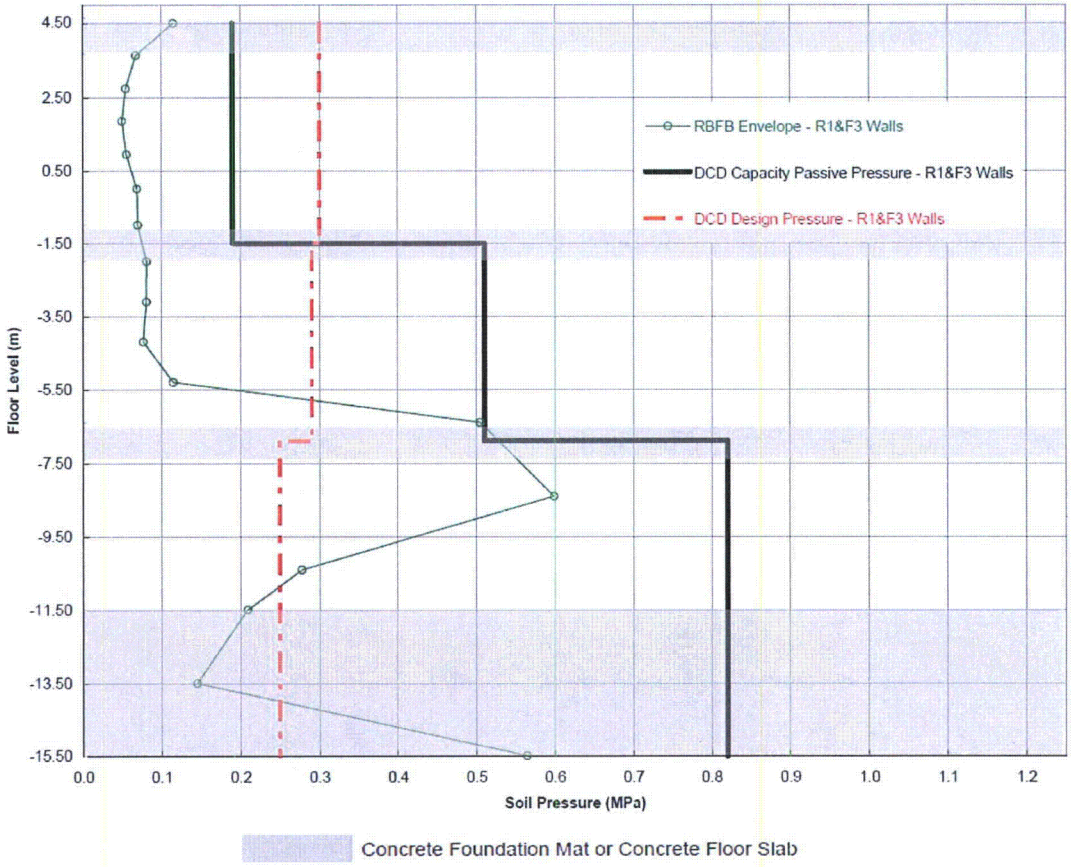

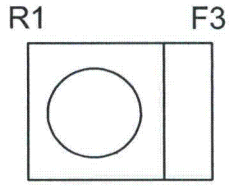

(c) Engineered Backfill – UB Rock/Soil Profile – Walls on Column Rows R1 and F3

Figure 28 SSI Lateral Soil Pressure RB/FB

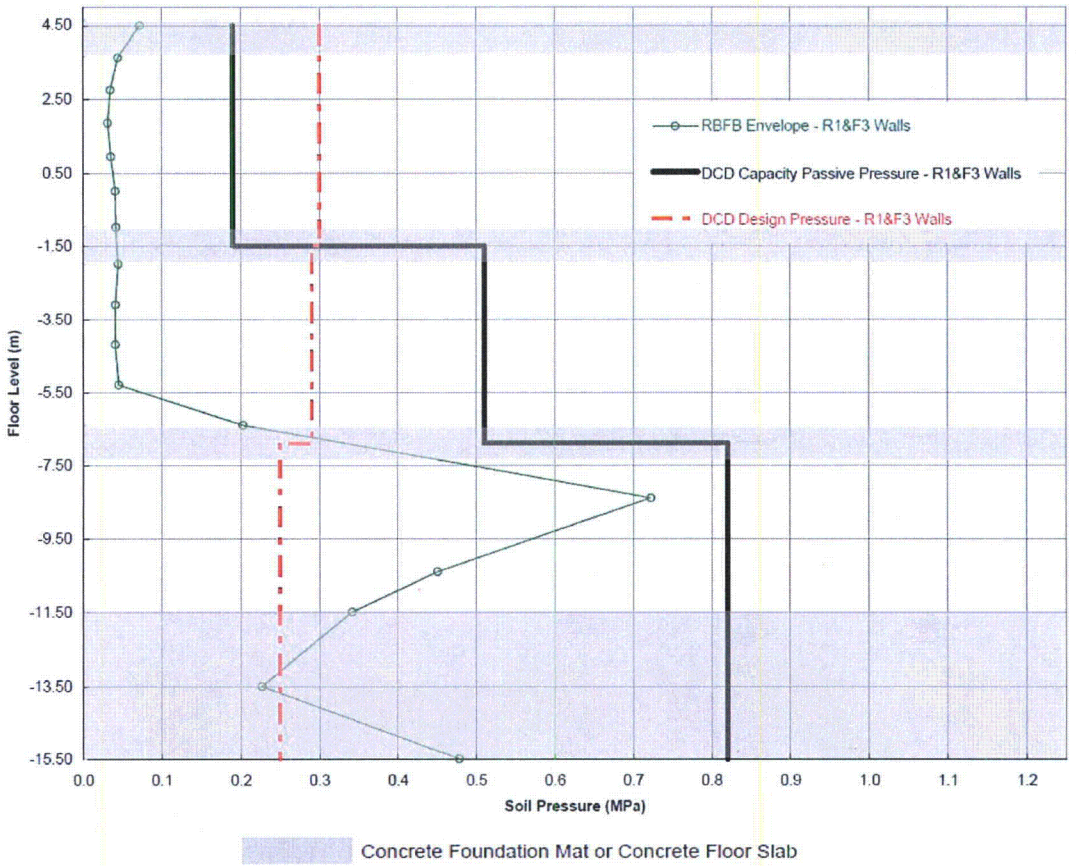

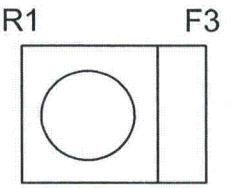

(d) Engineered Backfill – LB Rock/Soil Profile – Walls on Column Rows R1 and F3

Figure 29 SSI Lateral Soil Pressure RB/FB

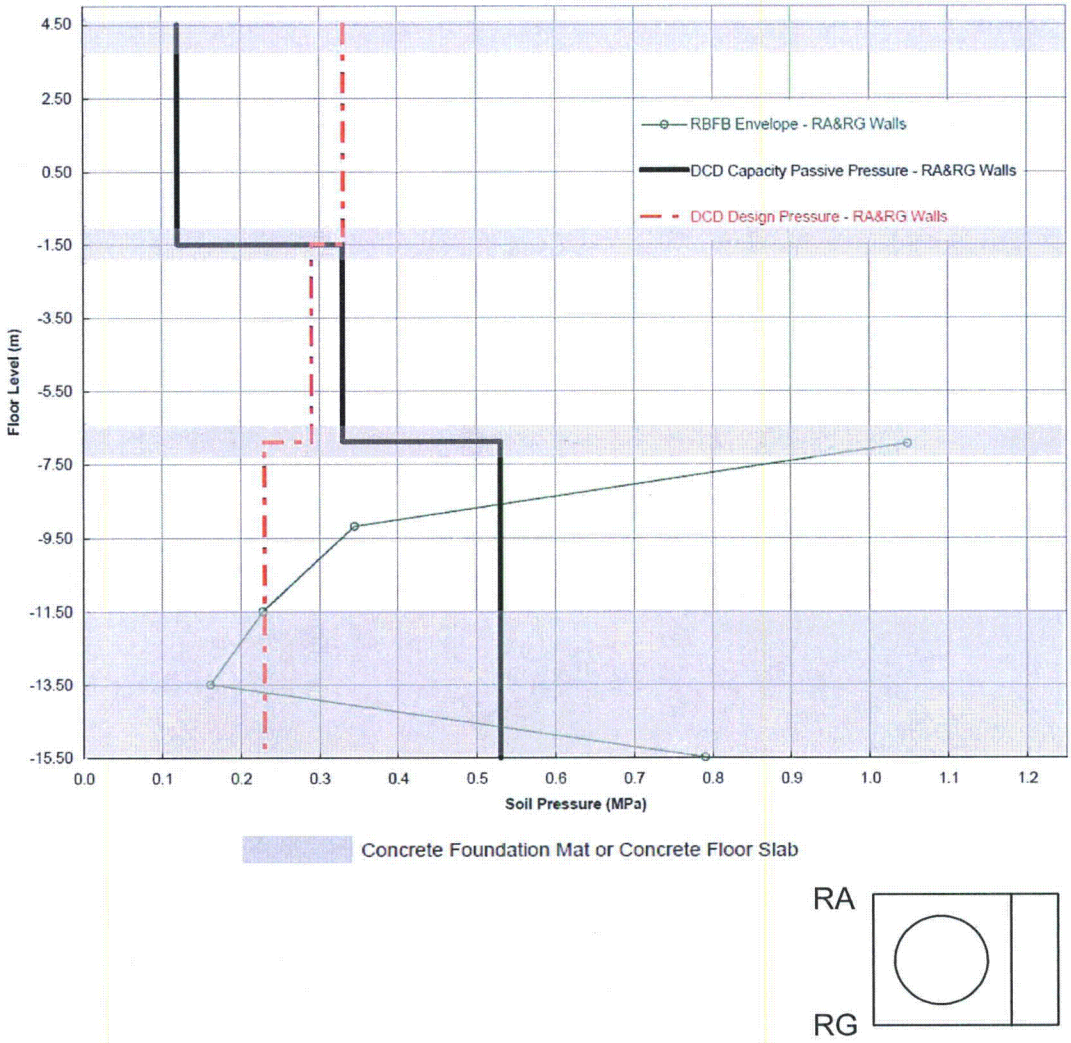

(e) Licensing Basis Envelope – Walls on Column Rows RA and RG

Figure 30 SSI Lateral Soil Pressure RB/FB

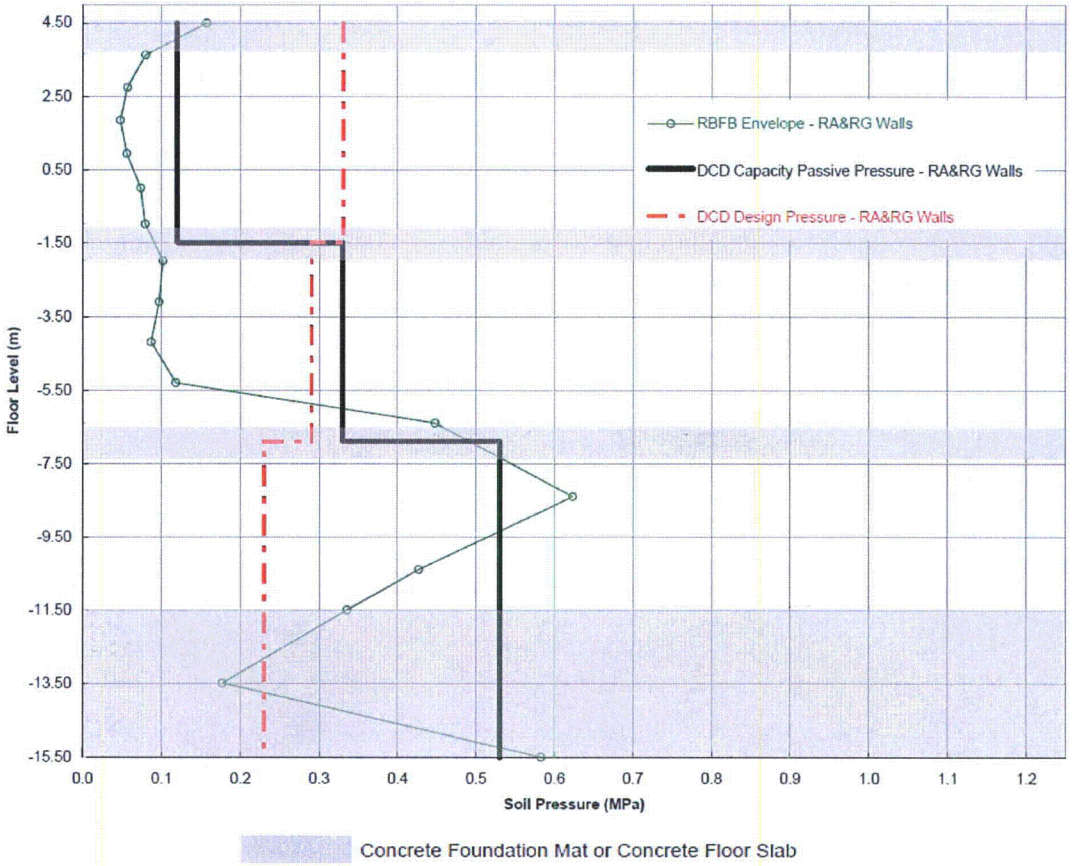

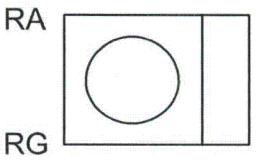

(f) Engineered Backfill Envelope – Walls on Column Rows RA and RG

Figure 31 SSI Lateral Soil Pressure RB/FB

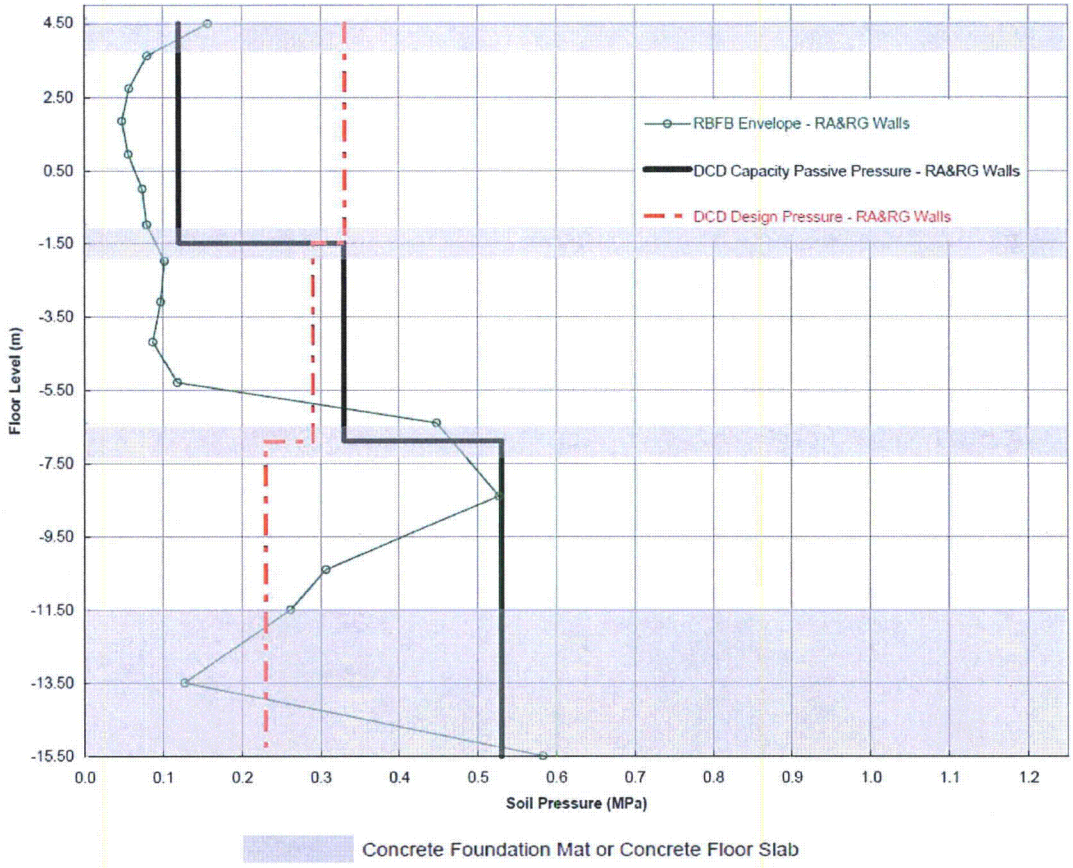

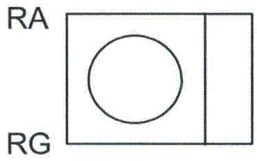

(g) Engineered Backfill – UB Rock/Soil Profile – Walls on Column Rows RA and RG

Figure 32 SSI Lateral Soil Pressure RB/FB

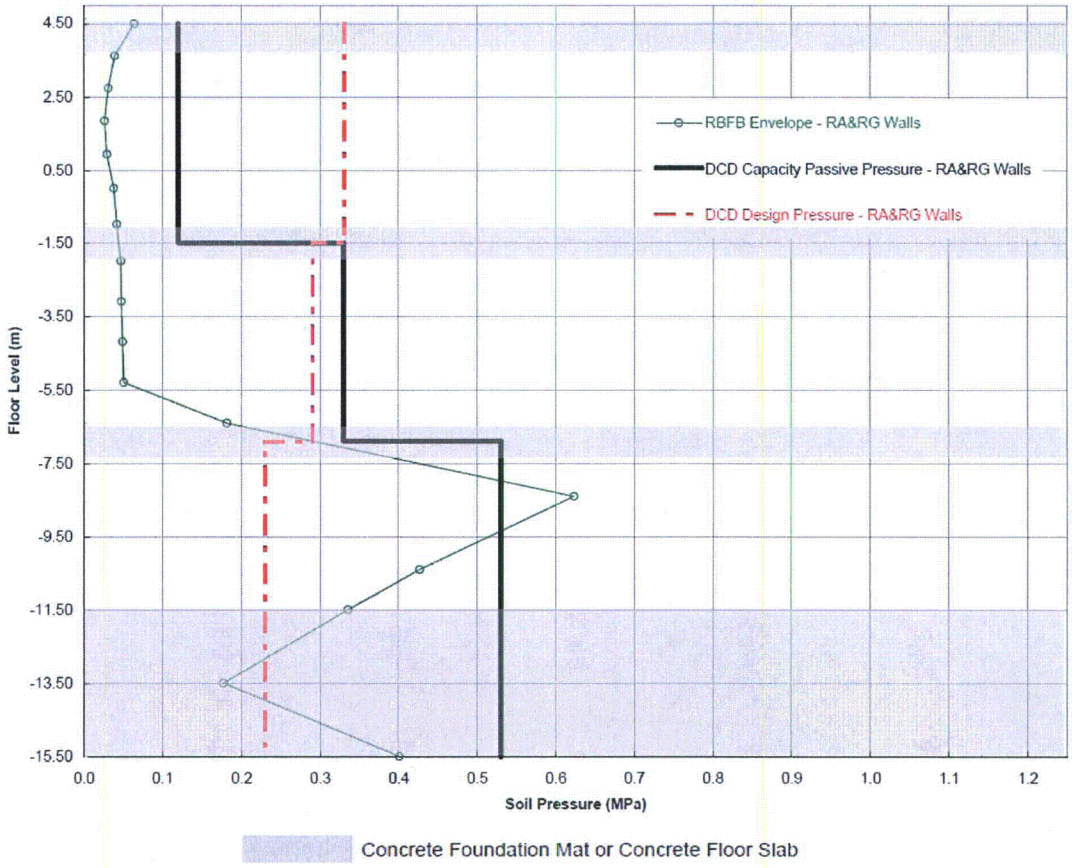

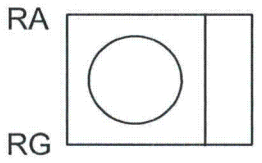

(h) Engineered Backfill – LB Rock/Soil Profile – Walls on Column Rows RA and RG

Figure 33 SSI Lateral Soil Pressure CB

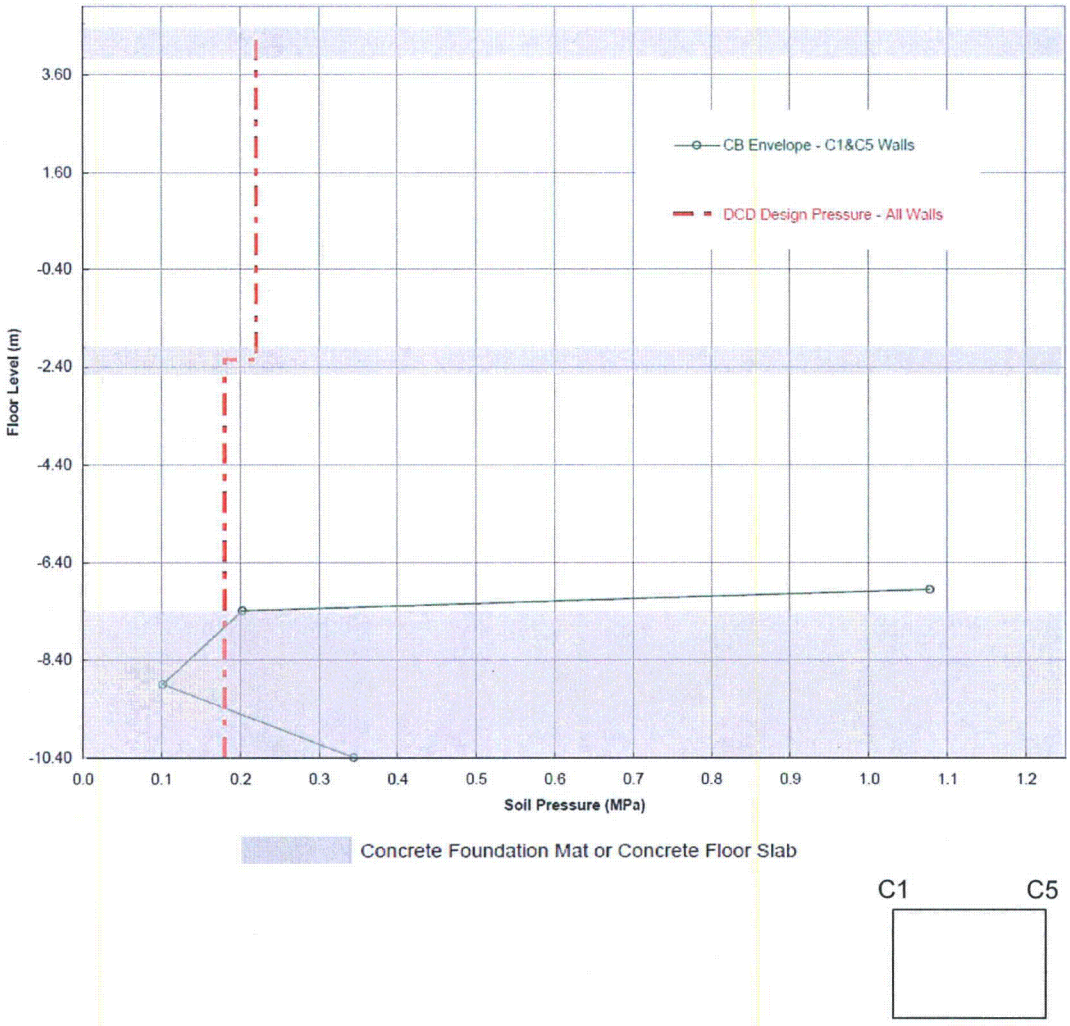

(a) Licensing Basis Envelope – Walls on Column Rows C1 and C5

Figure 34 SSI Lateral Soil Pressure CB

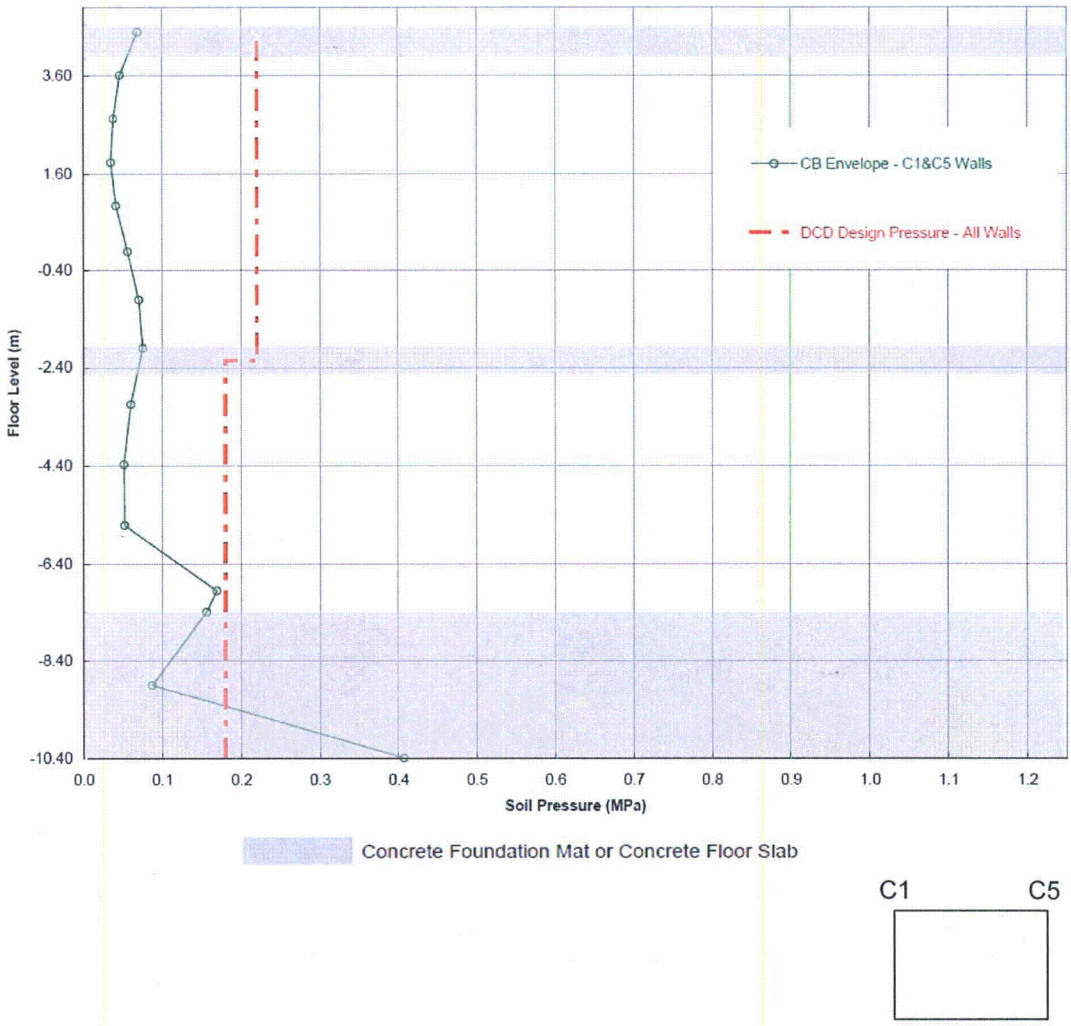

(b) Engineered Backfill Envelope – Walls on Column Rows C1 and C5

Figure 35 SSI Lateral Soil Pressure CB

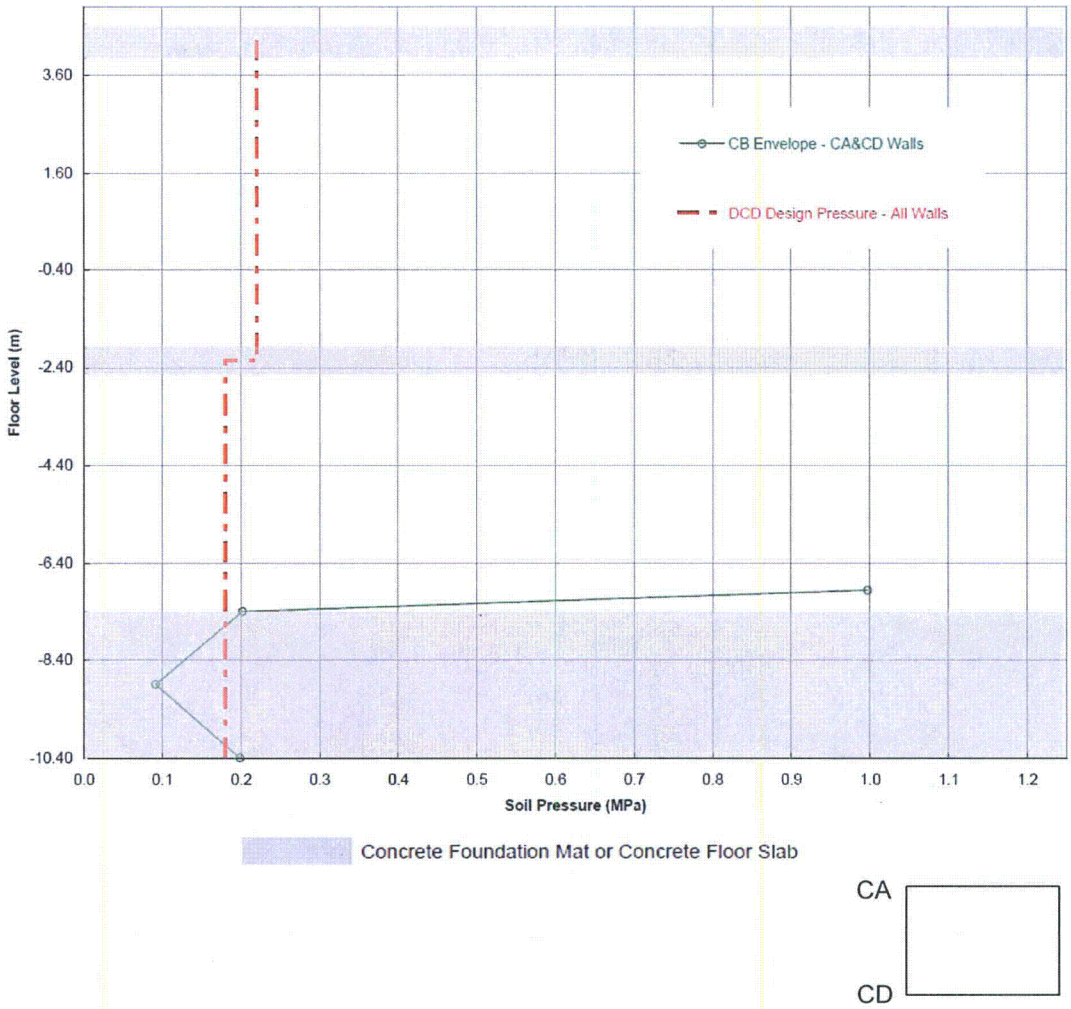

(c) Licensing Basis Envelope – Walls on Column Rows CA and CD

Figure 36 SSI Lateral Soil Pressure CB

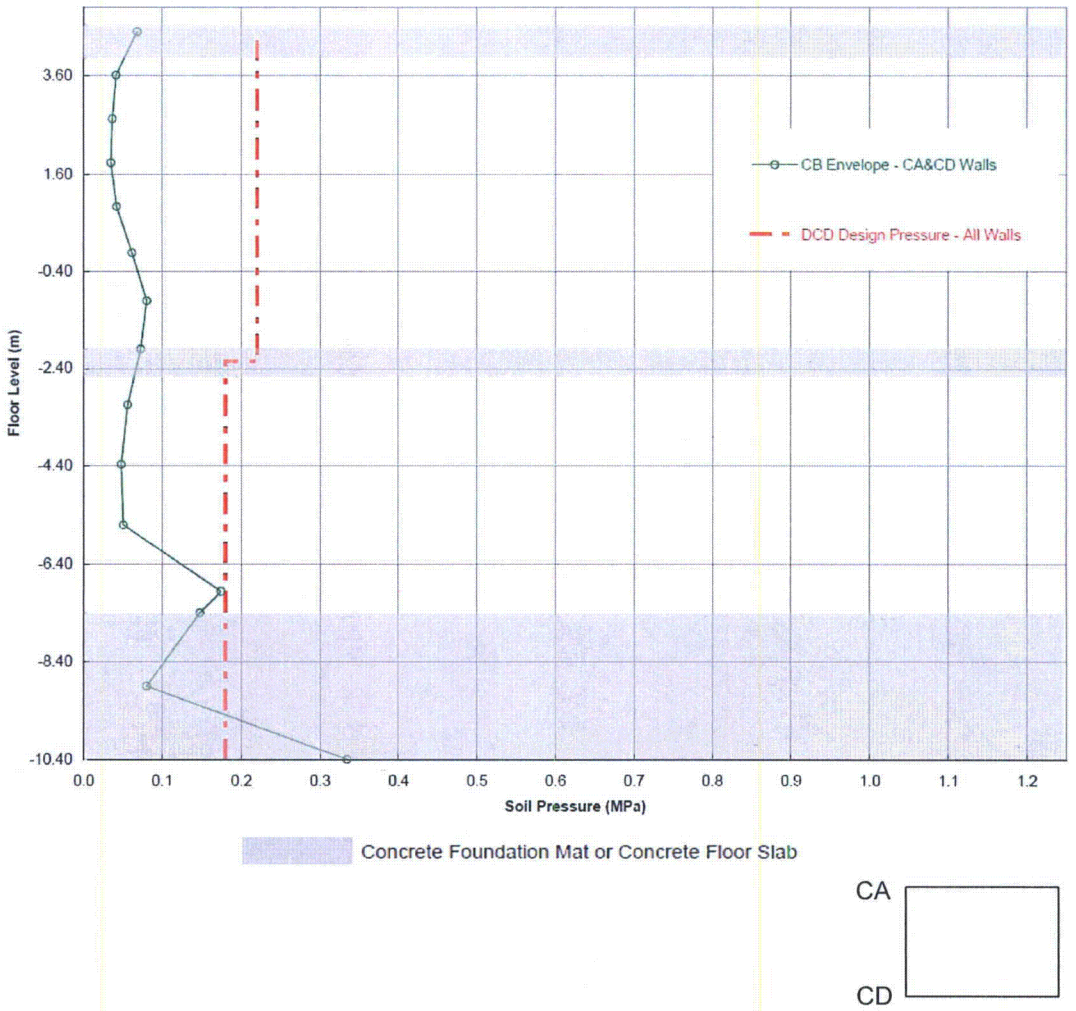

(d) Engineered Backfill Envelope – Walls on Column Rows CA and CD

Figure 37 SSSI Lateral Soil Pressure CB

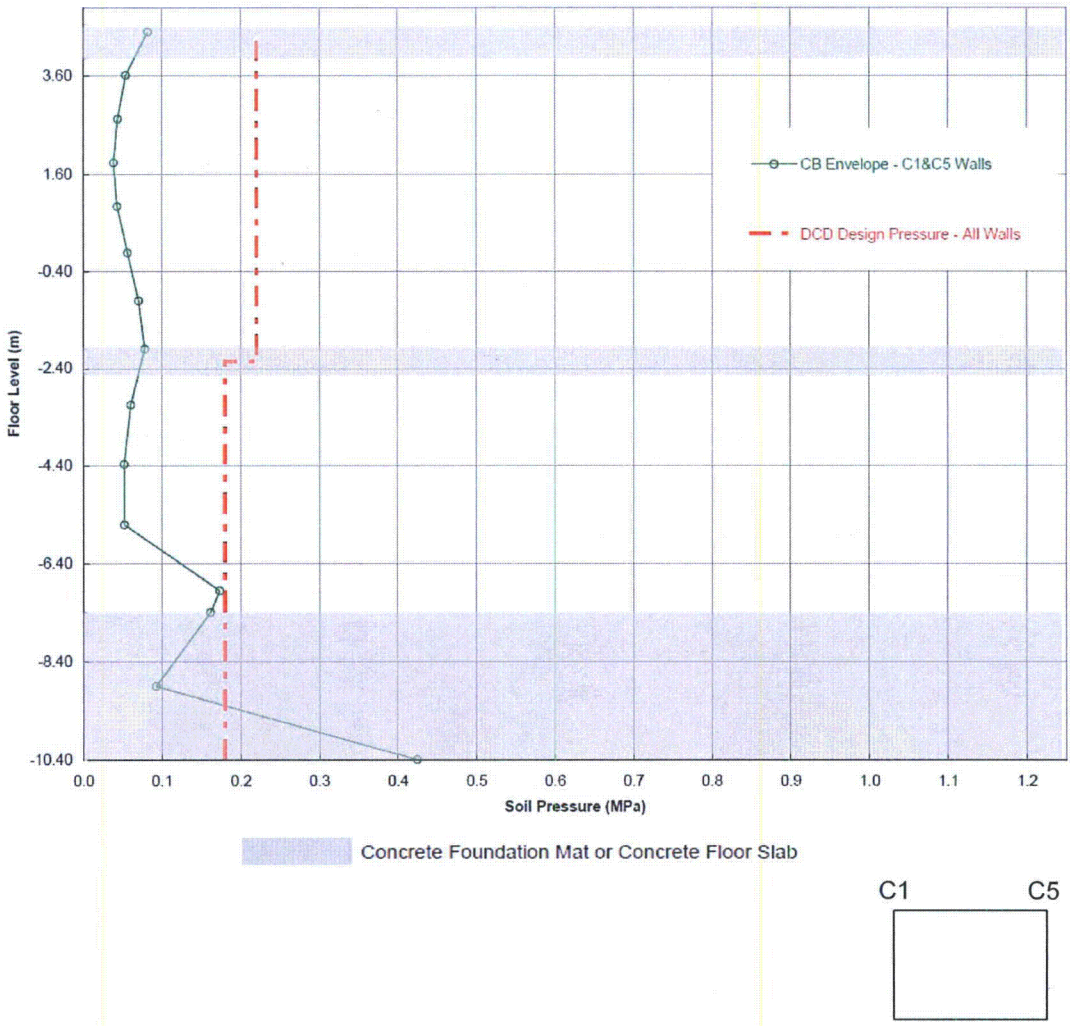

(a) Engineered Backfill Envelope – Walls on Column Rows C1 and C5

Figure 38 SSSI Lateral Soil Pressure CB

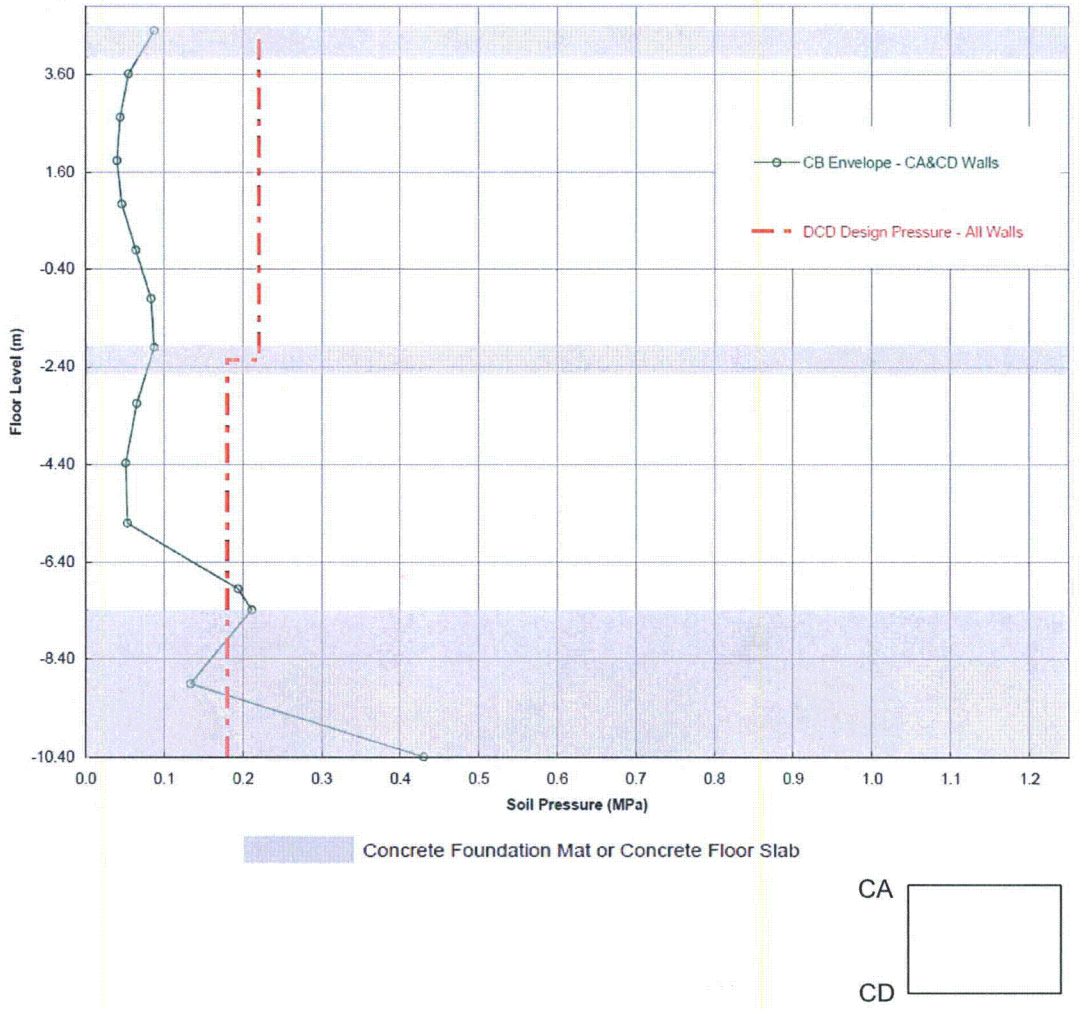

(b) Engineered Backfill Envelope – Walls on Column Rows CA and CD

Figure 39: Comparison of floor slab oscillator response spectra – Control Building (EL +13.8 m), DCD node 9001, z direction

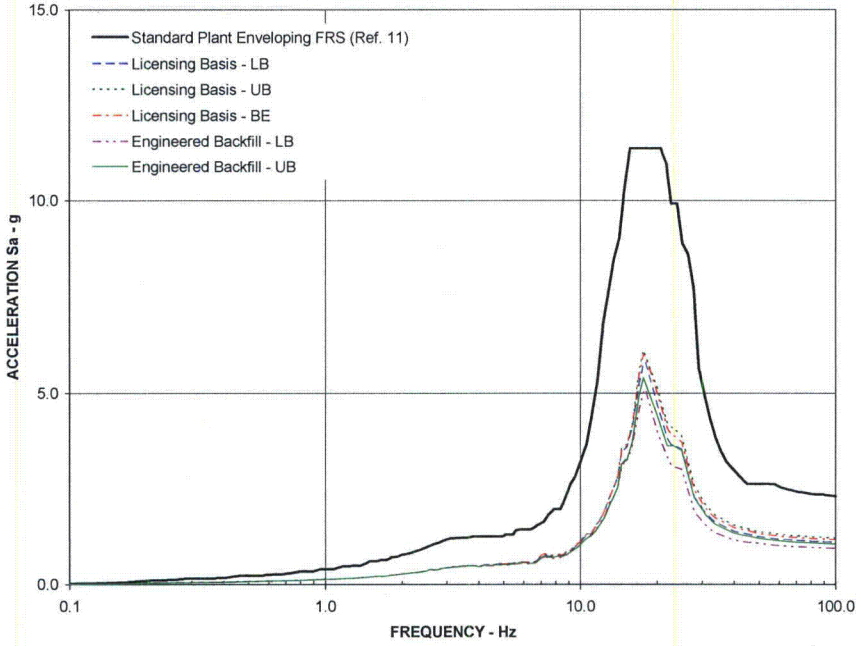

Figure 40: Comparison of floor slab oscillator response spectra – Control Building (EL +13.8 m), DCD node 9002, z direction

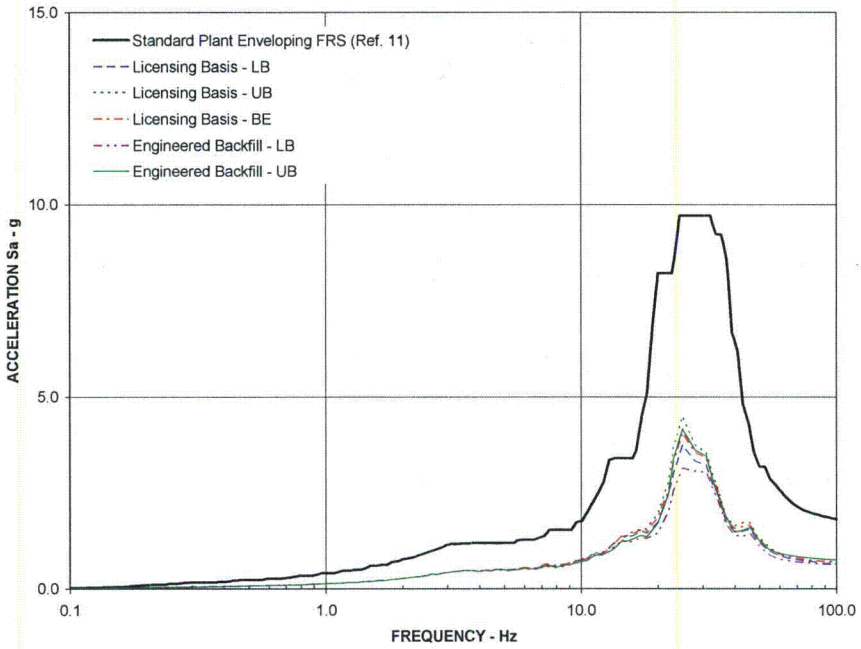

Figure 41: Comparison of floor slab oscillator response spectra – Control Building (EL +13.8 m), DCD node 9003, z direction

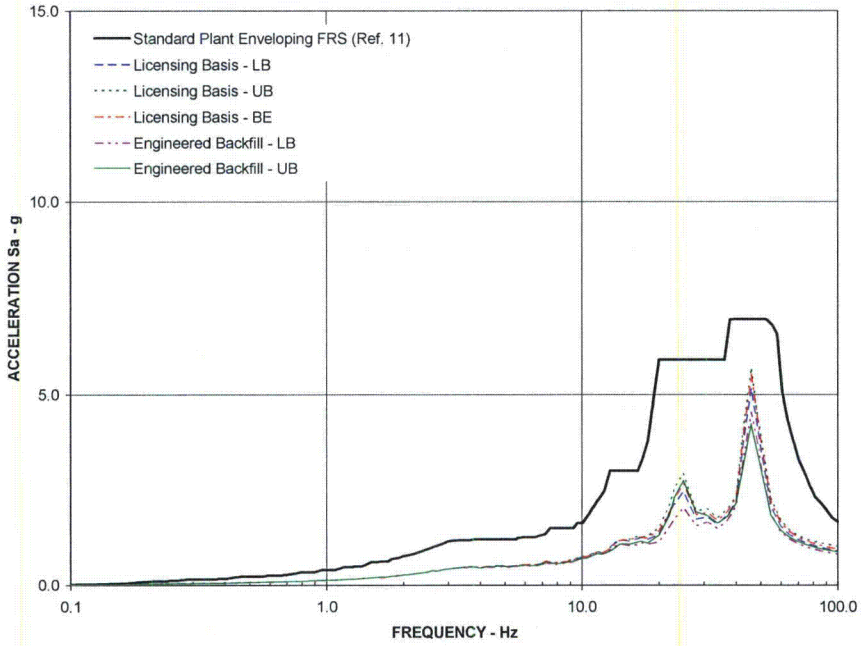

Figure 42: Comparison of floor slab oscillator response spectra – Control Building (EL +9.06 m), DCD node 9101, z direction

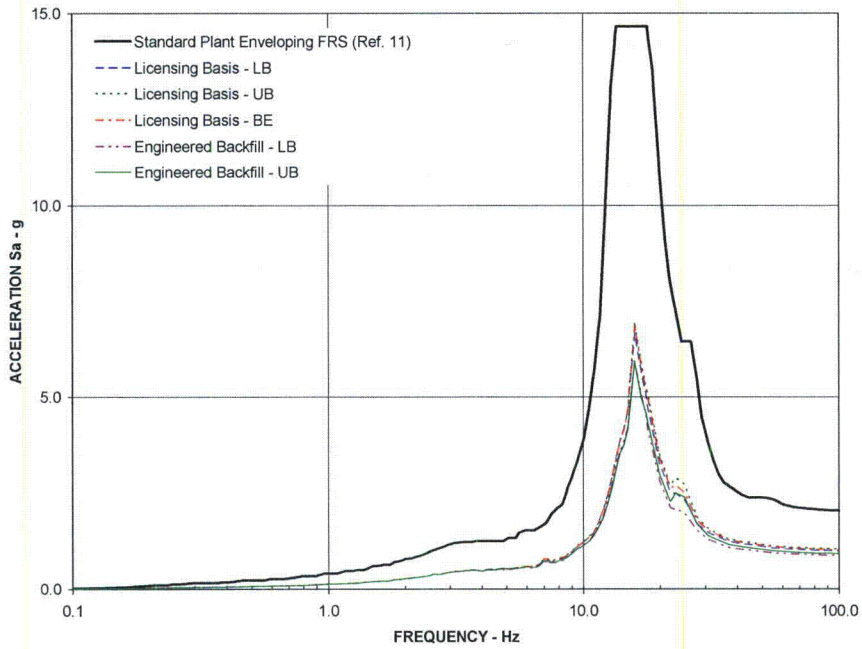

Figure 43: Comparison of floor slab oscillator response spectra – Control Building (EL +9.06 m), DCD node 9102, z direction

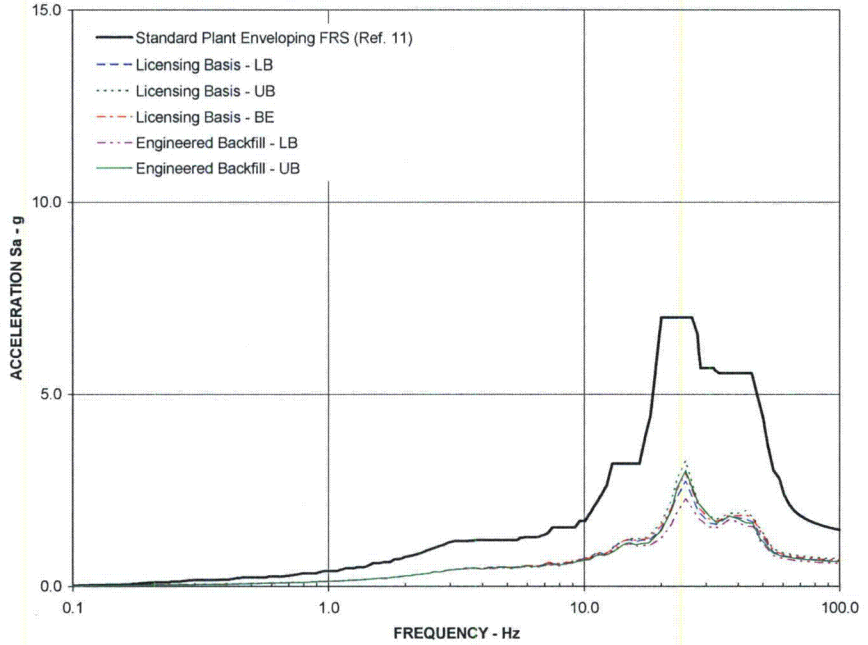

Figure 44: Comparison of floor slab oscillator response spectra – Control Building (EL +9.06 m), DCD node 9103, z direction

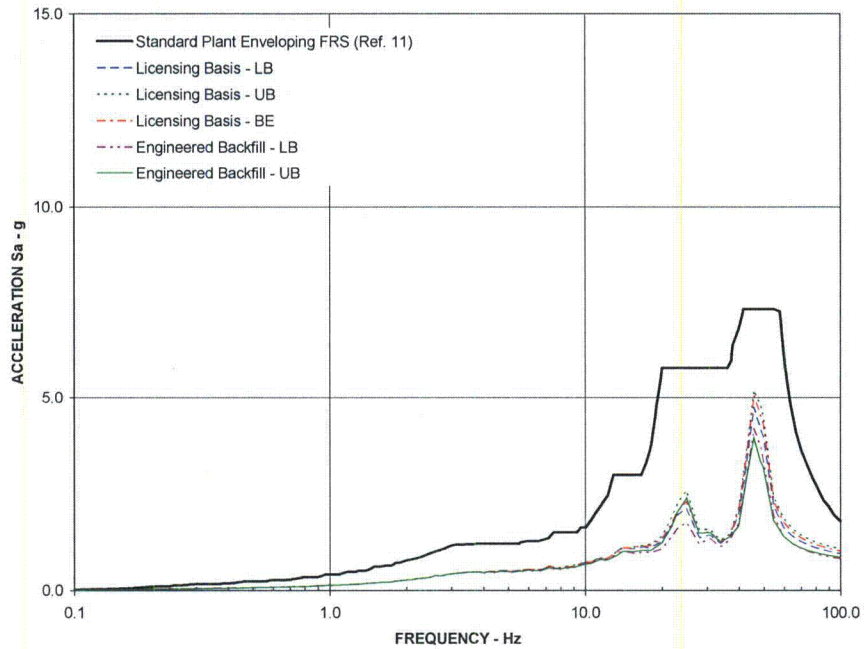

Figure 45: Comparison of floor slab oscillator response spectra – Control Building (EL +4.65 m), DCD node 9201, z direction

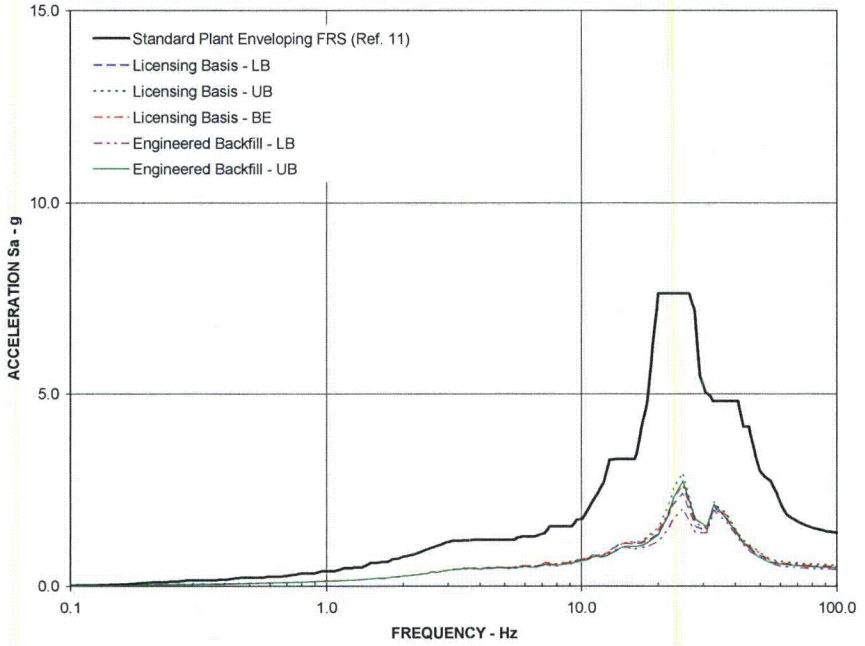

Figure 46: Comparison of floor slab oscillator response spectra – Control Building (EL +4.65 m), DCD node 9202, z direction

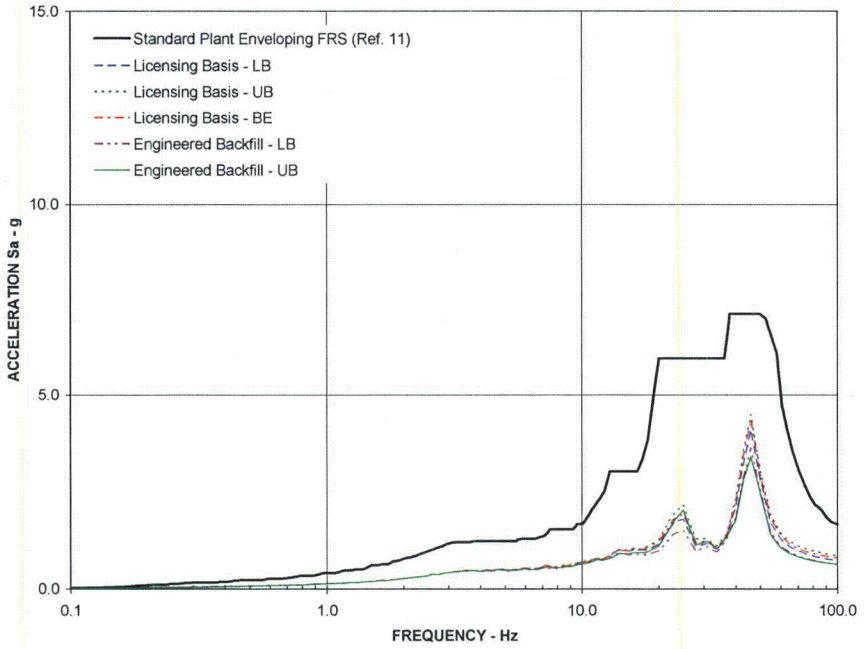

Figure 47: Comparison of floor slab oscillator response spectra – Control Building (EL -2.00 m), DCD node 9301, z direction

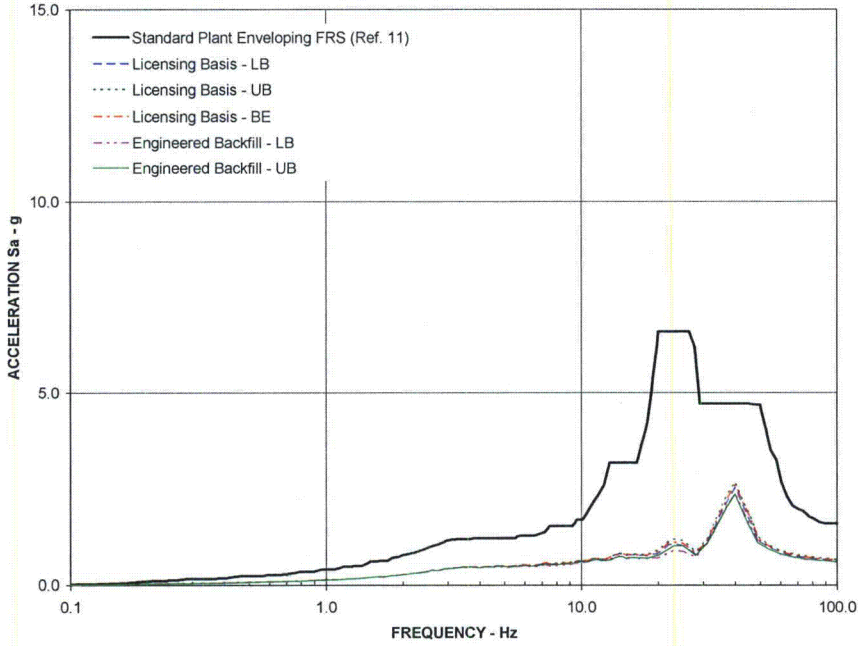

Figure 48: Comparison of floor slab oscillator response spectra – Reactor Building/Fuel Building (EL +52.4 m), DCD node 9101, z direction

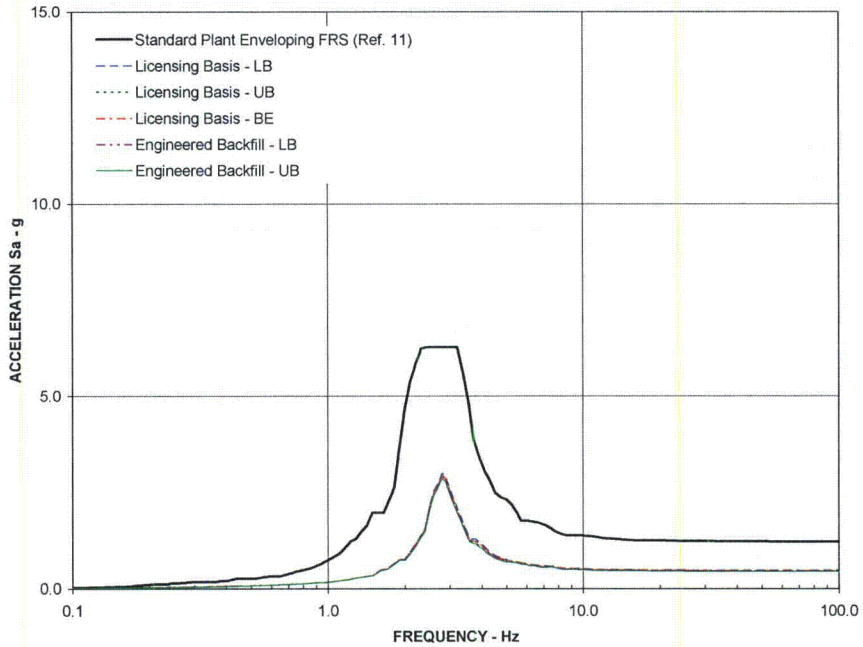

Figure 49: Comparison of floor slab oscillator response spectra – Reactor Building/Fuel Building (EL +52.4 m), DCD node 9102, z direction

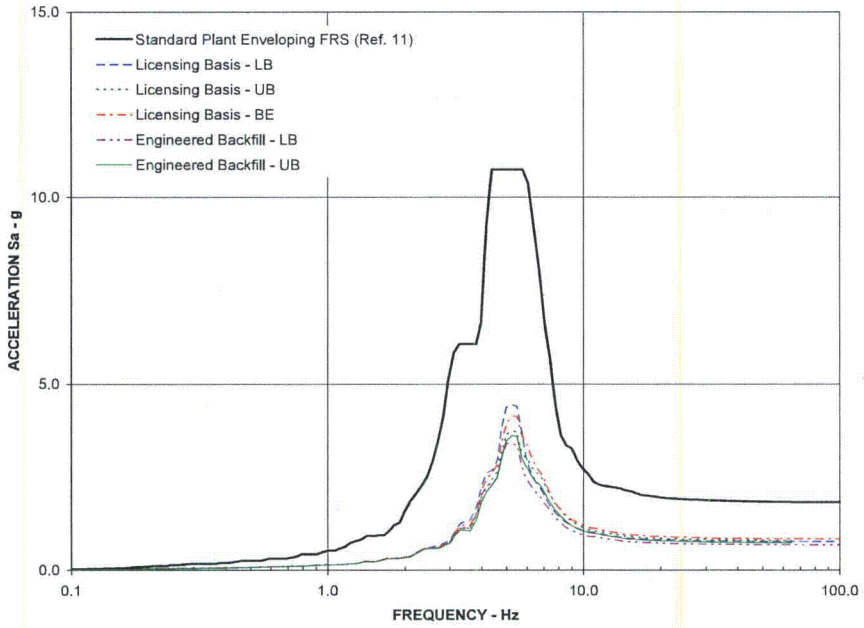

Figure 50: Comparison of floor slab oscillator response spectra – Reactor Building/Fuel Building (EL +52.4 m), DCD node 9103, z direction

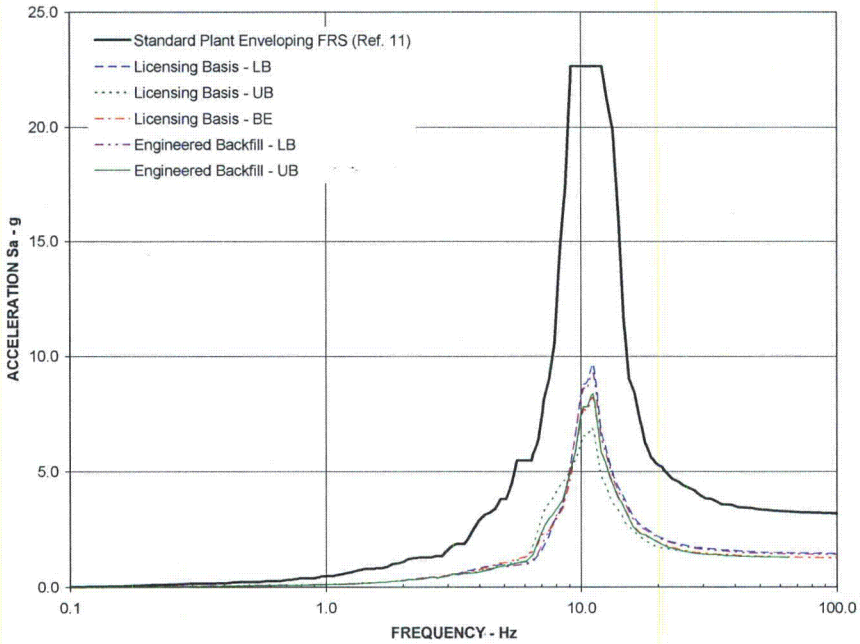

Figure 51: Comparison of floor slab oscillator response spectra – Reactor Building/Fuel Building (EL +52.4 m), DCD node 9104, z direction

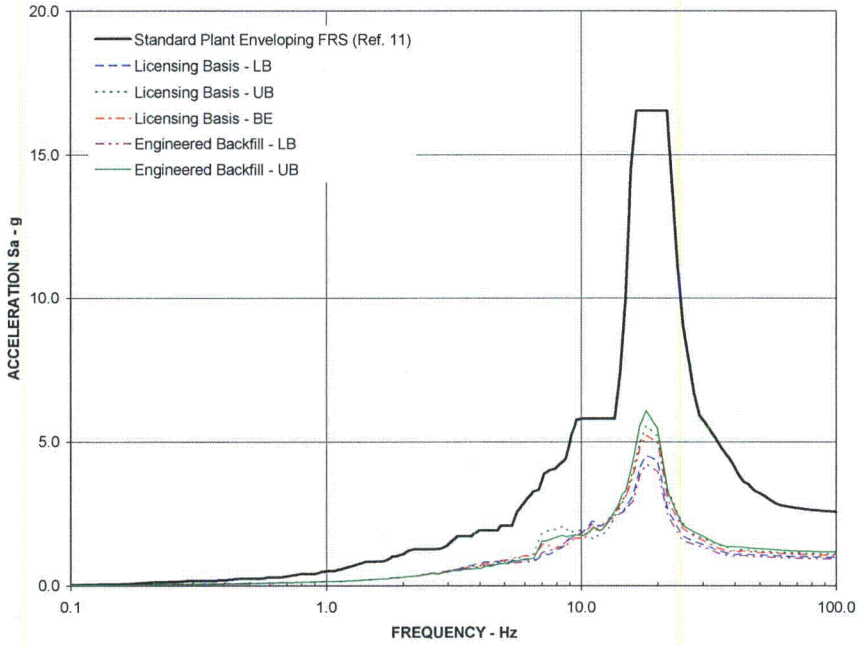

Figure 52: Comparison of floor slab oscillator response spectra – Reactor Building/Fuel Building (EL +52.4 m), DCD node 9105, z direction

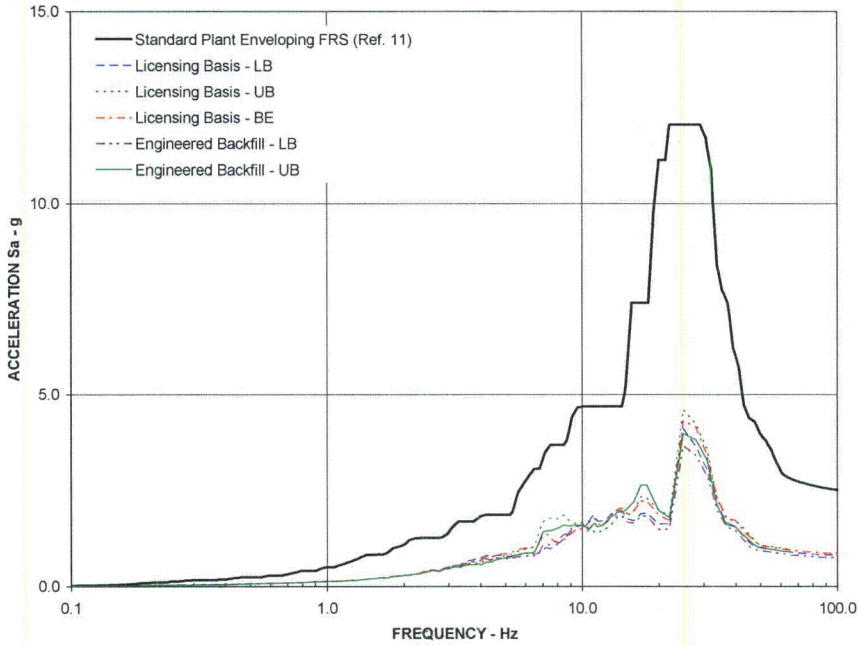

Figure 53: Comparison of floor slab oscillator response spectra – Reactor Building/Fuel Building (EL +52.4 m), DCD node 9106, z direction

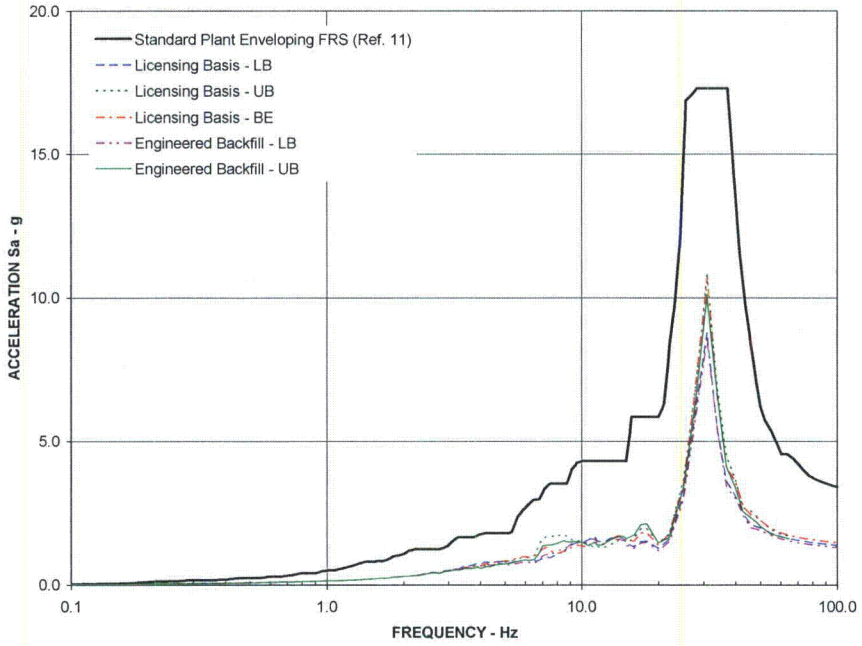

Figure 54: Comparison of floor slab oscillator response spectra – Reactor Building/Fuel Building (EL +52.4 m), DCD node 9107, z direction

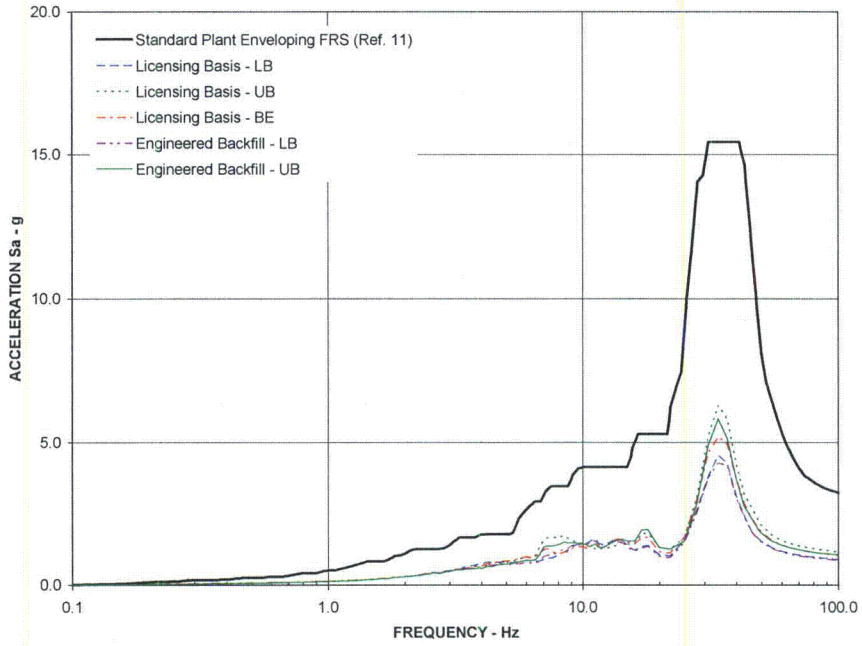

Figure 55: Comparison of floor slab oscillator response spectra – Reactor Building/Fuel Building (EL +52.4 m), DCD node 9108, z direction

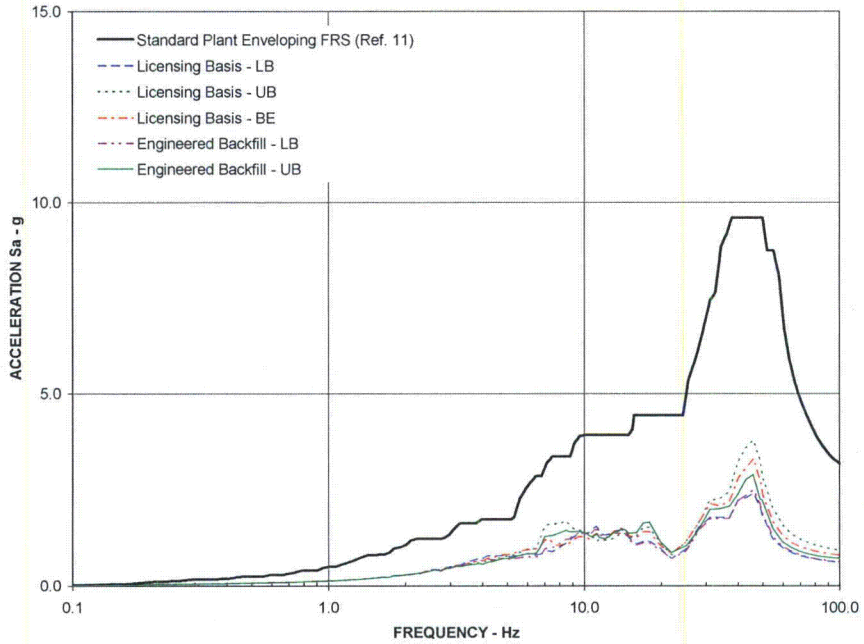

Figure 56: Comparison of floor slab oscillator response spectra – Reactor Building/Fuel Building (EL -6.4 m), DCD node 9011, z direction

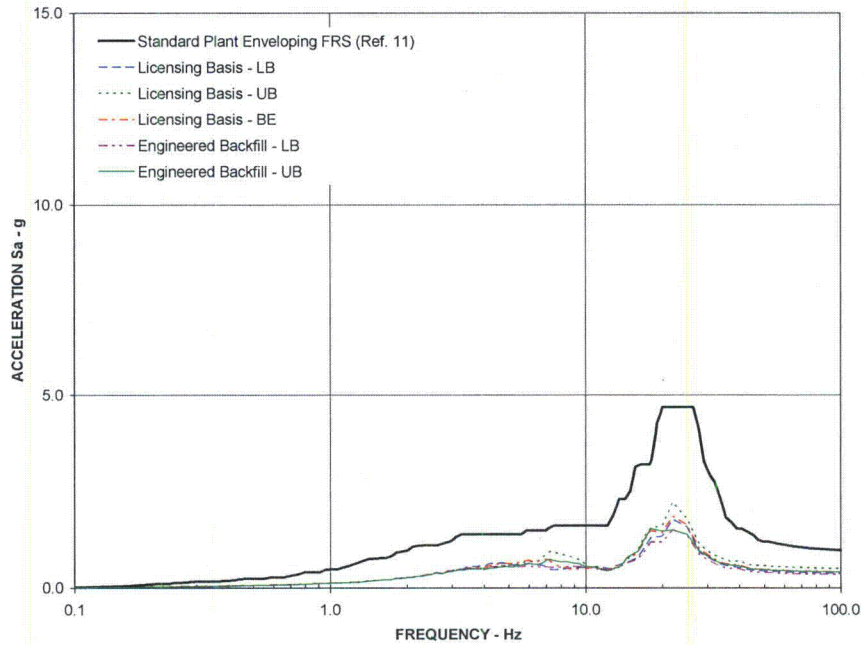

Figure 57: Comparison of floor slab oscillator response spectra – Reactor Building/Fuel Building (EL -6.4 m), DCD node 9012, z direction

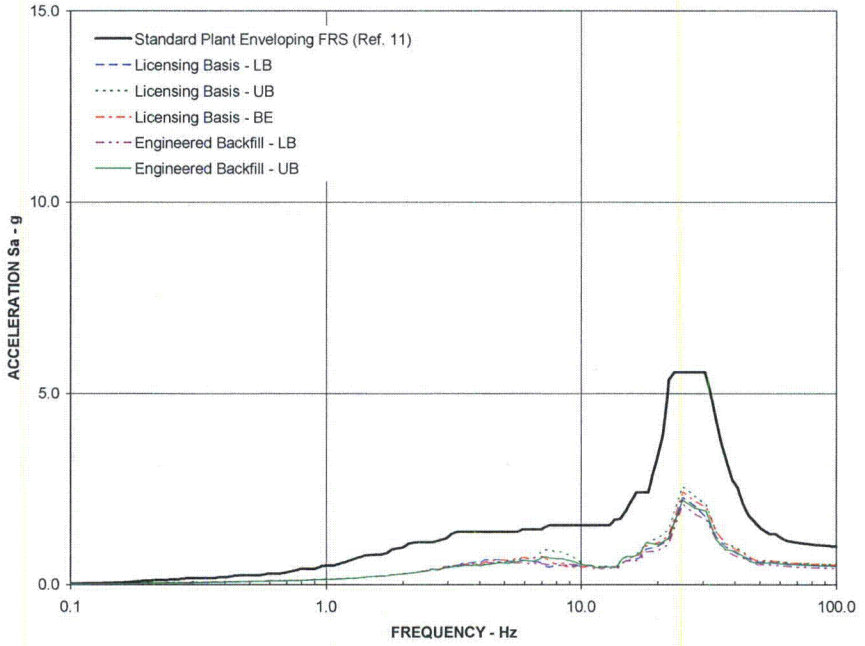

Figure 58: Comparison of floor slab oscillator response spectra – Reactor Building/Fuel Building (EL -6.4 m), DCD node 9013, z direction

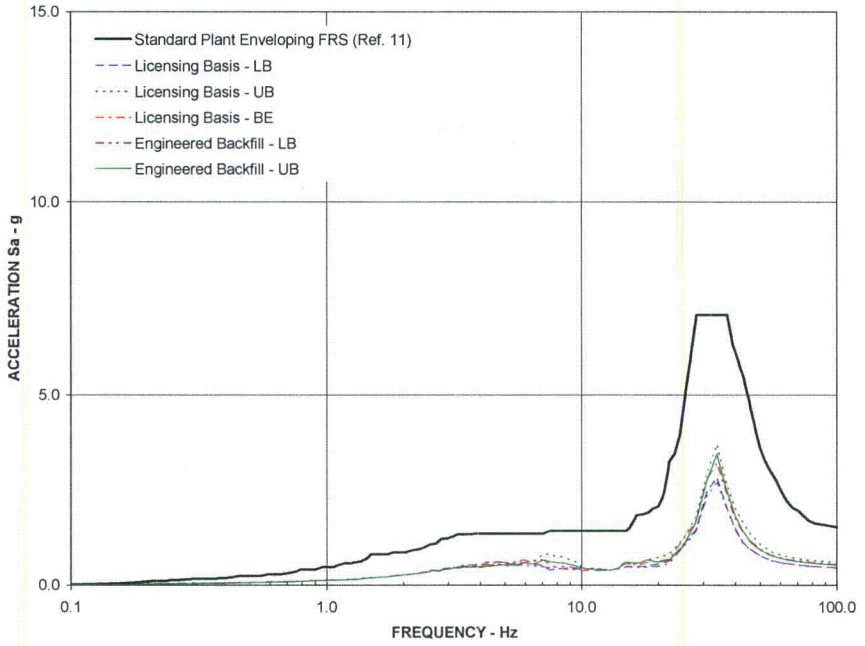

Figure 59: Comparison of floor slab oscillator response spectra – Reactor Building/Fuel Building (EL -1.0 m), DCD node 9021, z direction

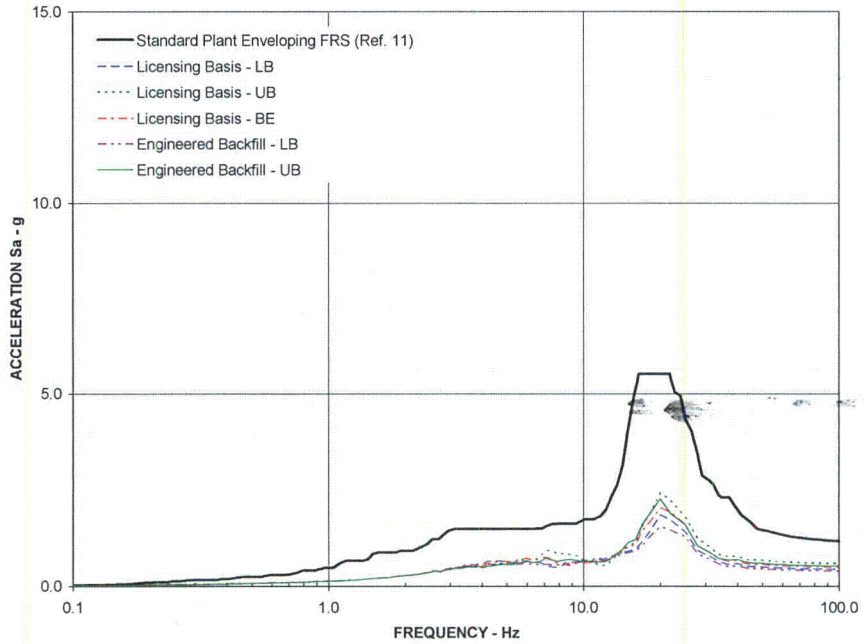

Figure 60: Comparison of floor slab oscillator response spectra – Reactor Building/Fuel Building (EL -1.0 m), DCD node 9022, z direction

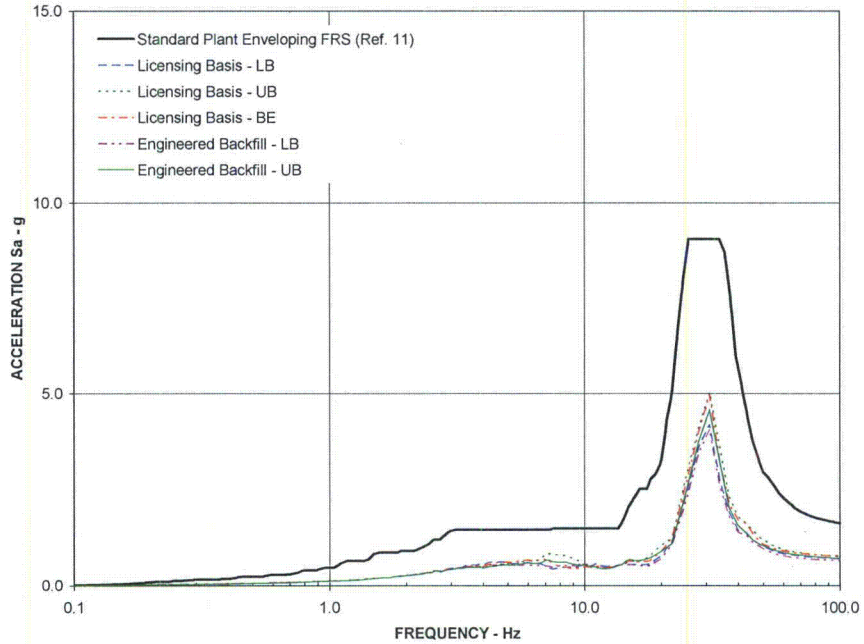

Figure 61: Comparison of floor slab oscillator response spectra – Reactor Building/Fuel Building (EL -1.0 m), DCD node 9023, z direction

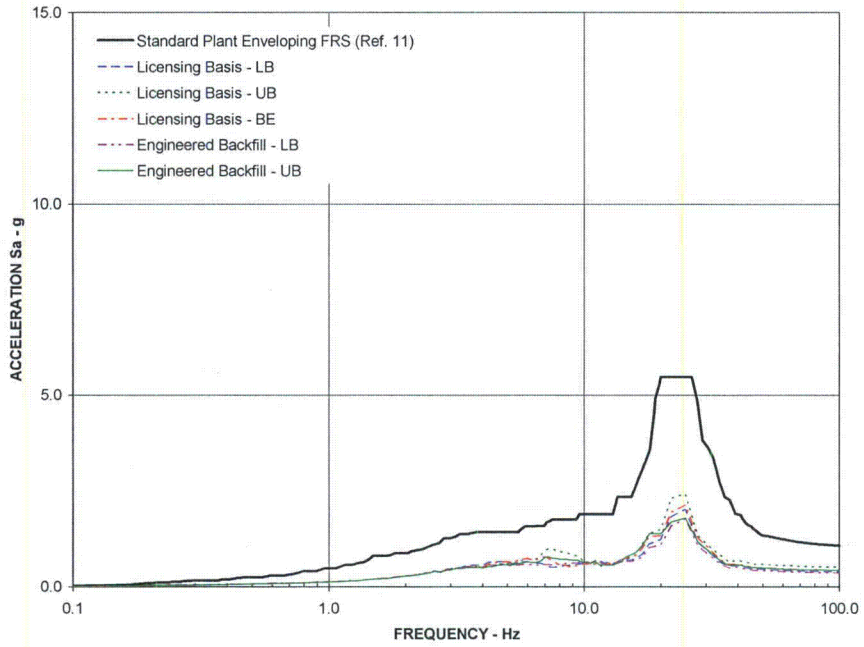

Figure 62: Comparison of floor slab oscillator response spectra – Reactor Building/Fuel Building (EL -1.0 m), DCD node 9024, z direction

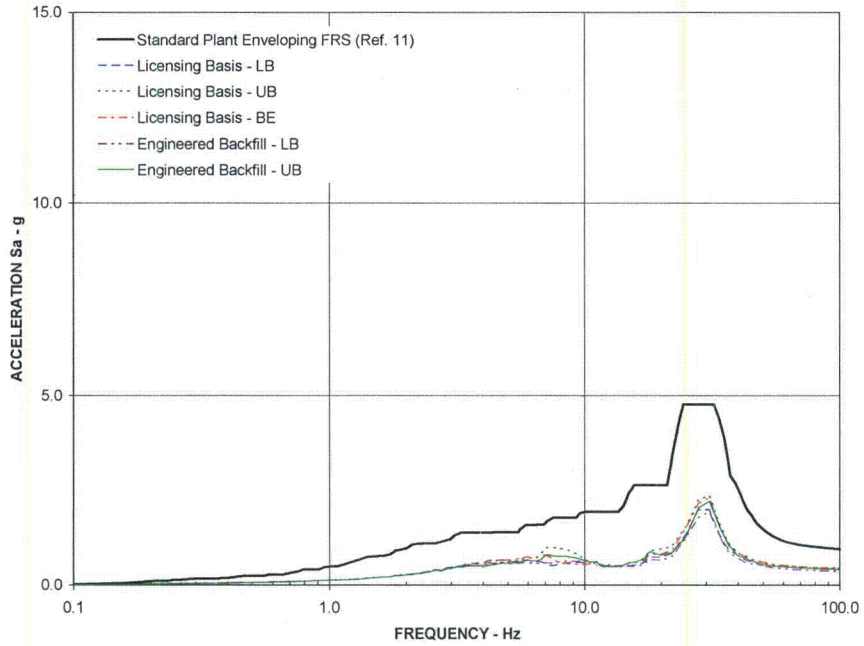

Figure 63: Comparison of floor slab oscillator response spectra – Reactor Building/Fuel Building (EL -1.0 m), DCD node 9025, z direction

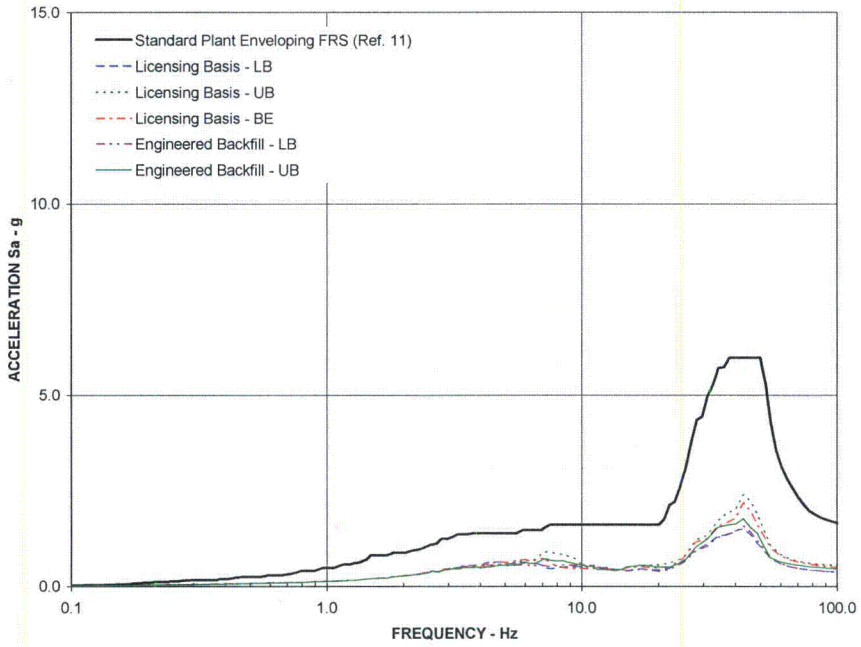

Figure 64: Comparison of floor slab oscillator response spectra – Reactor Building/Fuel Building (EL -1.0 m), DCD node 9026, z direction

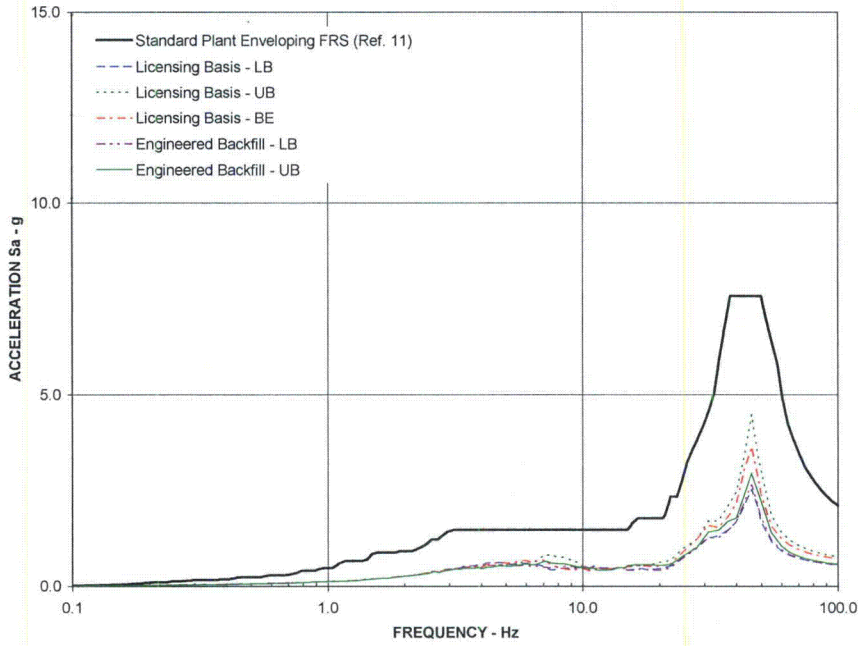

Figure 65: Comparison of floor slab oscillator response spectra – Reactor Building/Fuel Building (EL -1.0 m), DCD node 9027, z direction

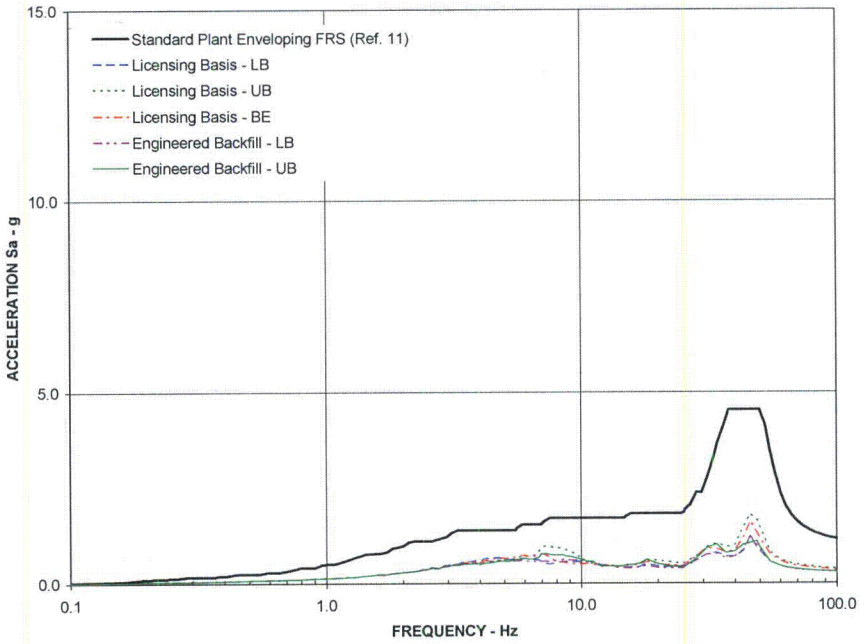

Figure 66: Comparison of floor slab oscillator response spectra – Reactor Building/Fuel Building (EL +4.65 m), DCD node 9031, z direction

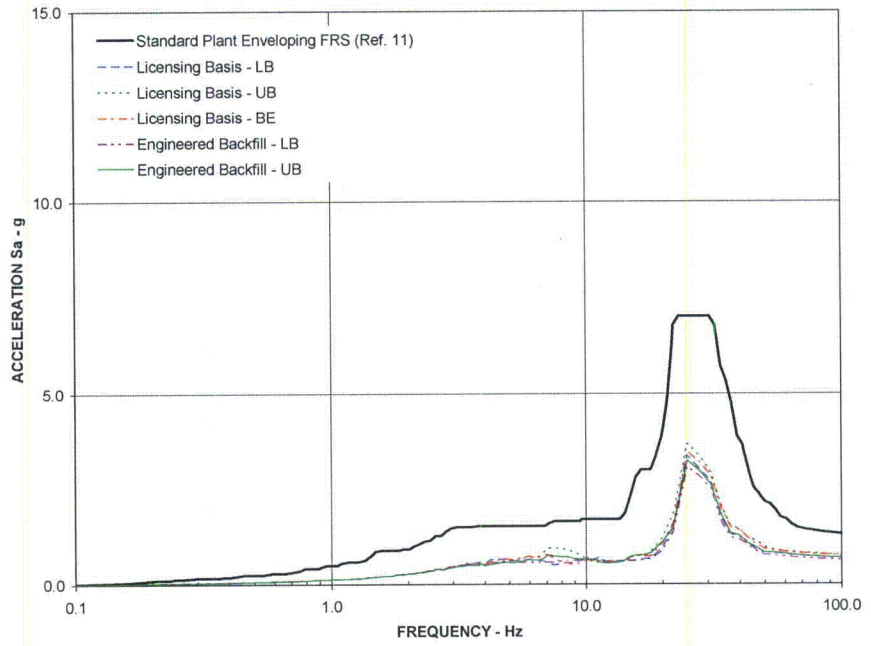

Figure 67: Comparison of floor slab oscillator response spectra – Reactor Building/Fuel Building (EL +4.65 m), DCD node 9032, z direction

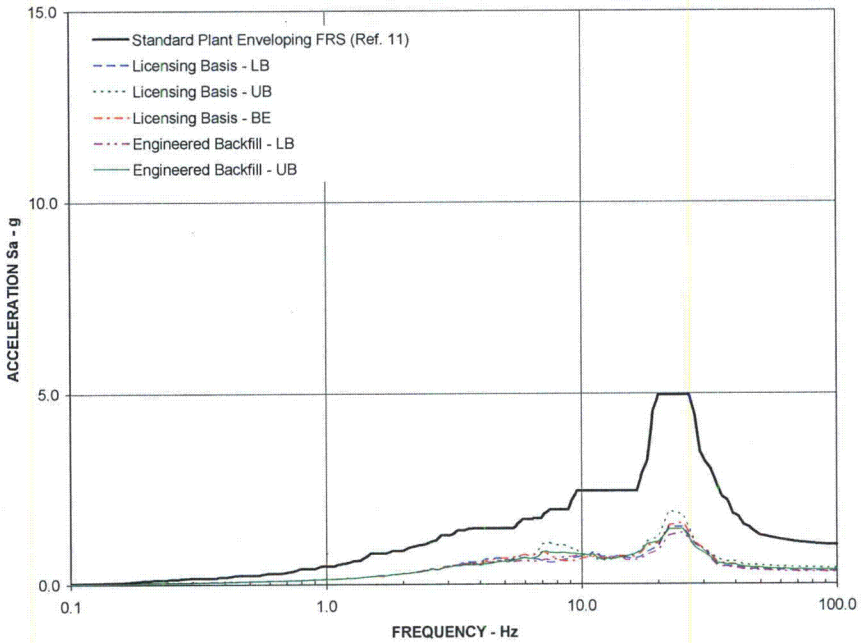

Figure 68: Comparison of floor slab oscillator response spectra – Reactor Building/Fuel Building (EL +4.65 m), DCD node 9033, z direction

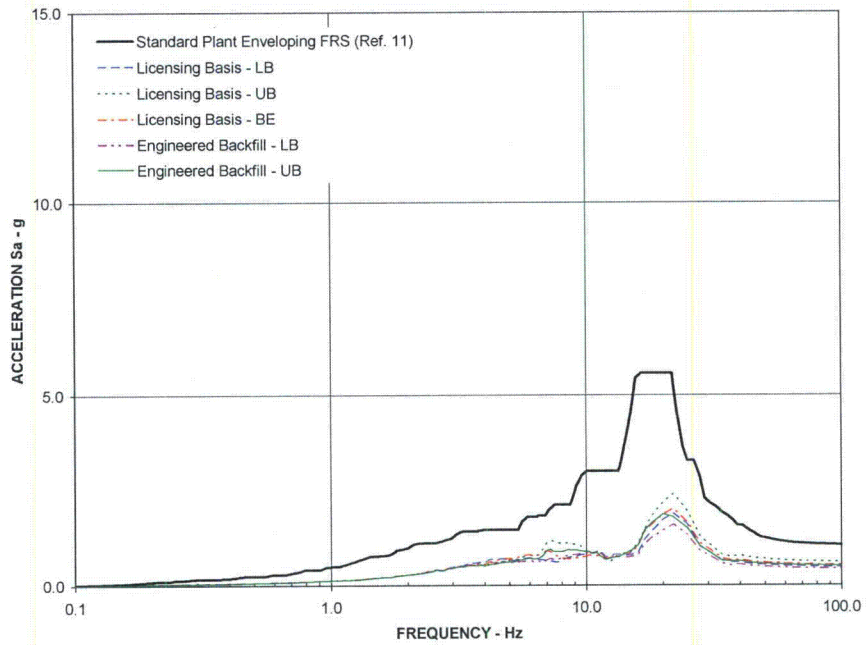

Figure 69: Comparison of floor slab oscillator response spectra – Reactor Building/Fuel Building (EL +4.65 m), DCD node 9034, z direction

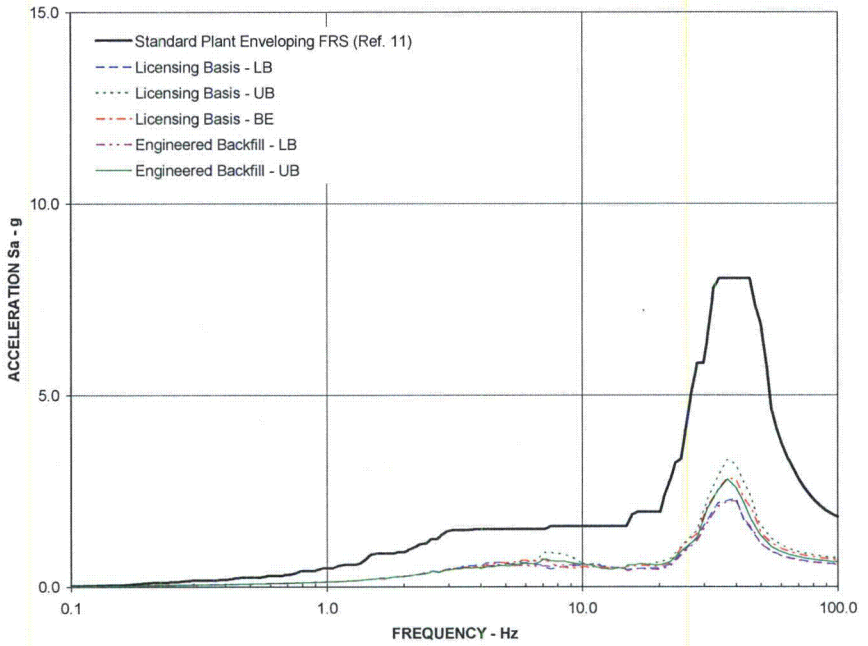

Figure 70: Comparison of floor slab oscillator response spectra – Reactor Building/Fuel Building (EL +4.65 m), DCD node 9035, z direction

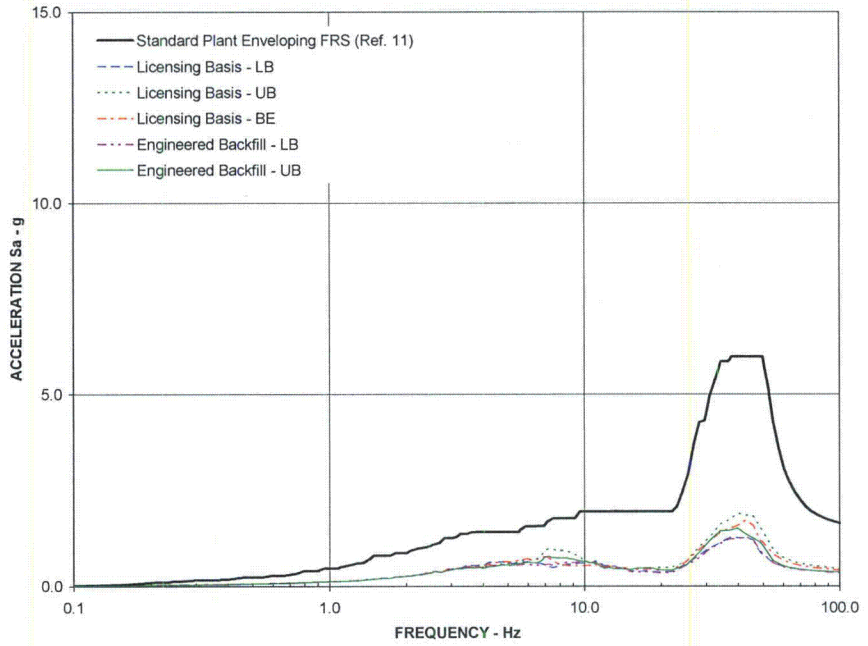

Figure 71: Comparison of floor slab oscillator response spectra – Reactor Building/Fuel Building (EL +9.06 m), DCD node 9041, z direction

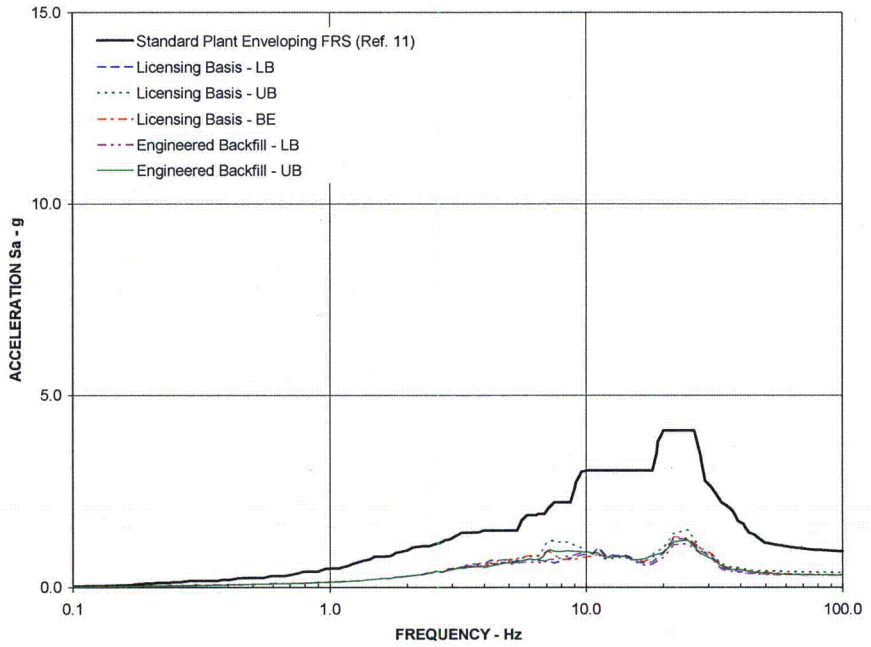

Figure 72: Comparison of floor slab oscillator response spectra – Reactor Building/Fuel Building (EL +9.06 m), DCD node 9042, z direction

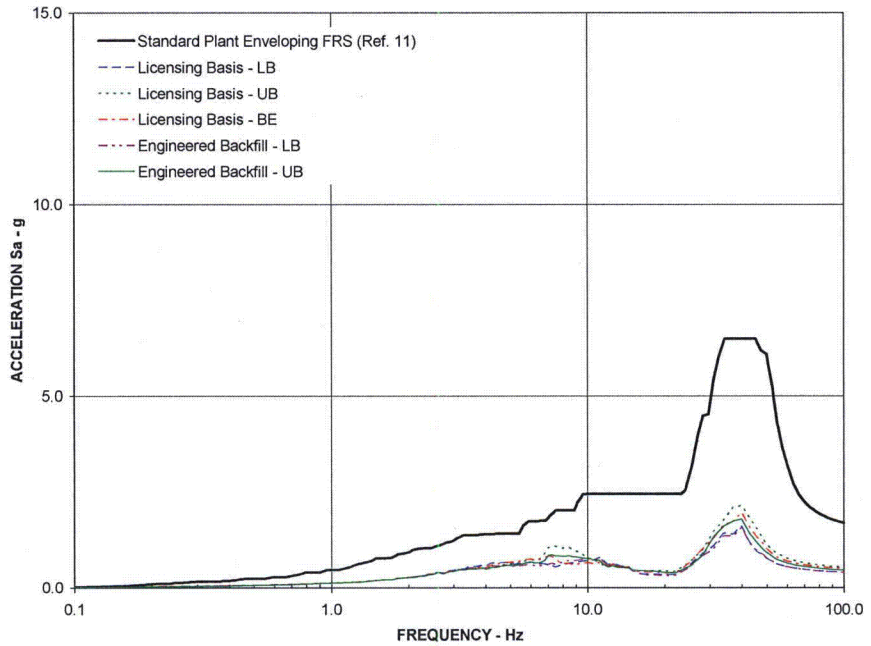

Figure 73: Comparison of floor slab oscillator response spectra – Reactor Building/Fuel Building (EL +13.57 m), DCD node 9051, z direction

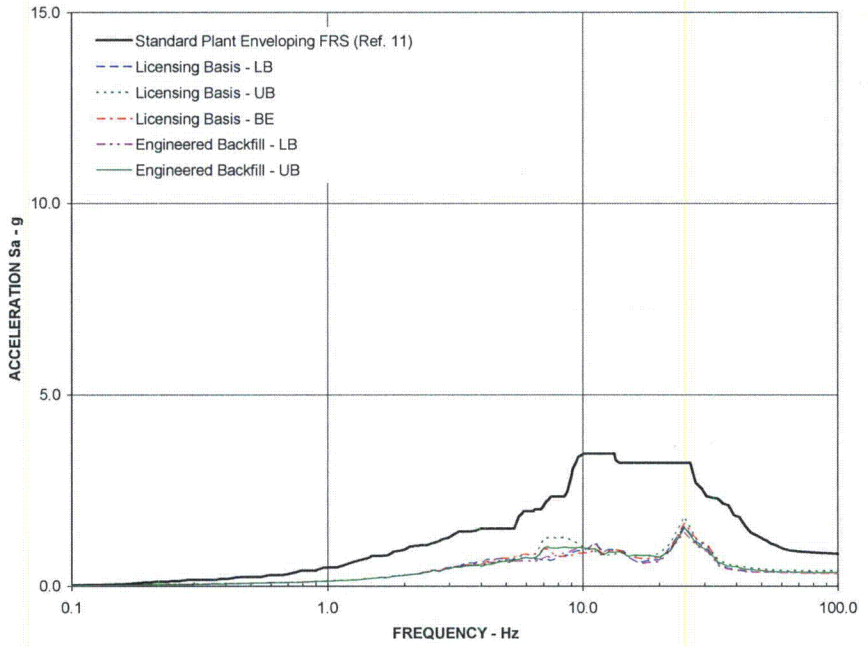

Figure 74: Comparison of floor slab oscillator response spectra – Reactor Building/Fuel Building (EL +13.57 m), DCD node 9052, z direction

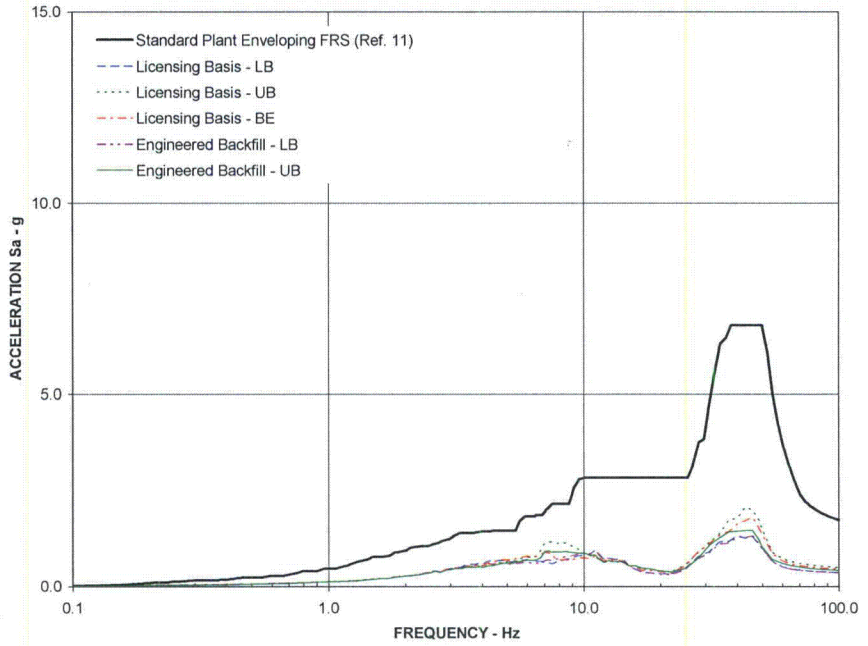

Figure 75: Comparison of floor slab oscillator response spectra – Reactor Building/Fuel Building (EL +17.5 m), DCD node 9061, z direction

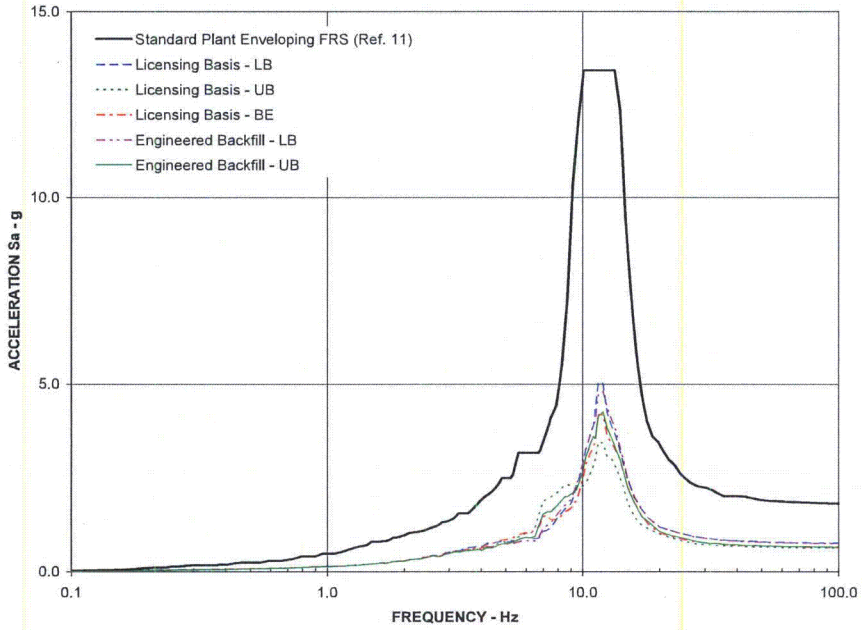

Figure 76: Comparison of floor slab oscillator response spectra – Reactor Building/Fuel Building (EL +17.5 m), DCD node 9062, z direction

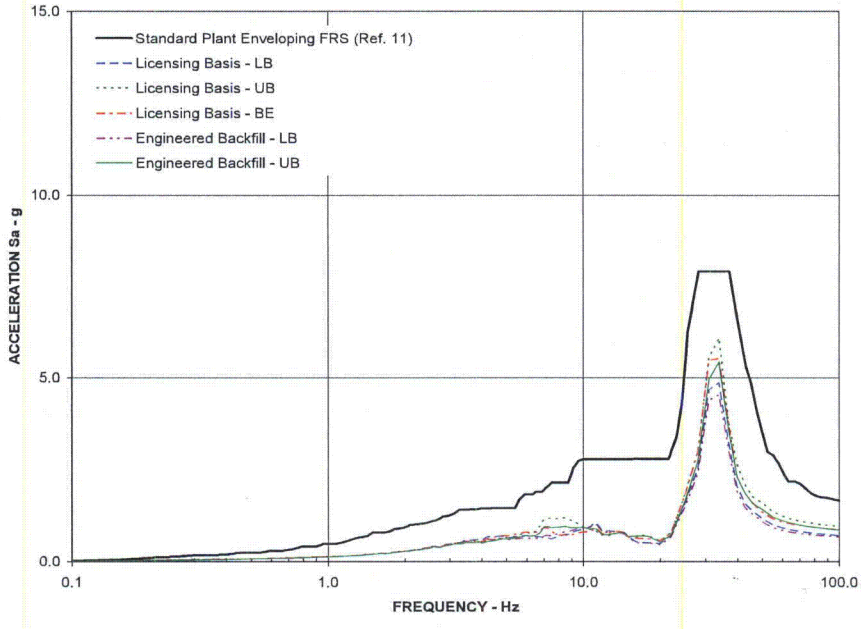

Figure 77: Comparison of floor slab oscillator response spectra – Reactor Building/Fuel Building (EL +17.5 m), DCD node 9063, z direction

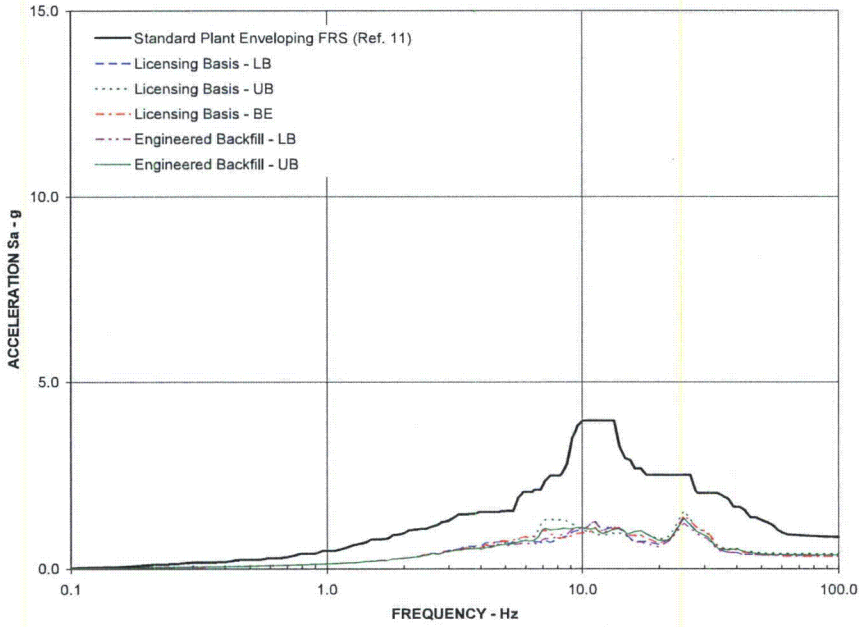

Figure 78: Comparison of floor slab oscillator response spectra – Reactor Building/Fuel Building (EL +17.5 m), DCD node 9064, z direction

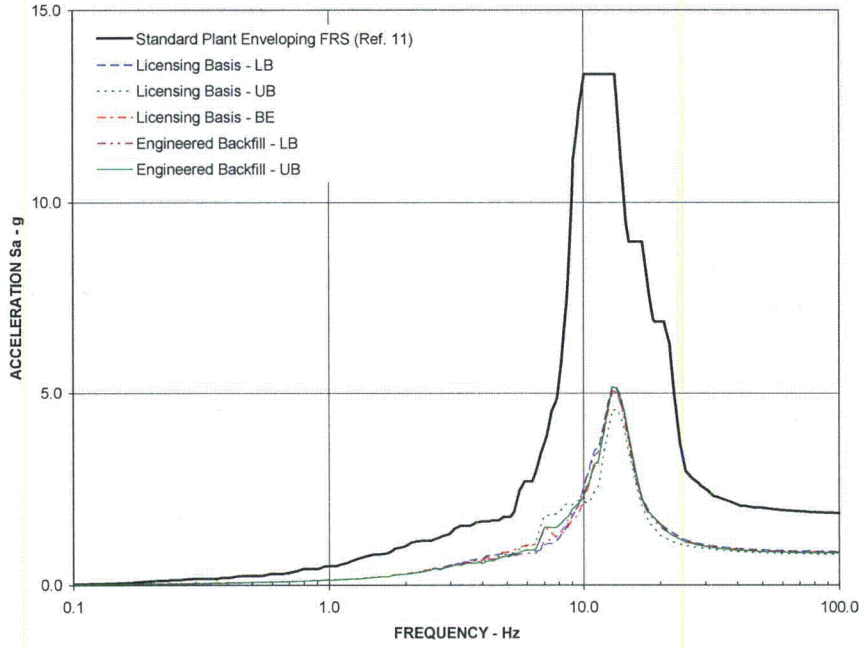

Figure 79: Comparison of floor slab oscillator response spectra – Reactor Building/Fuel Building (EL +17.5 m), DCD node 9065, z direction

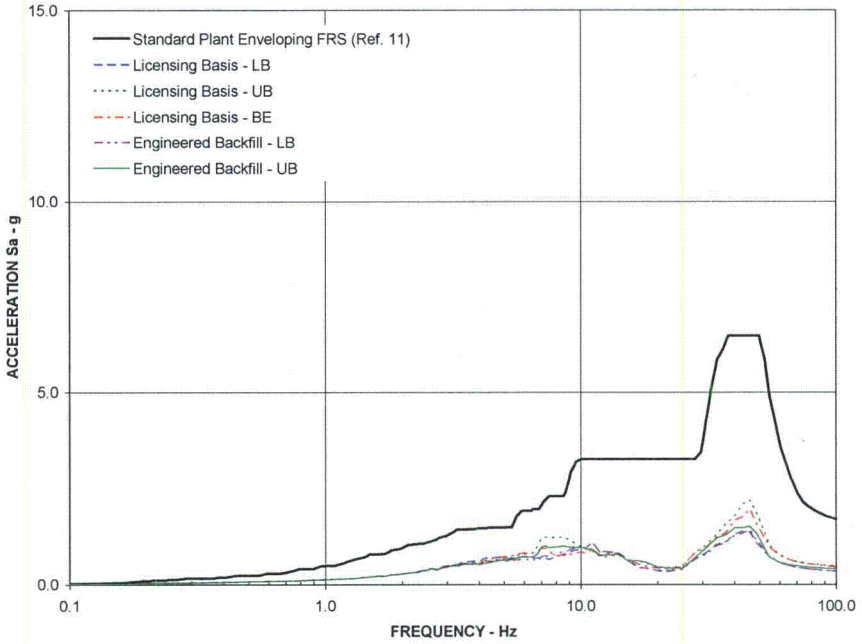

Figure 80: Comparison of floor slab oscillator response spectra – Reactor Building/Fuel Building (EL +22.5 m), DCD node 9071, z direction

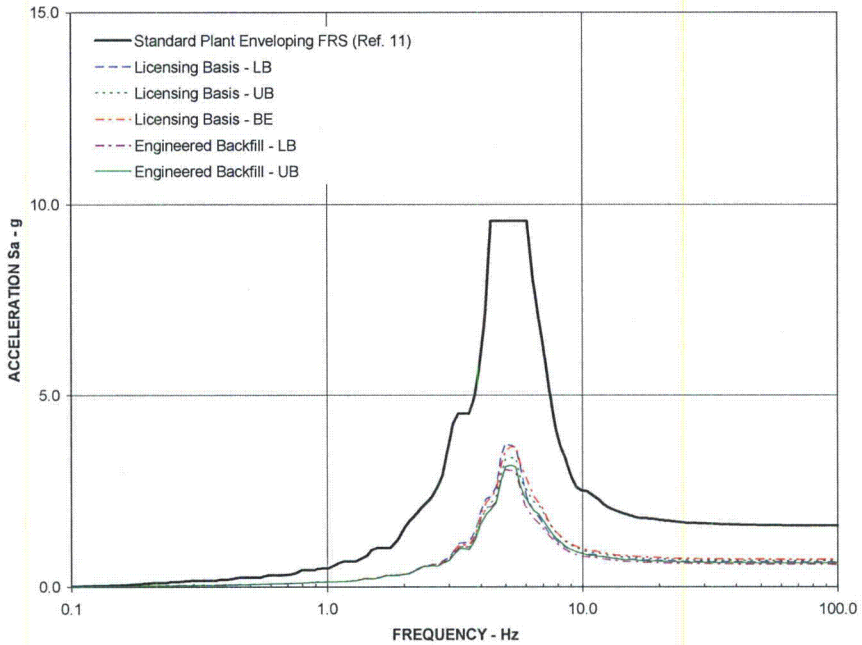

Figure 81: Comparison of floor slab oscillator response spectra – Reactor Building/Fuel Building (EL +22.5 m), DCD node 9072, z direction

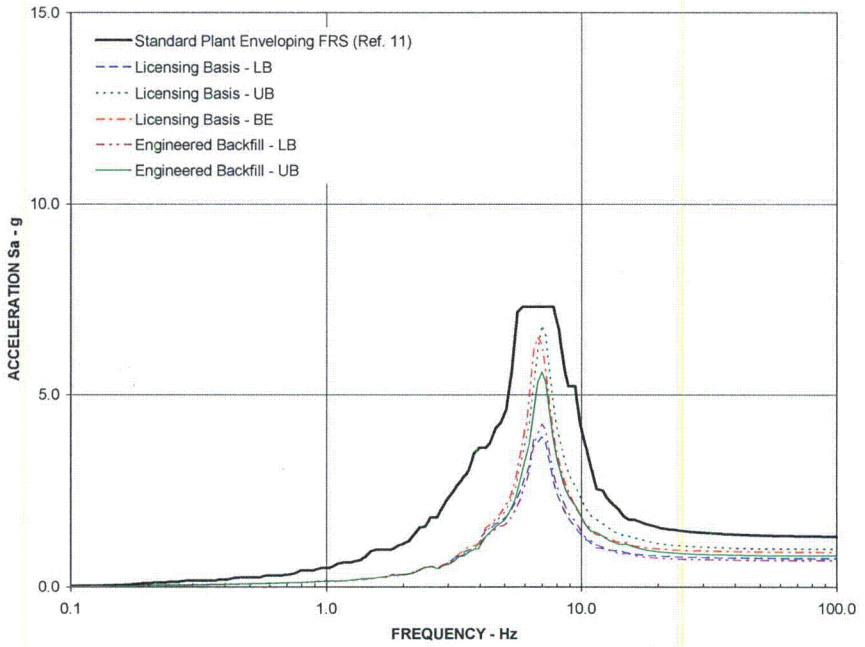

Figure 82: Comparison of floor slab oscillator response spectra – Reactor Building/Fuel Building (EL +22.5 m), DCD node 9073, z direction

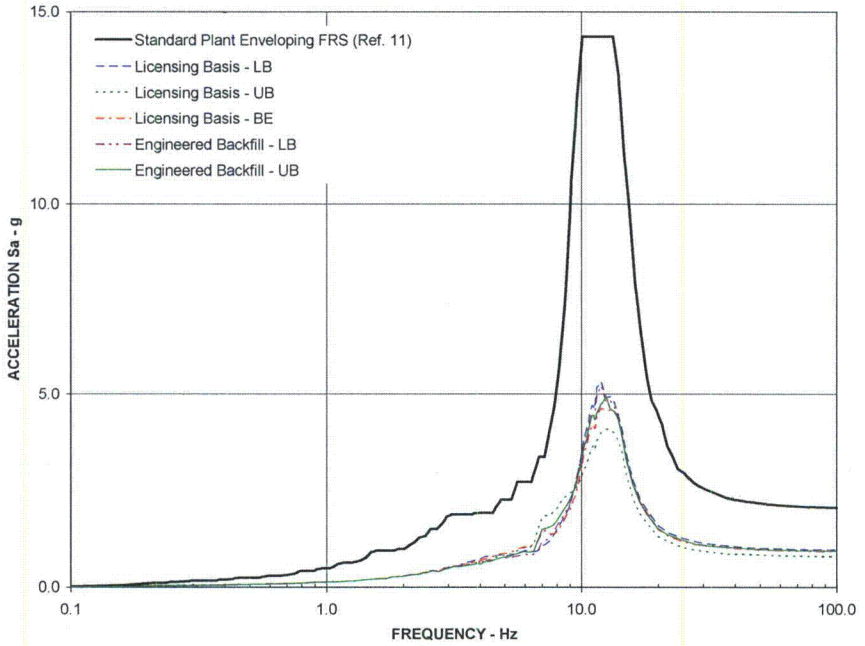

Figure 83: Comparison of floor slab oscillator response spectra – Reactor Building/Fuel Building (EL +22.5 m), DCD node 9074, z direction

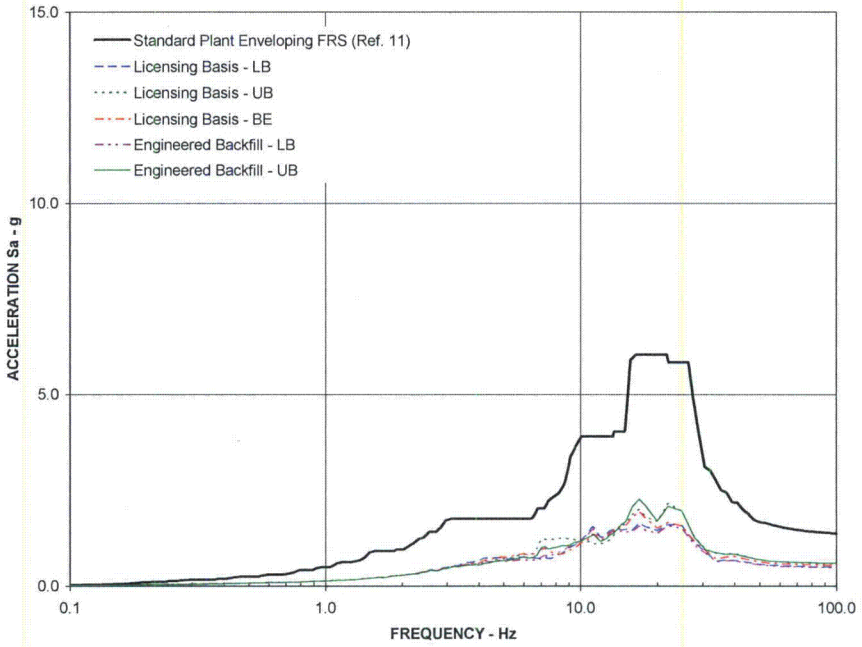

Figure 84: Comparison of floor slab oscillator response spectra – Reactor Building/Fuel Building (EL +22.5 m), DCD node 9075, z direction

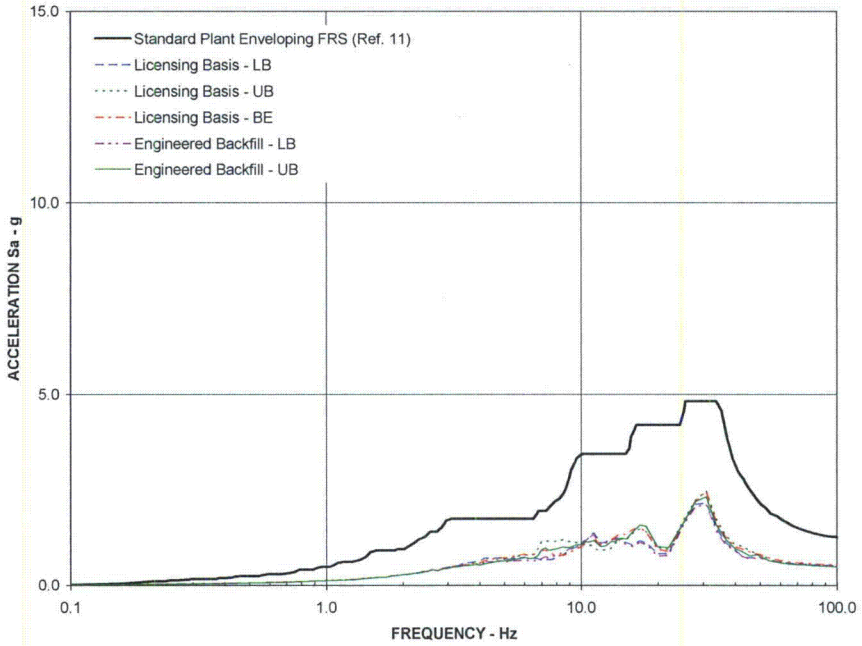

Figure 85: Comparison of floor slab oscillator response spectra – Reactor Building/Fuel Building (EL +27.0 m), DCD node 9081, z direction

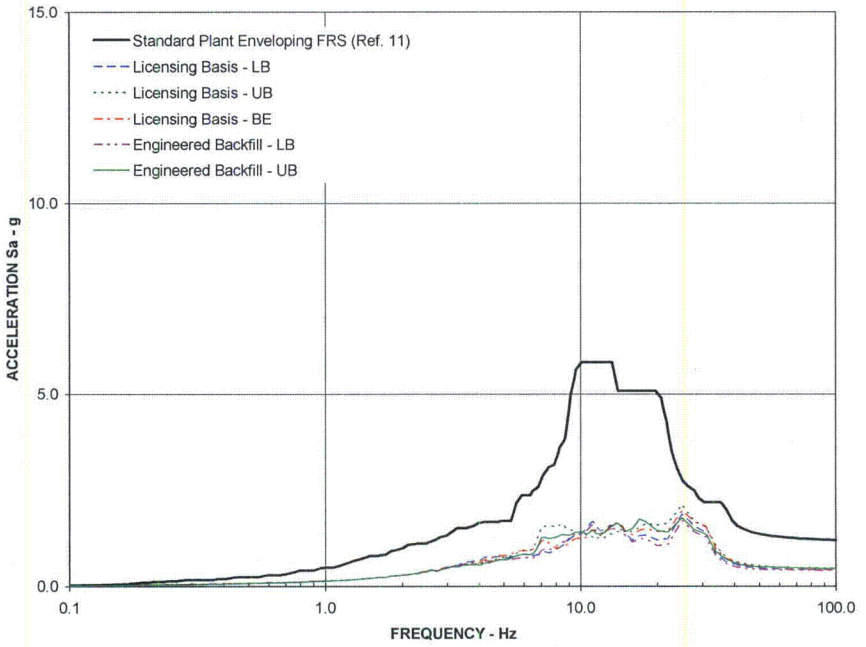

Figure 86: Comparison of floor slab oscillator response spectra – Reactor Building/Fuel Building (EL +27.0 m), DCD node 9082, z direction

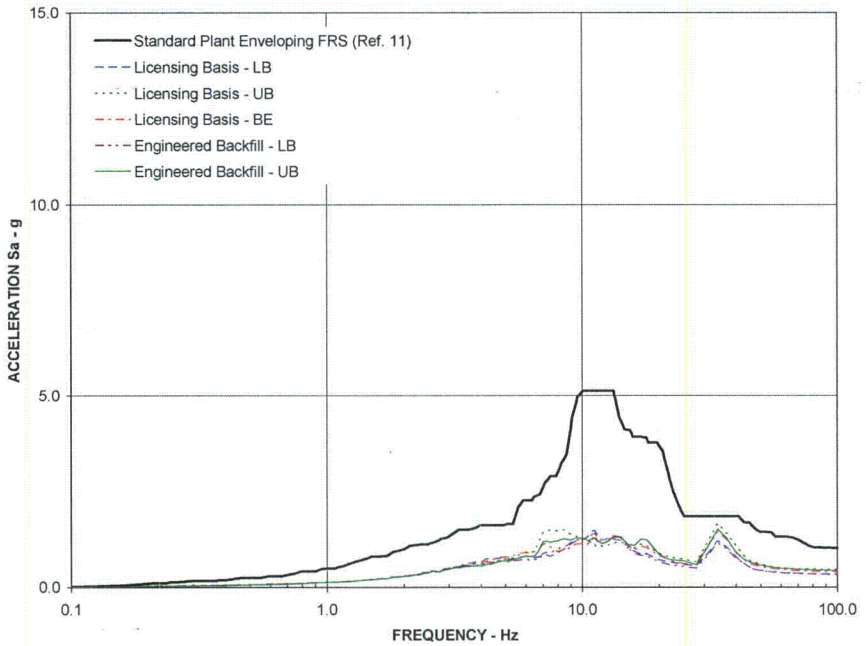

Figure 87: Comparison of floor slab oscillator response spectra – Reactor Building/Fuel Building (EL +27.0 m), DCD node 9083, z direction

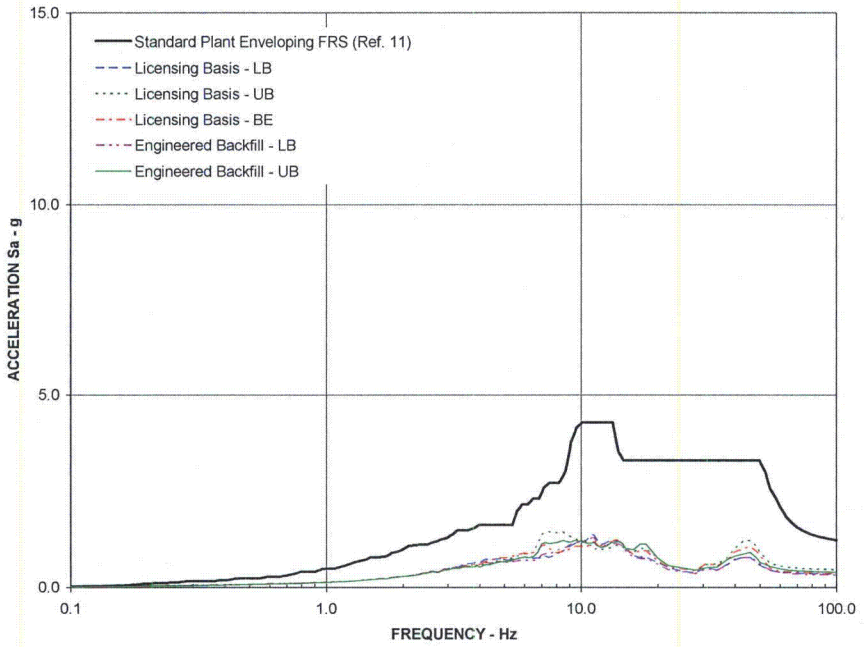

Figure 88: Comparison of floor slab oscillator response spectra – Reactor Building/Fuel Building (EL +27.0 m), DCD node 9084, z direction

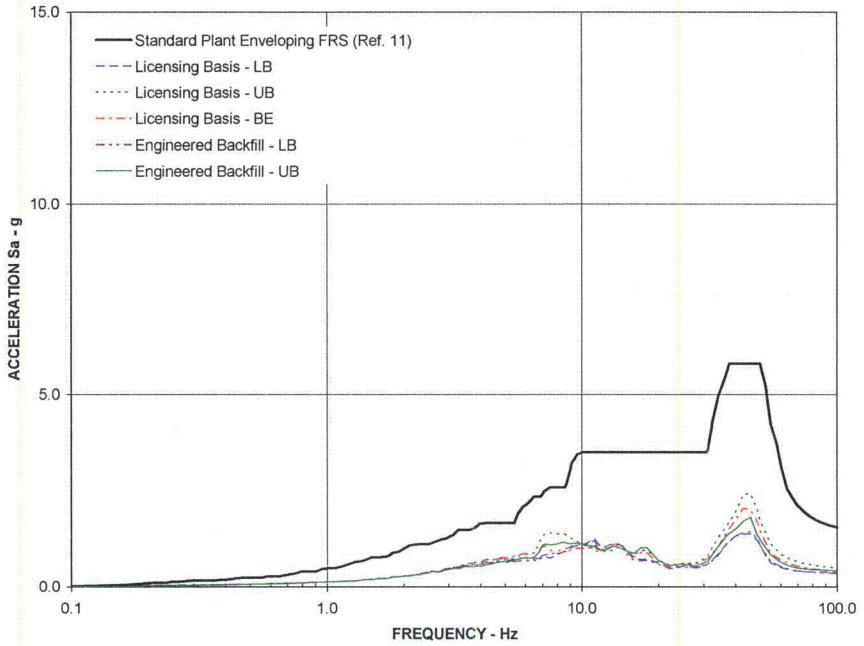

Figure 89: Comparison of floor slab oscillator response spectra – Reactor Building/Fuel Building (EL +27.0 m), DCD node 9085, z direction

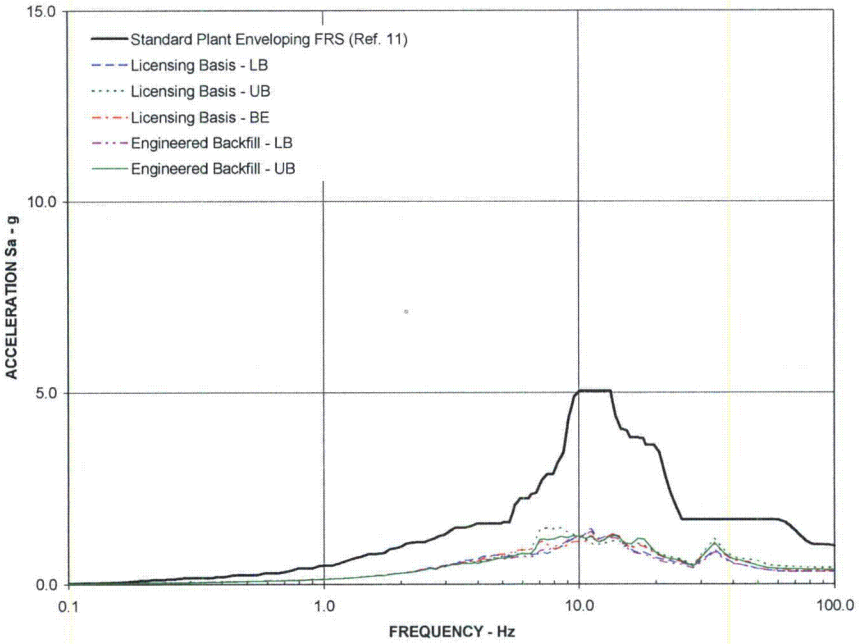

Figure 90: Comparison of floor slab oscillator response spectra – Reactor Building/Fuel Building (EL +34.0 m), DCD node 9091, z direction

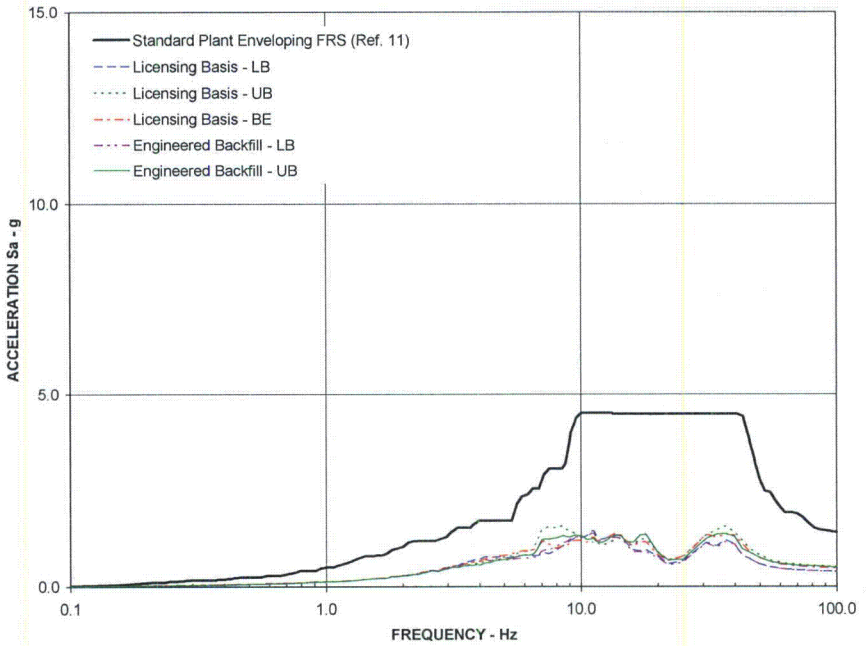

Figure 91: Comparison of floor slab oscillator response spectra – Reactor Building/Fuel Building (EL +34.0 m), DCD node 9092, z direction

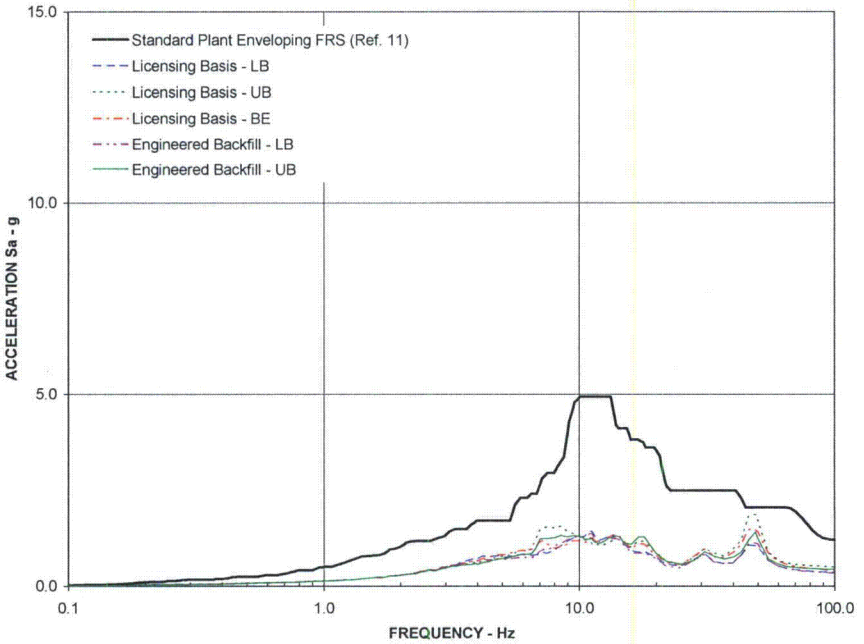

Figure 92: Comparison of horizontal oscillator 99981 RS and ESBWR standard plant enveloping RS for north-south direction (input motion from node 109).

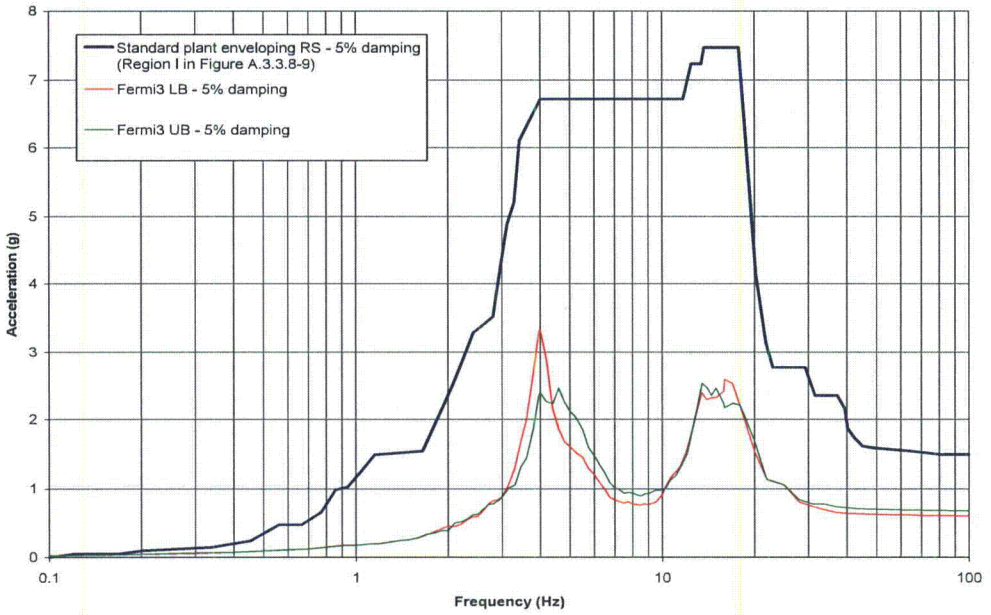

Figure 93: Comparison of horizontal oscillator 99982 RS and ESBWR standard plant enveloping RS for north-south direction (input motion from node 109).

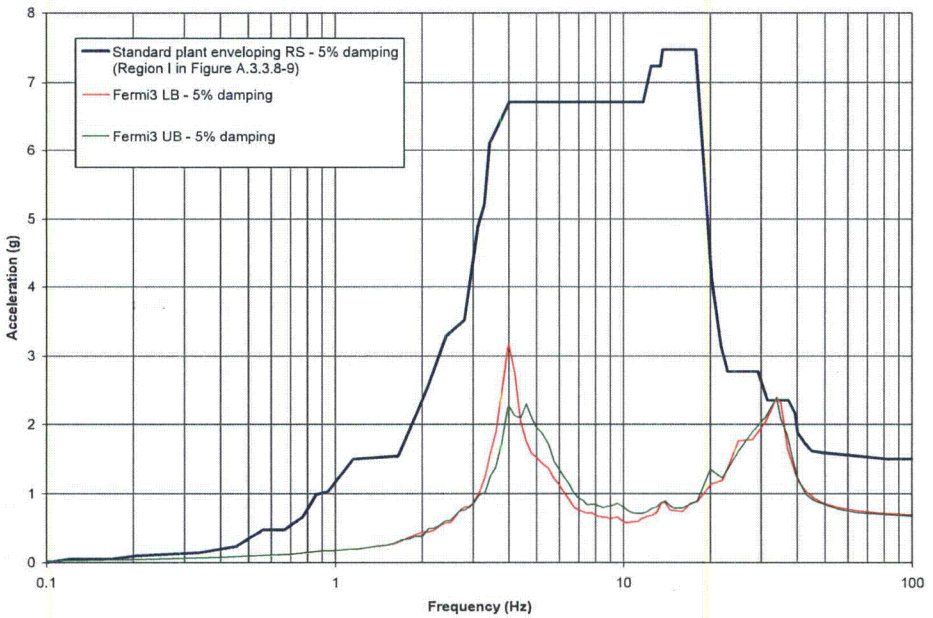

Figure 94: Comparison of horizontal oscillator 99983 RS and ESBWR standard plant enveloping RS for east-west direction (input motion from node 109).

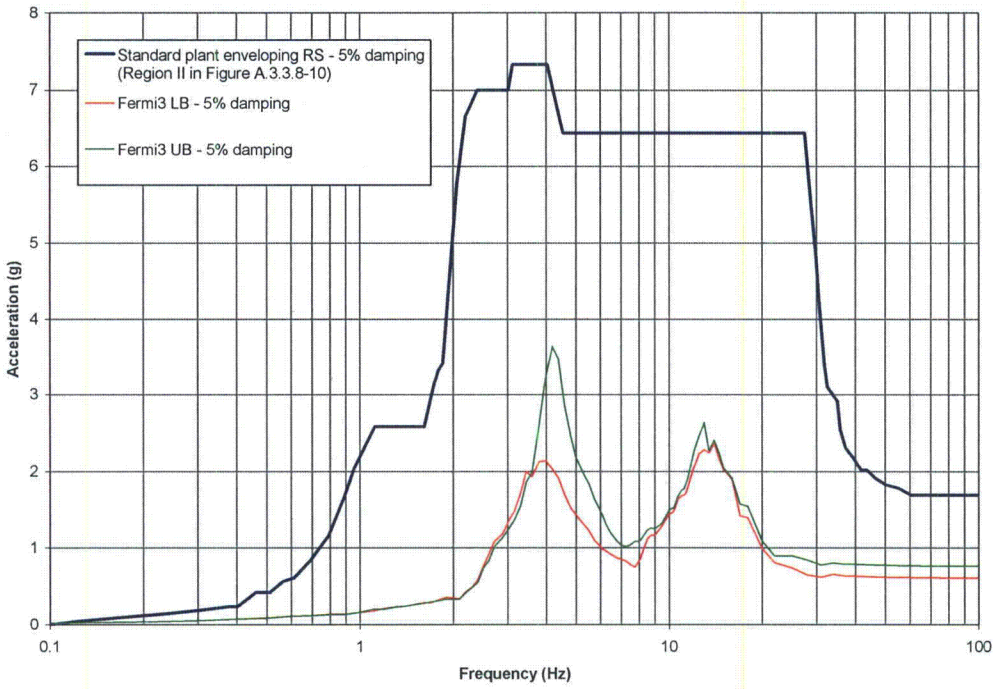

Figure 95: Comparison of horizontal oscillator 99984 RS and ESBWR standard plant enveloping RS for east-west direction (input motion from node 109).

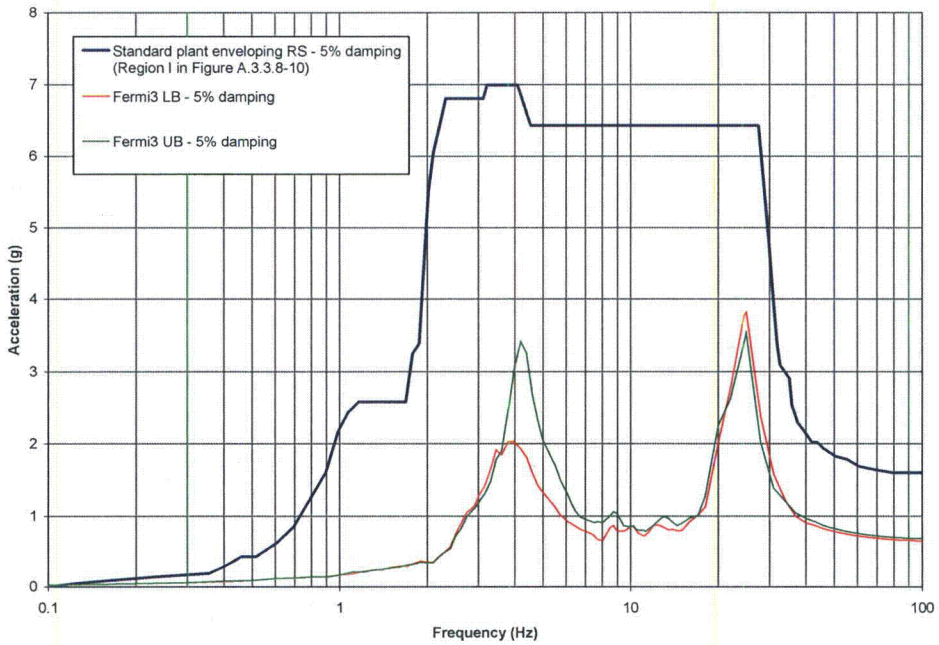

Figure 96: Comparison of horizontal oscillator 99985 RS and ESBWR standard plant enveloping RS for east-west direction (input motion from node 109).

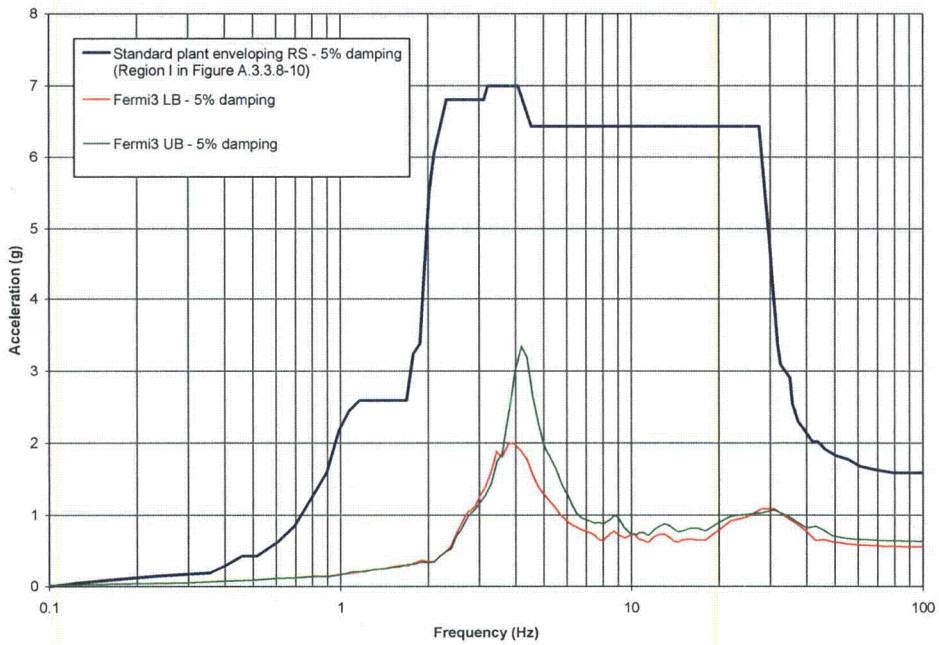

Figure 97: Comparison of horizontal oscillator 99981 RS and ESBWR standard plant enveloping RS for north-south direction (input motion from node 110).

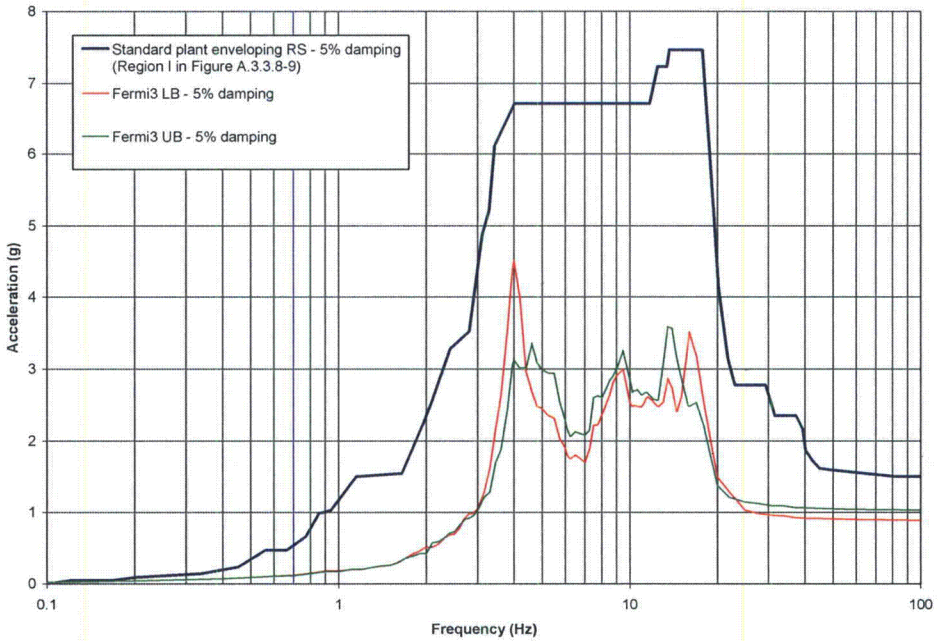

Figure 98: Comparison of horizontal oscillator 99982 RS and ESBWR standard plant enveloping RS for north-south direction (input motion from node 110).

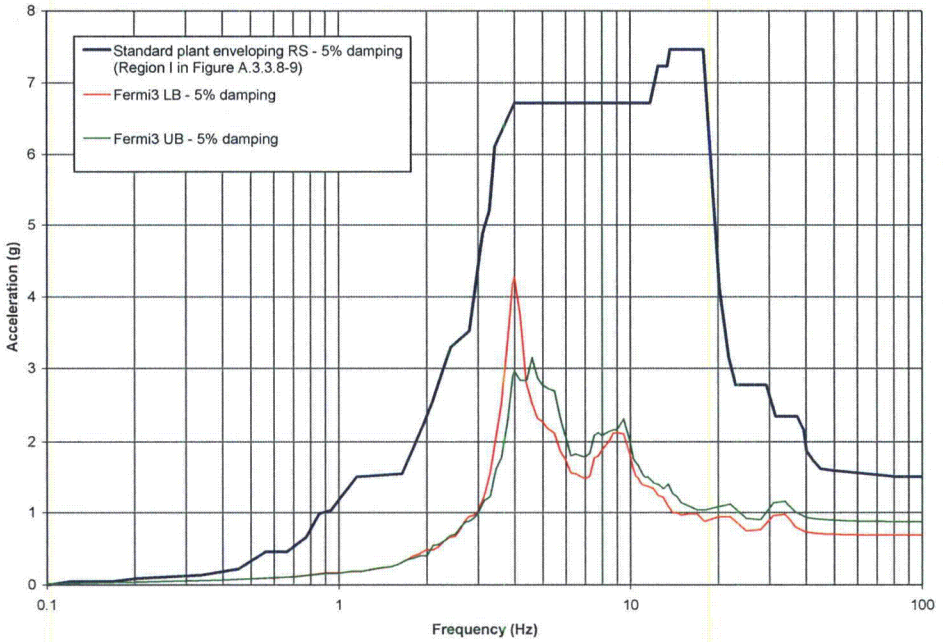

Figure 99: Comparison of horizontal oscillator 99983 RS and ESBWR standard plant enveloping RS for east-west direction (input motion from node 110).

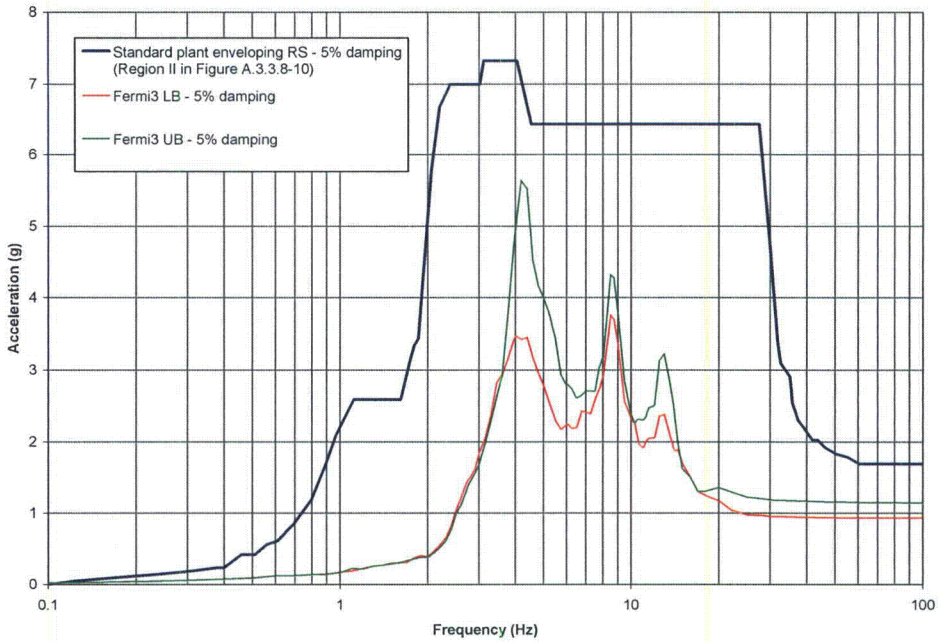

Figure 100: Comparison of horizontal oscillator 99984 RS and ESBWR standard plant enveloping RS for east-west direction (input motion from node 110).

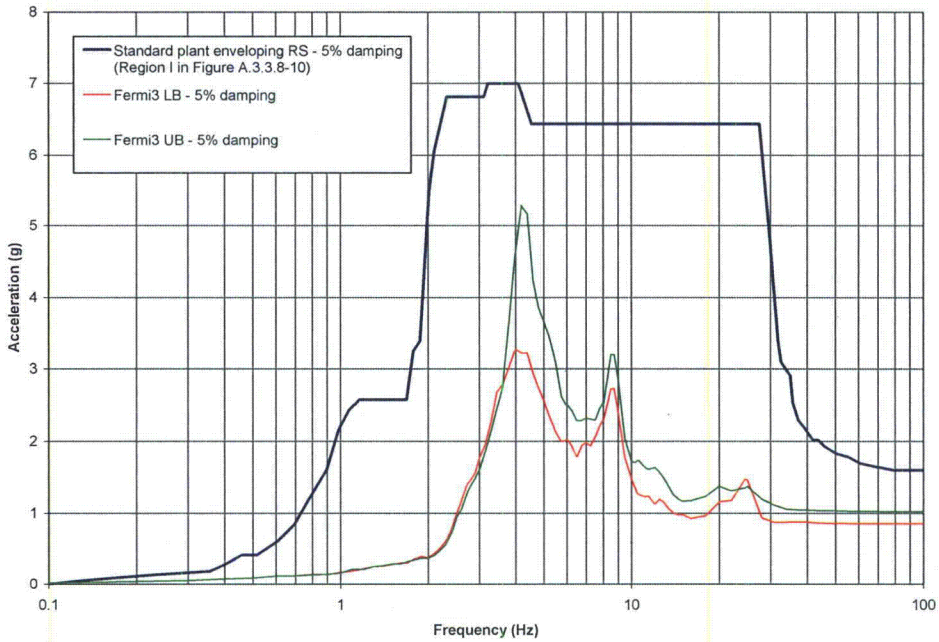

Figure 101: Comparison of horizontal oscillator 99985 RS and ESBWR standard plant enveloping RS for east-west direction (input motion from node 110).

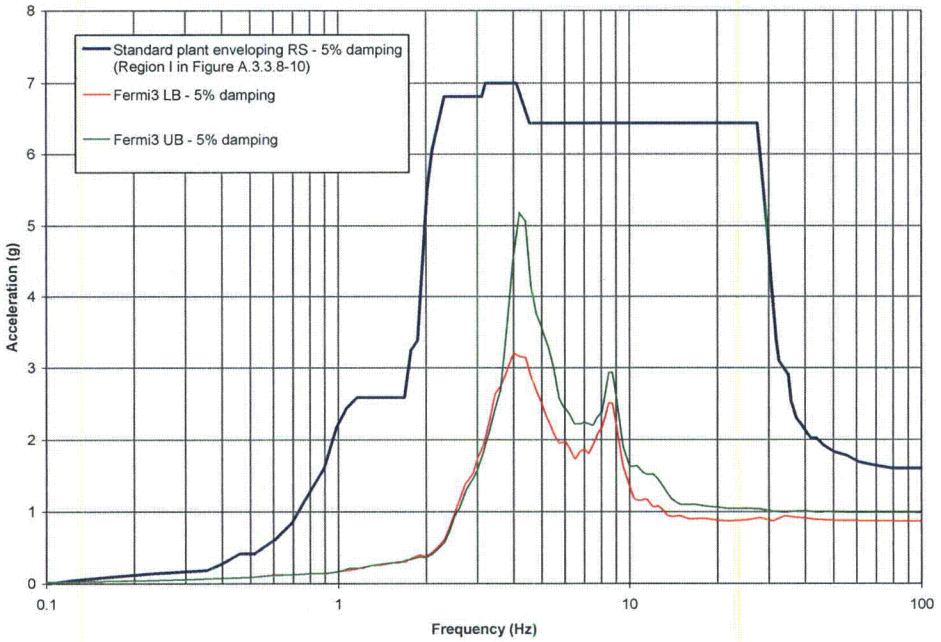

Figure 102: Comparison of horizontal oscillator 99982 lower-bound RS and ESBWR standard plant enveloping RS for east-west direction

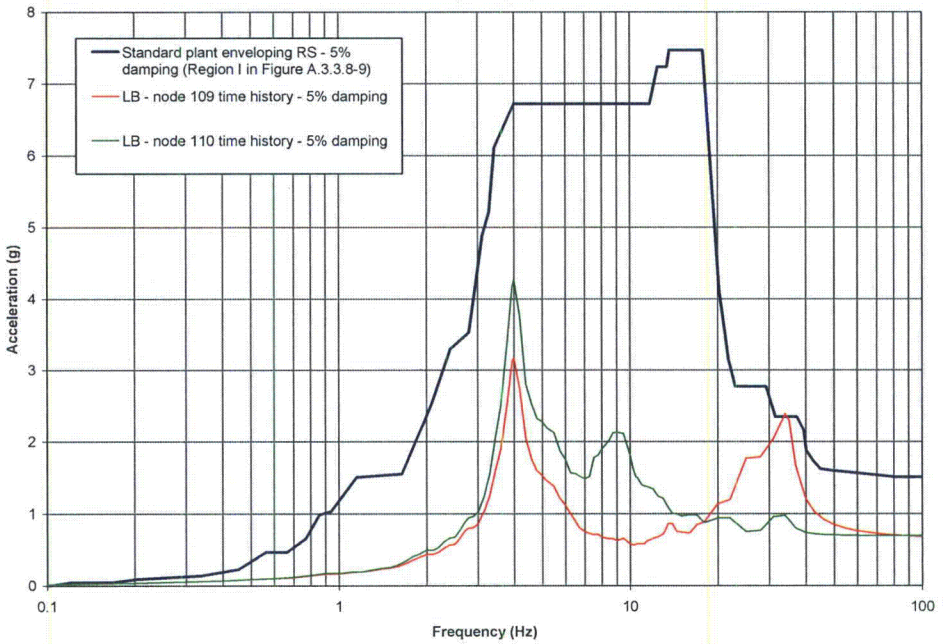

Figure 103: Comparison of horizontal oscillator 99982 upper-bound RS and ESBWR standard plant enveloping RS for east-west direction